

UNIVERSIDADE DE SÃO PAULO
INSTITUTO DE ASTRONOMIA, GEOFÍSICA E CIÊNCIAS ATMOSFÉRICAS
DEPARTAMENTO DE CIÊNCIAS ATMOSFÉRICAS

MONIQUE SILVA COELHO

**REACTIVE HYDROCARBONS (C₆-C₁₁) IN THE METROPOLITAN AREA
OF SÃO PAULO**

São Paulo
2023

Monique Silva Coelho

Reactive hydrocarbons (C₆-C₁₁) in the Metropolitan Area of São Paulo

Corrected version. The original is available in the Institute.

Thesis submitted in partial fulfillment of the requirements for the degree of Doctor of Sciences in the Institute of Astronomy, Geophysics and Atmospheric Sciences, post-graduation program in Meteorology.

Research field: Atmospheric Chemistry
Supervisor: Ph.D. Adalgiza Fornaro
Joint supervisor: Ph.D. Daniel C. Zacharias

São Paulo
2023

CONTENTS

Chapter 1. Introduction	16
Chapter 2. Non-methane hydrocarbons in the vicinity of a petrochemical complex in the Metropolitan Area of São Paulo, Brazil (Coelho et al., 2021).	18
2.1. Introduction	19
2.2. Materials and methods.....	23
2.2.1. Study area and sampling strategy	23
2.2.2. HCs identification	26
2.2.3. Estimating the formation of secondary pollutants.....	32
2.3. Results and discussions.....	34
2.3.1. Data overview	34
2.3.2. Meteorological and air quality conditions.....	39
2.3.3. BTEX mixing ratios comparison.....	45
2.3.4. Ratios and correlation between BTEX species	48
2.3.5. O ₃ and SOA formation potentials (OFP and SOAFP)	52
2.3.6. Exposure risk	54
2.4. Conclusions.....	56
Chapter 3. Air Quality Impact Estimation Due to Uncontrolled Emissions from Capuava Petrochemical Complex in the Metropolitan Area of São Paulo (MASP), Brazil (Coelho et al., 2023).....	58
3.1. Introduction	58
3.2. Materials and Methods	64
3.2.1. Gaussian Plume Model (AERMOD).....	64
3.2.2. Air Quality Data Analysis.....	68
3.3. Results and Discussions	69
3.3.1. Air Quality Data	69
3.3.2. Air Quality Modeling	77
3.4. Conclusions.....	83
Chapter 4. Six years (2017-2022) of benzene and toluene monitoring: Trends and impacts for São Paulo state, Brazil.	85
4.1. Introduction	85
4.2. Materials and Methods	87

4.2.1. Estimating the formation of secondary pollutants	88
4.2.2. Risk assessment	88
4.3. Results and discussion	89
4.3.1. Air quality station characteristics	89
4.3.2. Data overview	100
4.3.3. Seasonal and diurnal profiles	105
4.3.4. Ratios and correlation for benzene and toluene	108
4.3.5. O ₃ and SOA formation potentials	111
4.3.6. Exposure risk	113
4.5. Conclusions.....	115
Chapter 5. Conclusions.....	117
Chapter 6. Future perspectives	120
APPENDIX I: Publications and presentations at scientific meetings.....	121
APPENDIX II: Publishing rights - license details	122
References	124

I dedicate this work to my mother, Heloisa, to my grandparents Maria das Graças and Helvécio, in gratitude for the love, encouragement and support.

ACKNOWLEDGMENTS

I would like to thank the Comissão de Aperfeiçoamento de Pessoal do Nível Superior (CAPES) for the financial support and scholarship (post-graduate program in Meteorology, IAG-USP).

I would like to thank my supervisor Prof. Dr. Adalgiza Fornaro for this doctoral opportunity, for her support and contribution during the development of this project. And to Dr. Daniel C. Zacharias for teaching and mentoring during the modelling topics developed at this project.

I wish to acknowledge the help provided by Dr. Pamela Dominutti and Prof Dr. Thiago Nogueira, for his teaching and mentoring during all steps of this work.

I would also like to extend my thanks to my colleagues of IAG-USP: Tailine, Natanael, Jeová and Noelia.

Finally, I want to thank my husband, Felipe, for the unconditional support and for always encouraging me to achieve my goals.

Resumo

Os compostos orgânicos voláteis (COVs) são fundamentais nas reações atmosféricas, produzindo ozônio troposférico (O_3) e aerossóis orgânicos secundários (SOA). Dentre os COVs, destacam-se os hidrocarbonetos (HCs), incluindo os compostos aromáticos (ex. (BTEX: benzeno, tolueno, etilbenzeno, m,p- e o-xilenos) sendo emitido diretamente na atmosfera, em áreas urbanas, por escapamentos de veículos, evaporação de combustível, uso de solventes, emissões de gás natural e processos industriais. São Paulo é o estado brasileiro com maior ocupação territorial e mais de 47 milhões de habitantes, somado ao maior desenvolvimento econômico e à maior frota automotiva, causando degradação da qualidade do ar. Na região metropolitana de São Paulo (RMSP), em particular, a frota de mais de 7 milhões de veículos tem sido reconhecida como a principal causa de eventos de poluição do ar, mas problemas de saúde e queixas da população do entorno de um importante complexo industrial e petroquímico do MASP também receberam atenção. Nesse contexto, o presente estudo avaliou os HCs próximos ao Complexo Petroquímico de Capuava (CPC) na RMSP, no período de 2016 a 2022. Na primeira etapa foram analisados dados de diferentes HCs com base em amostragens horárias em dois locais diferentes durante, 2016-2017. Na segunda parte do estudo foram analisadas as emissões descontroladas de material particulado (PM) e COVs, que ocorreu entre abril e maio de 2021 no CPC, com base nos dados da estação de qualidade do ar de Capuava (CETESB) e aplicando o modelo de pluma gaussiana – AERMOD (*steady-state plume model*), estimamos as concentrações de COV e PM_{10} . Finalmente, uma análise dos dados horários de benzeno e tolueno foi fornecida, para seis estações de qualidade do ar (Capuava, Paulínia, Cubatão, Pinheiros, São José dos Campos e São José-Vista Verde) inseridas no estado de São Paulo, de 2017 a 2022. Os resultados de amostragem (cartuchos *Tenax*) e análise (GC-FID) mostraram que no entorno do CPC, os compostos mais abundantes foram tolueno ($1,5 \pm 1,1$ ppbv), cis-2-hexeno ($1,4 \pm 1,9$ ppbv), benzeno ($0,55 \pm 0,66$ ppbv) e m+p-xileno ($0,58 \pm 0,3$ ppbv). As correlações e proporções entre BTEX mostraram a influência de fontes industriais, apesar das emissões veiculares terem sido as principais fontes desses compostos no entorno do CPC. A estimativa dos potenciais impactos associados às emissões de CPC para a formação de poluentes secundários mostrou que os compostos aromáticos representaram ~98 % e ~68% da formação total de SOA e O_3 , respectivamente. A estimativa do risco de câncer ao longo da vida devido ao benzeno foi seis vezes maior do que a recomendação da EPA e pode afetar negativamente a saúde da população nesta região. Quando comparamos o episódio de emissões descontroladas (abril-maio de 2021) em relação aos quatro anos anteriores mostrou-se um aumento nas concentrações médias por um fator de 2 para PM_{10} , benzeno e tolueno, atingindo valores máximos durante o episódio: $174 \mu g m^{-3}$

(PM₁₀), 22,8 ppb (benzeno) e 14,3 ppb (tolueno). Além disso, as simulações com o AERMOD demonstraram que a pluma de COV teve potencial para atingir grande parte dos municípios de Mauá e Santo André, podendo afetar a saúde de mais de 1 milhão de habitantes. Por fim, nas análises dos dados das estações da CETESB, para o período (2017-2022), o benzeno apresentou maiores concentrações médias anuais nas estações localizadas em áreas industrializadas (Capuava – 2017: 0,78 ppb; Cubatão – 2018: 0,70 ppb; Capuava – 2019: 0,78 ppb, 2020: 0,72 ppb, 2021: 1,15 ppb e 2022: 0,78 ppb). Entretanto, um perfil menos nítido foi observado para o tolueno, pois as maiores concentrações foram observadas para áreas industriais ou de tráfego urbano (Capuava – 2017: 1,3 ppb; Pinheiros – 2018: 1,7 ppb; 2019: 1,2 ppb; São José dos Campos – 2020: 1,7 ppb; Capuava – 2021: 1,4 ppb e Cubatão – 2022: 1,5 ppb). Além disso, os perfis diurnos de tolueno em áreas industriais não correspondem às emissões típicas do tráfego. A estimativa do risco de câncer devido à exposição ao benzeno variou de $1,0 \times 10^{-6}$ a $1,0 \times 10^{-5}$, chegando a ser dez vezes maior do que a recomendação da EPA. Essa observação fornece uma visão geral das concentrações para os demais complexos industriais do estado de São Paulo. Os resultados forneceram informações significativas sobre os efeitos das emissões atmosféricas do complexo petroquímico e industrial de Capuava na qualidade do ar, em uma área densamente urbanizada, analisando dados oficiais (CETESB), modelados (AERMOD) e resultados de amostragens (cartuchos *TENAX*) para uma área com alto potencial de contaminação do ar no Brasil.

Palavras-chave: BTEX, emissões industriais, potencial de formação de ozônio e SOA (OFP, SOAFP), risco de câncer, modelagem de dispersão atmosférica.

Abstract

Volatile organic compounds (VOCs) are fundamental in the atmospheric reactions, producing tropospheric ozone (O₃) and secondary organic aerosols (SOA). Among the VOCs, hydrocarbons (HCs) stand out, including the aromatics compounds (e.g., BTEX: benzene, toluene, ethylbenzene, m,p- and o-xylenes) being emitted directly into the atmosphere, in urban areas, by vehicle exhausts, fuel evaporation, solvent use, emissions of natural gas, and industrial processes. São Paulo is the Brazilian state with the largest territorial occupation and more than 47 million inhabitants, added to the greater economic development and the largest automotive fleet, causing degradation of air quality. At metropolitan area of São Paulo (MASP) the vehicle fleet of more than 7 million vehicles has been recognized as the main cause of air pollution events. But health problems and complaints from the population around an important industrial and petrochemical complex at MASP have also received special attention. In this context, the present study evaluated the HCs close to the Capuava Petrochemical Complex (CPC) in MASP, from 2016 to 2022. In the first step were analyzed data of different HCs based hourly sampling in two different sites during different days, 2016-2017. In the second part were analyzed severe uncontrolled emissions of particulate matter (PM) and VOCs (April-May 2021) from the CPC, based in Capuava air quality station (AQS, CETESB) data and applying the Gaussian plume model – AERMOD (steady-state plume model), estimating the concentrations of VOC and particulate matter (PM₁₀). Finally, an analysis of benzene and toluene hourly data was provided from six air quality stations (Capuava, Paulínia, Cubatão, Pinheiros, São José dos Campos e São José-Vista Verde) of São Paulo state, from 2017 to 2022. The results of sampling (Tenax tubes) and analysis (GC-FID) showed that in the surroundings of the CPC, the most abundant compounds were toluene (1.5 ± 1.1 ppb_v), cis-2-hexene (1.4 ± 1.9 ppb_v), benzene (0.55 ± 0.66 ppb_v) and m+p-xylene (0.58 ± 0.3 ppb_v). The correlations and ratios among BTEX showed the influence from industrial sources despite vehicular emissions have been the main sources of these compounds around CPC. The estimation of the potential impacts associated to CPC emissions for the formation of secondary pollutants showed that aromatic compounds represented ~98 % and ~68% of the total SOA and O₃ formation, respectively. The estimation of the lifetime cancer risk (LCR) due to benzene was six times higher than the EPA recommendation and could negatively affect the populations health in this region. The episode of uncontrolled emissions (April-May 2021) compared to the four previous years showed increase in the mean concentrations by a factor of 2 for PM₁₀, benzene, and toluene, reaching maximum values during the episode: 174 µg m⁻³ (PM₁₀), 22.8 ppb (benzene) and 14.3 ppb (toluene). AERMOD showed that the VOC plume had the potential to reach a large part of Mauá and Santo André municipalities, with the potential to affect the health of more than 1 million inhabitants. Finally, the CETESB AQS

analyses for the period (2017-2022), benzene shows higher annual mean concentrations at the sites located in industrialized areas (Capuava – 2017: 0.78 ppb; Cubatão – 2018: 0.70 ppb; Capuava – 2019: 0.78 ppb, 2020: 0.72 ppb, 2021: 1.15 ppb and 2022: 0.78 ppb), however, a less clear profile was observed for toluene, since the higher concentrations were observed for industrial or urban-traffic areas (Capuava – 2017: 1.3 ppb; Pinheiros – 2018: 1.7 ppb; 2019: 1.2 ppb; São José dos Campos – 2020: 1.7 ppb; Capuava – 2021: 1.4 ppb and Cubatão – 2022: 1.5 ppb). Additionally diurnal profiles of toluene at industrial areas do not corresponds to typical traffic emissions. The estimation of LCR due to benzene was ranged from 1.0×10^{-6} to 1.0×10^{-5} , reaching up ten times higher than the EPA recommendation. This observation provides an overview of the concentrations for the other industrial areas in São Paulo state. Results provided significantly important information on the effects of airborne emissions from the Capuava petrochemical and industrial complex on air quality in a densely urbanized area, analyzing data from an official AQS, modeled (AERMOD) and measurements results for an area with high potential of air contamination in Brazil.

Keywords: BTEX, industrial emissions, ozone and SOA formation potential (OFP, SOAFP), cancer risk, dispersion modeling.

LIST OF FIGURES

Figure 2.1. Sampling area localization: Great ABC Region (grey shaded area) in the southeast of the Metropolitan Area of São Paulo (MASP). Red stars represent the sampling points: Federal University of ABC (UFABC) and Bernaldo de Toledo Piza school (BTP) located at 4000 and 300m far from the Petrochemical and Industrial Complex (yellow highlighted area), respectively. Blue square denotes the air quality and meteorological site (Capuava Station, CETESB).....	24
Figure 2.2. Air sampling system: (a) vacuum pump; (b) adapter for fitting the tubes in duplicate and (c) flow meter.....	25
Figure 2.3. Standard gas mixture (Ozone precursor mix standard, Spectra Gases – Restek) chromatogram for (C ₆ -C ₁₂) eluted in the methyl silicone column. m,p-xylenes coeluted in this chromatographic system.	29
Figure 2.4. Chromatograms obtained from a duplicate sample collected in BTP on July 14, 2017 (13:35 - 14:35 local time).....	30
Figure 2.5. Chromatogram obtained from analysis of blank from samples.....	31
Figure 2.6. Average mixing ratios and standard deviation for the most abundant hydrocarbons at the BTP (left) and UFABC (right) sampling sites, for periods ranging from 8:00 a.m. to 6:00 p.m. during 2016-2017.....	35
Figure 2.7. Monthly meteorological and pollutants variability for the period under study (July 2016 to July 2017) for: a) wind speed (m s ⁻¹) and direction (°) (Capuava Station, CETESB, 2020); b) monthly accumulated precipitation (mm) and mean temperature (°C) (IAG/ USP Meteorological Station); c) monthly boxplots of air pollutant concentrations for PM ₁₀ , O ₃ and SO ₂ (µg m ⁻³) (Capuava Station, CETESB, 2020). In boxplot width, the lower and upper hinges correspond to the first and third quartiles (the 25th and 75th percentiles). Lower whisker = smallest observation greater than or equal to lower hinge - 1.5 * IQR. Upper whisker = largest observation less than or equal to upper hinge + 1.5 * IQR. Middle is median, 50% quantile and the point is mean value. The circles point represents the arithmetic mean. Data beyond the end of the whiskers are called "outlying" points.	40
Figure 2.8. Average diurnal profiles of the most abundant hydrocarbons (A) and relative mass contribution for thirty-five hydrocarbons (B) grouped by alkanes (17), alkenes (2) and aromatics (16) at the BTP and UFABC sampling sites, during 2016-2017.....	44
Figure 2.9. Hourly average mixing ratios of benzene and toluene obtained in the present study and those from CETESB Air Quality Monitoring Stations in São Paulo State, in 2017 (CETESB, 2018). ¹ SJC and ² SJC refers to São José dos Campos (Vista Verde) Station and São José dos Campos Station, respectively. *Sampling sites of Present study (UFABC and BTP).....	46
Figure 2.10. Comparison of relative BTEX mass contributions (%) observed in industrial and urban areas: Rio de Janeiro, Brazil (Silva et al., 2017), Dunquerque, France (Roukos et al., 2009), Lanzhou, China (Jia et al., 2016), Texas, United States (Leuchner and Rappenglück, 2010), Ulsan, Korea (Kim et al., 2019), Windsor, Canada (Miller et al., 2011), Yokohama, Japan (Tiwari et al., 2010). *Present study represents the averaged concentrations for both sampling sites. ‡Rio de Janeiro, Brazil represents the averaged concentrations for two sampling sites (Air Basins I and III) that represents industrialized urban areas.....	48
Figure 2.11. Scatter plots and respective linear regression for BTEX at the two sampling sites, BTP (red) and UFABC (blue). Cor is the correlation coefficient (Pearson) and the curves represent the mixing ratios distribution at both sites (in ppb).....	51

Figure 2.12. (a) Ozone Formation Potential (OFP) and (b) Secondary Organic Aerosol Formation Potential (SOAFP) estimation for most abundant compounds, at BTP (red) and UFABC (blue) sampling sites.....	53
Figure 3.1. Metropolitan area of São Paulo (MASP) with Braskem and RECAP industries, and the CETESB, Capuava Air Quality Station, and AQS (identified by the red triangles). Source: OpenStreetMap.....	60
Figure 3.2. Braskem and RECAP industrial plants on tridimensional modeling. In blue are the buildings or tanks, in red are the point sources (stacks/flare). Source: Google Earth (accessed on 11 March 2023)	68
Figure 3.3. Annual boxplots of 1 h concentrations ($\mu\text{g m}^{-3}$) for PM10, benzene, and toluene at Capuava AQS, from 2017 to 2022, and for each episode. Boxplot width and the lower and upper hinges correspond to the first and third quartiles (the 25th and 75th percentiles). Lower whisker: smallest observation greater than or equal to lower hinge - 1.5 * IQR (interquartile range), above 75th percentile. Upper whisker: largest observation less than or equal to upper hinge + 1.5 * IQR, below 25th percentile. The middle is the median (50% quantile), and the red point is the mean value. Points beyond the end of the whiskers are “outliers”, which correspond to values > 1.5 and < 3 times the standard deviation (sd). The data were presented on the Y axis with an appropriate scale for good visualization of the percentiles and the mean in relation to the median. Obs.: The episode corresponds to April–May of 2021, 2021 corresponds to the other months of this year, the data available for 2020 were only from January to March, and 2022 was only from January to June.	71
Figure 3.4. Normalized concentrations in relation to the mean value profiles for PM10, benzene, and toluene at Capuava AQS, from April to May for each year from 2017 to 2022. Episode represents the 2021 concentrations.....	72
Figure 3.5. Changes in benzene, toluene and PM ₁₀ mean hourly concentrations at Capuava station, depending on wind directions. a) Polar annulus plots from 2017 – 2020 and b) Polar annulus plots for episode from April to May 2021. Color scale represents concentrations ($\mu\text{g m}^{-3}$), the thickness in the circle represents the hour of the day: 00:00 inside to 11:00 p.m. outside. Blank spaces are missing values.	75
Figure 3.6. Hourly concentrations of PM10 at Capuava AQS, during the episode (April to May 2021). Rectangles represent the peaks observed from 1:00 a.m. to 4:00 a.m.....	77
Figure 3.7. (a) Hourly mean concentrations for benzene, toluene, and PM10 at Capuava AQS, VOC, and PM (AERMOD: modeled data) during the episode (April to May 2021), white spaces are missing values. (b) The wind rose shows the wind speed (m s^{-1}) and wind direction ($^{\circ}$), data were filtered by the preferential wind direction from the Capuava Petrochemical Complex (0° to 180°) (c) “Correlation” is the correlation coefficient of Pearson.....	78
Figure 3.8. The maximum concentration of 1 h average ($\mu\text{g m}^{-3}$) of VOC in the affected area during the CPC maintenance period.	80
Figure 3.9. The maximum concentration of 24 h average ($\mu\text{g m}^{-3}$) of PM in the affected area during the CPC maintenance period.	82
Figure 4.1. Part of São Paulo State with the demarcations of CETESB Air Quality Station (AQS) (identified by the red pins) and the respective municipality of each station (with pins). Source: Google Earth.....	88

Figure 4.2. Cubatão (CB) Air Quality Station (AQS) (red pin) and the respective distance of industrial area (~1 km) of Presidente Bernardes Refinery (RPBC) (with arrow). Source: Google Earth.	89
Figure 4.3. Changes in benzene and toluene mean hourly concentrations at Cubatão station, depending on wind directions. Polar annulus plots from 2017 – 2022. Color scale represents concentrations ($\mu\text{g m}^{-3}$), the thickness in the circle represents the hour of the day: 00:00 inside to 11:00 p.m. outside. Blank spaces are missing values.	90
Figure 4.4. Capuava (CP) Air Quality Station (AQS) (red pin) and the respective distance of industrial area (~0.5 km) of Capuava Refinery (RPBC) (with arrow). Source: Google Earth.	91
Figure 4.5. Changes in benzene and toluene mean hourly concentrations at Capuava station, depending on wind directions. Polar annulus plots from 2017 – 2022. Color scale represents concentrations ($\mu\text{g m}^{-3}$), the thickness in the circle represents the hour of the day: 00:00 inside to 11:00 p.m. outside. Blank spaces are missing values.	92
Figure 4.6. Paulínia (PL) Air Quality Station (AQS) (red pin) and the respective distance of industrial area (~2 km) of Planalto Paulista Refinery (REPLAN) (with arrow). Source: Google Earth.	93
Figure 4.7. Changes in benzene and toluene mean hourly concentrations at Paulínia station, depending on wind directions. Polar annulus plots from 2017 – 2022 (insufficient number of measurements for 2020). Color scale represents concentrations ($\mu\text{g m}^{-3}$), the thickness in the circle represents the hour of the day: 00:00 inside to 11:00 p.m. outside. Blank spaces are missing values.	94
Figure 4.8. Pinheiros (PN) Air Quality Station (AQS) (red pin) and the respective distance of Marginal Pinheiros (~0.2 km) (with arrow). Source: Google Earth.	95
Figure 4.9. Changes in benzene and toluene mean hourly concentrations at Pinheiros station, depending on wind directions. Polar annulus plots from 2017 – 2021 (there is no valid data for 2022). Color scale represents concentrations ($\mu\text{g m}^{-3}$), the thickness in the circle represents the hour of the day: 00:00 inside to 11:00 p.m. outside. Blank spaces are missing values.	96
Figure 4.10. São José dos Campos (SJC) and São José dos Campos – Vista Verde (SJC-VV) Air Quality Stations (AQS) (red pins) and the respective distance of industrial area of Henrique Lage Oil Refinery (REVAP) (with arrow). Source: Google Earth.	97
Figure 4.11. Changes in benzene and toluene mean hourly concentrations at São José dos Campos station, depending on wind directions. Polar annulus plots from 2017 – 2022. Color scale represents concentrations ($\mu\text{g m}^{-3}$), the thickness in the circle represents the hour of the day: 00:00 inside to 11:00 p.m. outside. Blank spaces are missing values.	98
Figure 4.12. Changes in benzene and toluene mean hourly concentrations at São José dos Campos – Vista Verde station, depending on wind directions. Polar annulus plots from 2017 – 2022. Color scale represents concentrations ($\mu\text{g m}^{-3}$), the thickness in the circle represents the hour of the day: 00:00 inside to 11:00 p.m. outside. Blank spaces are missing values.	99
Figure 4.13. Annual boxplots of 1 h concentrations ($\mu\text{g m}^{-3}$) for benzene, and toluene at CETESB AQS, from 2017 to 2022, were CB: Cubatão, CP: Capuava, PL: Paulínia, PN: Pinheiros, SJC: São José dos Campos and SJC_VV: São José dos Campos – Vista Verde. Boxplot width and the lower and upper hinges correspond to the first and third quartiles (the 25th and 75th percentiles). Lower whisker: smallest observation greater than or equal to lower hinge - 1.5 * IQR (interquartile range), above 75th percentile. Upper whisker: largest observation less than or equal to upper	

hinge + 1.5 * IQR, below 25th percentile. The middle is the median (50% quantile), and the red point is the mean value. Points beyond the end of the whiskers are “outliers”, which correspond to values > 1.5 and < 3 times the standard deviation (sd). The data were presented on the Y axis with an appropriate scale for good visualization of the percentiles and the mean in relation to the median. 104

Figure 4.14. Seasonal trends for benzene and toluene at CETESB AQS, from 2017 to 2022, were CB: Cubatão, CP: Capuava, PL: Paulínia, PN: Pinheiros, SJC: São José dos Campos and SJC_VV: São José dos Campos – Vista Verde. Points corresponds to the monthly mean concentrations. Autumn: March, April and May; Winter: June, July and August; Spring: September, October and November; Summer: December, January and February. 106

Figure 4.15. Average profiles for benzene, and toluene at CETESB AQS, from 2017 to 2022, were CB: Cubatão, CP: Capuava, PL: Paulínia, PN: Pinheiros, SJC: São José dos Campos and SJC_VV: São José dos Campos – Vista Verde. 107

Figure 4.16. Scatter plots and respective linear regression for benzene and toluene at CETESB AQS, from 2017 to 2022, were CB: Cubatão, CP: Capuava, PL: Paulínia, PN: Pinheiros, SJC: São José dos Campos and SJC_VV: São José dos Campos – Vista Verde. The correlation coefficient (Pearson) is presented in different colors, that corresponds with each station, and the curves represent the concentration distribution at sites (in $\mu\text{g m}^{-3}$). 110

Figure 4.17. Ozone Formation Potential (OFP) and Secondary Organic Aerosol Formation Potential (SOAFP) estimation for benzene and toluene at CETESB AQS, from 2017 to 2022, were CB: Cubatão, CP: Capuava, PL: Paulínia, PN: Pinheiros, SJC: São José dos Campos and SJC_VV: São José dos Campos – Vista Verde. 112

LIST OF TABLES

Table 2.1. Chromatographic analytical conditions for hydrocarbons analyses.....	26
Table 2.2. Recovery values for each hydrocarbon on TENAX absorption test.....	28
Table 2.3. Values of constant rate of reaction with respect to the hydroxyl radical (k_{OH}), Maximum Incremental Reactivity (MIR), Secondary Organic Aerosol Potentials (SOAP), Fractional Aerosol Coefficient (FAC) and Detection and Quantification limits (DL, QL) for some hydrocarbons sampled of the petrochemical and industrial complex in Metropolitan Area of São Paulo.	33
Table 2.4. Summary of statistical analysis for C6-C11 NMHCs hourly mixing ratios (ppb _v) in the Metropolitan Area of São Paulo (MASP), for each sampling sites University Federal of ABC (UFABC) and Beneraldo de Toledo Piza school (BTP) for periods ranging from 8:00 a.m. to 6:00 p.m. during 2016-2017.....	37
Table 2.5. Comparison of ratios (B/T and X/B) observed indifferent countries and areas (industrial and urban).	49
Table 2.6. Calculated values of exposure concentration (EC), lifetime cancer risk (LCR), hazard quotient (HQ) and hazard index (HI) for the sampling sites of the present study. Inhalation exposure reference (RFC) and inhalation risk (IR) were obtained from U.S. EPA (IRIS) for each compound.....	55
Table 3.1. Summary of AERMOD input data extracted from Environmental Licenses of Braskem and RECAP.....	66
Table 3.2. Summary of statistical analysis of AERMET input data.....	70
Table 3.3. Summary of statistical analysis for hourly concentrations ($\mu\text{g m}^{-3}$) in the Capuava AQS, during 2017-2022 and modeled data provided by AERMOD.....	70
Table 4.1. Summary of statistical analysis for hourly concentrations ($\mu\text{g m}^{-3}$), for all sites, during 2017-2022. Years in bold represent data without annual representation.....	100
Table 4.2. Comparison of B/T ratios observed in different AQS, for each year of monitoring (2017-2022). Ratios ≥ 0.5 are bolded.	109
Table 4.3. Calculated values of exposure concentration (EC), lifetime cancer risk (LCR), hazard quotient (HQ) and hazard index (HI) for CETESB AQS, from 2017 to 2022, were CB: Cubatão, CP: Capuava, PL: Paulínia, PN: Pinheiros, SJC: São José dos Campos and SJC_VV: São José dos Campos – Vista Verde. Inhalation exposure reference (RFC) and inhalation risk (IR) were obtained from U.S. EPA (IRIS) for each compound.....	114

Chapter 1. Introduction

In the southeast region of Metropolitan Area of São Paulo (MASP) there are seven important municipalities, known as the ABC region, with more than 2.8 million inhabitants; this is where Capuava Petrochemical Complex (CPC), the most important industrial complex of MASP, is located. In addition, in the São Paulo state, there is other three petrochemical complexes: Planalto Paulista Refinery (Paulínia), Henrique Lage Refinery (São José dos Campos) and Presidente Bernardes Refinery (Cubatão). In the vicinity of these industrial areas, the Environmental Agency of São Paulo State (CETESB) conducted the air quality monitoring.

The complex in focus at the present study is the CPC stands out among the industrial emissions, as it is the only included in the MASP, contributing to the deterioration of air quality in a region highly impacted by traffic emissions (Coelho et al., 2021; Evo et al., 2011; Saiki et al., 2007). The CPC is composed of the Capuava Oil Refinery (RECAP), and other industries, in a range of ~ 8.5 km² inside a densely populated (~ 3400 inhabitants/km²) urban area.

The purpose of the present study is to improve the understanding about reactive hydrocarbons (HCs) (C₆-C₁₁) emitted by industrial sources in the atmosphere of the MASP. In this general perspective, the study includes specific work steps:

- I. Air Samples – Hourly sampling and analyze of the measurements (Gas Chromatograph – GC/FID); Chapter 2.
- II. Analyzed uncontrolled emissions from petrochemical complex – Air Quality station data and applying the Gaussian plume model (AERMOD); Chapter 3.
- III. Data overview of official air quality stations, that monitoring benzene and toluene at industrial areas of the São Paulo state, on last six years; Chapter 4.

The combination of these steps generated topics of special importance for the study of the subject in the region, as described above:


- Understand the role of HCs from industrial emissions;
- Understand the impact of industrial emissions for an impacted area like the MASP;
- Provided information about emissions sources;
- Characterize diurnal, seasonal and multi-year trends for HCs;
- Understand the role of secondary pollutants, with HCs as precursors;
- Provided information about human health impacts;
- Understand the range and proportion of uncontrolled industrial emissions and their impact on air quality at MASP.

Chapter 2. Non-methane hydrocarbons in the vicinity of a petrochemical complex in the Metropolitan Area of São Paulo, Brazil.

Air Quality, Atmosphere & Health
<https://doi.org/10.1007/s11869-021-00992-1>

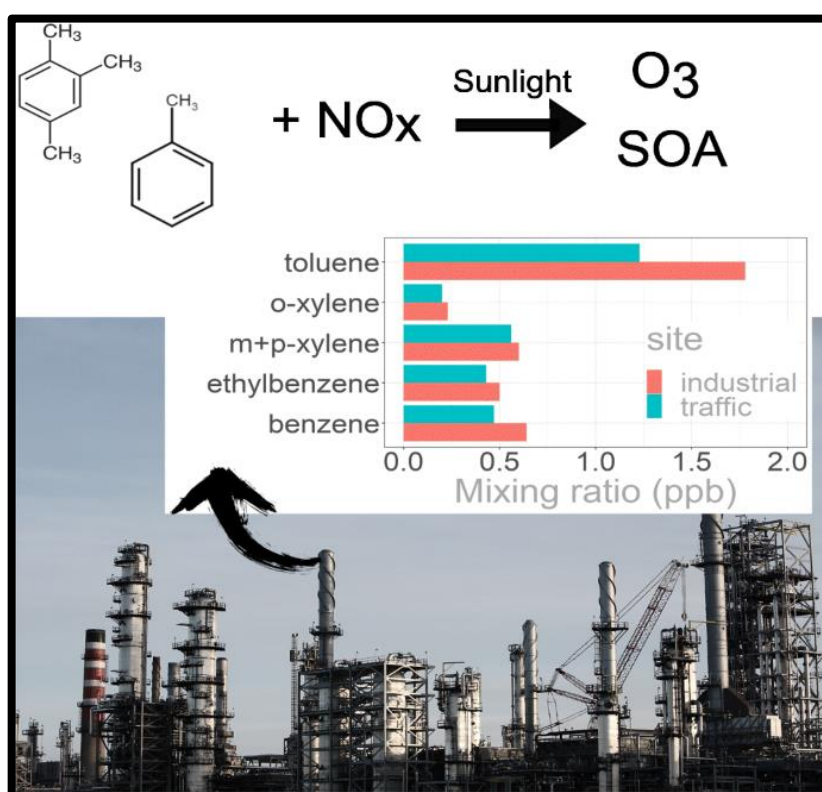


Non-methane hydrocarbons in the vicinity of a petrochemical complex in the Metropolitan Area of São Paulo, Brazil

Monique Silva Coelho^{1,2} · Pamela A. Dominutti^{1,3,4}  · Cláudia Boian² · Tailine Corrêa dos Santos¹ · Thiago Nogueira¹ · Cristina A. Vilas Boas de Sales Oliveira¹ · Adalgiza Fornaro¹

Received: 17 September 2020 / Accepted: 2 February 2021
© The Author(s), under exclusive licence to Springer Nature B.V. part of Springer Nature 2021

GRAPHICAL ABSTRACT



2.1. Introduction

Volatile organic compounds (VOCs) are among the most important gaseous pollutants in the atmosphere, including not only a wide range of non-methane hydrocarbons (HCs) but also aldehydes, ketones, alcohols, ethers among other compounds (Jacobson, 2002). Each of these species has its own intrinsic chemical characteristics, affecting its atmospheric reactivity and in consequence their lifetime in the atmosphere (Monks et al., 2009). Except for methane, VOCs are found in the troposphere at mixing ratios ranging from few parts per trillion (pptv) to a few ten parts per billion (ppbv) (Kansal, 2009). In spite of presenting low concentrations in the atmosphere, some of VOCs can exert a detrimental effect on human health, affecting the respiratory system and, in some cases, provoking depressing central nervous system or acting as carcinogenic (NTP, 2016). VOCs can be emitted directly into the atmosphere by a wide range of anthropogenic and natural sources. However, in urban areas, they are mainly released by anthropogenic sources, such as vehicle exhausts, fuel evaporation, solvent use, emissions of natural gas and industrial processes (Friedrich and Obermeier, 1999). In urban atmospheres, BTEX (benzene, toluene, ethylbenzene, m+p- and o-xylenes) represent a significant fraction of VOCs, reaching up to 50% in volume of total VOCs (Lee et al., 2002). Crude oil consists of 94% in weight of HCs, being 30% alkanes, 49% cycloalkanes and 15% aromatics (Simpson et al., 2010). In addition, fossil fuels or solvents containing aromatic compounds with less than 15 carbons, can easily evaporate into the air due to their high vapor pressures and low boiling points (Rajabi et al., 2020). However, the relative importance of different VOCs emission sources in urban areas remains under discussion, as it varies according to each region (Yuan et al., 2013; Salameh et al., 2015; Andrade et al., 2017; Ly et al., 2020). In the last years, several studies have applied source apportionment models in order to assign emission sources to VOCs observations obtained during field campaigns, (Salameh et al., 2015; Debevec et al., 2017; Weber et al., 2018; Thera et al., 2019). For instance, the source apportionment in the megacity of Seoul showed that traffic and

industrial emissions contributed, on average, to 40 and 25%, respectively for total VOCs concentrations (Song et al., 2019). Traffic emissions from combustion and gasoline contributed from 51 to 74% in winter and summer, respectively at sub-urban site in Beirut (Salameh et al., 2015). However, Istanbul had a different emission pattern, where traffic was not the main contributor of VOCs (15.8%), but a regional mixed source with contribution from biogenic and anthropogenic emissions (36.3%) (Thera et al., 2019).

Once released into the atmosphere, primary VOCs undergo chemical transformations due mainly to the presence of the OH radical during the day. VOCs have a fundamental role in the oxidizing capacity of the atmosphere due to the production of secondary pollutants, such as oxygenated compounds (organic acids, aldehydes, ketones), secondary organic aerosols (SOA) and tropospheric ozone (O_3) (Carter, 1994; Kroll; Seinfeld, 2008). In urban areas, O_3 is formed from the photochemical reactions among its precursors: nitrogen oxides ($NO_x = NO + NO_2$) and VOCs. In the last years, several photochemical models have been used to evaluate tropospheric O_3 by developing ozone formation potential (OFP) metrics (Bloss et al., 2005; Zheng et al., 2009; Cheng et al., 2010; Carter, 2010; Derwent et al., 2010; Jenkin et al., 2017). These metrics provide a specific scale for each VOCs species (related to the compound's reactivity) allowing to estimate the impact of VOCs emissions on O_3 formation, such as the Maximum Incremental Reactivity scale (MIR). MIR values were derived from chamber experiments, representing the change in mass of O_3 caused by addition of the one-unit mass of a specific VOCs (Carter, 2010). In addition to the ozone formation, the oxidation of VOCs gives rise to organic compounds with enough low vapor pressures to partition to the condensed particulate phase favoring SOA formation. On a global scale, it is estimated that aromatics such as toluene and xylenes contribute between 1.4 and 8.6 TgC.year⁻¹ to SOA formation (Zhang et al., 2017). The secondary organic aerosol potential (SOAP) estimates the SOA yield reflecting the propensity of each organic compound to form SOA, expressed in relation to toluene

(Derwent et al., 2010; Wu et al., 2017). The estimations obtained from these models and metrics have been successfully applied to communicate and develop public policy initiatives resulting in VOCs emission control strategies. In the last years, reductions in the VOCs and secondary pollutants concentrations have been observed in urban areas such as Los Angeles, London and Paris (Warneke et al., 2012; Waked et al., 2016). Similarly, previous studies developed in São Paulo (Brazil) showed that HCs concentrations, decreased from 2003 to 2013 by a factor of 2.3 in urban areas and 4.0 in suburban areas (Dominutti et al., 2016). Despite this decrease over the last years, and the implementation of vehicle emission control programs, O₃ and particles (PM₁₀ and PM_{2.5}) consistently exceeds the standard air quality in the Metropolitan Area of São Paulo (MASP) (CETESB, 2019).

The MASP with more than 22 million inhabitants encompasses ~12% of the total population in Brazil. It covers an area of 8000 km² and a densely urbanized area of ~2000 km², including 38 cities and the state Capital, São Paulo (IBGE, 2017). This area includes Great ABC region, widely known because of the great number of companies, including car manufacturers, petrochemical and industrial companies. The air quality in this area has been degraded over the last years, being O₃ and particulate matter (PM) the main air pollution concerns (CETESB, 2019). Average O₃ concentrations show the highest values during the spring and summer, from September to March (Carvalho et al., 2015). The contribution of aromatics to O₃ formation in the MASP is quite significant in winter (dry season in the MASP), when the incidence of radiation is lower and the presence of atmospheric aerosols increases (Orlando et al., 2010). During the winter, the meteorological conditions also provide a stable atmosphere and hinder dispersion processes. However, during the other seasons, alkenes > aldehydes > aromatics are the potential O₃ precursors (Alvim et al., 2011; Dominutti et al., 2016). These studies have shown that the presence of the HCs in the MASP atmosphere can significantly contribute to air quality degradation.

A few studies about biomonitoring, population health and VOCs in the atmosphere were carried out in the Great ABC region in the MASP (Saiki et al., 2007; Evo et al., 2011; Pereira et al., 2019; Zaccarelli-Marino, 2012; Zaccarelli-Marino et al., 2016). The biomonitoring of air pollution in the vicinity of the Petrochemical and Industrial Complex (PIC) evidenced the highest concentration of pollutants when compared to the areas of Santo André (part of Great ABC region) that were not under the influence of industries (Saiki et al., 2007). Furthermore, a considerable increase in the incidence of chronic autoimmune thyroiditis in residents in the vicinity of the PIC was observed, indicating atmospheric pollutants in that area may be a major risk factor for primary hypothyroidism in adults and children (Zaccarelli-Marino, 2012; Zaccarelli-Marino et al., 2016). Likewise, petrochemical biomarkers as hopanoids were observed in tree bark samples collected (Pereira et al., 2019). For the PIC area, the alkanes concentrations from refinery processes ($C_{15} - C_{26}$) were higher than those emitted by biogenic sources (Caumo et al., 2018). The presence of HCs in the atmosphere of the Great ABC region was quantified for the first time in 2013 by Boian et al. (2015).

Despite the few studies developed in the PIC area and the evidence of the health effects related to the industrial emissions, little is known about the gas-phase VOCs and their contribution to the local atmospheric composition and their effects on the formation of secondary pollutants.

In this paper, we provide a detailed analysis of the mixing ratios of 35 hydrocarbons measured in the PIC area for the first time. HCs species include alkanes (C_6-C_{11}), aromatics (C_6-C_{10}) and alkenes (cis/trans-2-hexene). Our measurements include extensive campaigns developed in two distinct sampling points over seven months. Here, we analyze the HCs daily profiles, exploring the correlation between species for emission sources evaluation. Furthermore, a spatial analysis of BTEX is provided, comparing the contribution of the MASP with other industrial areas worldwide. The potential impacts that these compounds could have in the formation

of secondary pollutants (O_3 and SOA) are also tackled, proposing a base for further understand the contribution from industrial emissions in megacities air quality. Finally, the potential cancer risk was calculated in order to estimate the effects on the health of population living around the PIC.

2.2. Materials and methods

2.2.1. Study area and sampling strategy

The Great ABC Region is located in the southeast of MASP, and characterized by industrial activities, starting with the opening of an oil refinery in 1954 and followed by the expansion of the petrochemical and industrial complex in 1972 (COFIP ABC, 2019). Over the years, beyond the industries installed, the population also increased and currently around 200 thousand inhabitants live nearby (IBGE, 2017).

The PIC is composed of the Capuava Oil Refinery and 14 other industries, in a range of ~ 8.5 km² in a densely populated urban area. This complex produces ethylene, propylene and polyethylene from the distillation of naphtha, as well as fertilizers and various intermediates with the capacity to process about 53,000 barrels of oil per day (COFIP ABC, 2019; Petrobras, 2020). The products of the petrochemical supply the industries in Great ABC region and MASP, the largest consumer market in South America, with great economic importance in Brazil. In addition, the petrochemical is responsible for the commercialization of $\sim 30\%$ of the total fuel volume consumed in MASP (Petrobras, 2020). Thus, the region is a strategic area for the development of atmospheric pollution measurements, due to its high degree of industrialization and urbanization.

Our measurements were developed at two different sampling sites (Figure 2.1). The first located nearby the Avenida dos Estados (Federal University of ABC, UFABC), an important traffic avenue connecting the cities of the Great ABC region (Santo André, São Bernardo, São Caetano do Sul and Mauá) to other in the MASP. The second

site is located near the PIC (~0.2 km), highly impacted by the industrial emissions (Beneraldo de Toledo Piza school - BTP) (Figure 2.1).

Air samples were hourly collected in periods ranging from 8:00 a.m. to 6:00 p.m. The total of 90 samples were regularly collected over a year on the following dates: 7/5/2016; 8/19/2016; 11/16/2016; 11/23/2016; 11/28/2016; 12/9/2016; 3/28/2017; 5/3/2017; 7/14/2017; 7/17/2017.

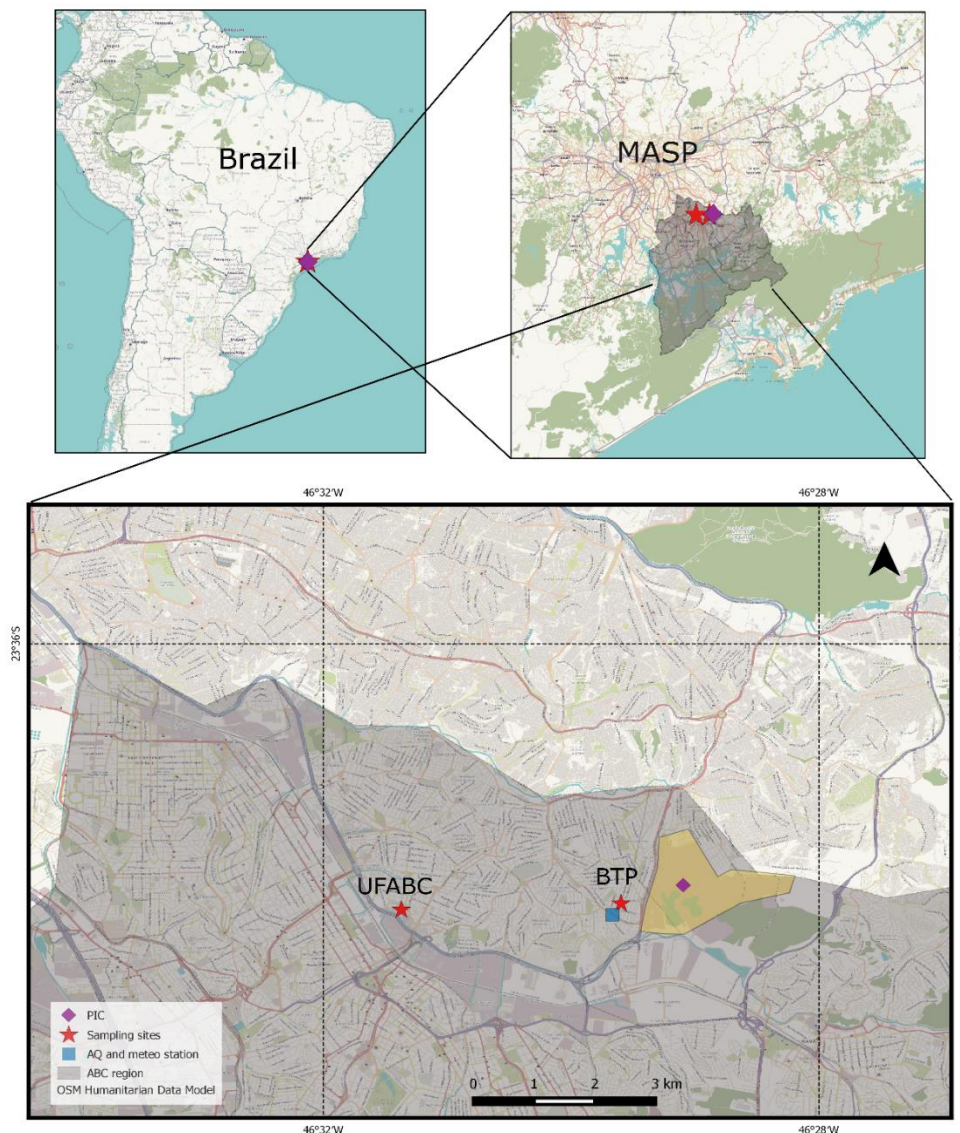


Figure 2.1. Sampling area localization: Great ABC Region (grey shaded area) in the southeast of the Metropolitan Area of São Paulo (MASP). Red stars represent the sampling points: Federal University of ABC (UFABC) and Beneraldo de Toledo Piza school (BTP) located at 4000 and 300m far from the Petrochemical and Industrial Complex (yellow highlighted area), respectively. Blue square denotes the air quality and meteorological site (Capuava Station, CETESB).

Air sampling was performed by TENAX TA® tubes, a polymer resin specifically designed for the retention of volatile and semi-volatile compounds in the atmosphere (PerkinElmer, 2020). This sorbent material was selected due to its affinity to sampling organic compounds with more than 6 carbons and its hydrophobic characteristics (Ras et al., 2009). For that, the air was sampled in duplicates for 1 hour using a vacuum pump with a constant flow (Figure 2.2). To determine the optimum constant flow rate during the air samples, the breakthrough Volume (BV) test was performed. BV is the volume of a sample retained in the backup tube (EPA, 1999), in which values of $\geq 5\%$ of any analyte were observed, being BV confirmed (EPA, 1999). The optimum flow rate for sampling was 50 mL min^{-1} , with volumes may vary depending (1 to 4 liters) on the time of exposure of the tube (EPA, 1999). The experiment was conducted with different sample volumes (adjusted flow rates: 55 mL min^{-1} , 35 mL min^{-1} and 30 mL min^{-1} for 60 minutes). Results showed that among the three different flow rates tested, the 55 mL min^{-1} (3.3 liters of volume) was the one that presented the best results for these compounds ($\text{C}_6\text{-C}_{11}$), with the lowest BV observed (Coelho et al., 2019).

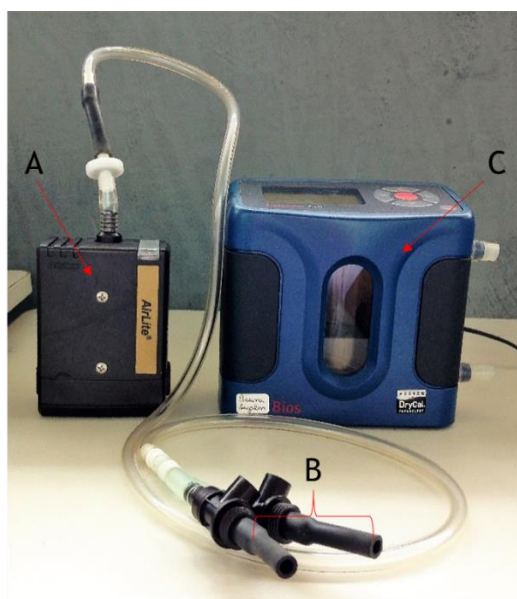


Figure 2.2. Air sampling system: (a) vacuum pump; (b) adapter for fitting the tubes in duplicate and (c) flow meter.

In addition, an analysis of air pollutants and meteorological parameters was performed. For that, we, used the data from Capuava station of CETESB air quality network (Environmental Agency of the State of São Paulo), which is located near BTP sampling point (~ 0.45 km). Data of pollutants (NO_x, CO, PM₁₀, O₃ and SO₂) and wind (speed and direction) are measured hourly and available online (<https://cetesb.sp.gov.br/ar/qualar/>). Precipitation and temperature data are also analyzed which was obtained from IAG/ USP meteorological station (<http://www.estacao.iag.usp.br/index.php>).

2.2.2. HCs identification

The sorbent tubes collected during field campaigns were later analyzed at the laboratory by a gas chromatograph with flame ionization detectors, GC-FID (Ozone Precursor Analyzer System, Clarus500®), coupled to a thermal desorption module (Turbo Matrix 650 ATD). More details about the chromatographic system and analytical conditions can be found in table 2.1.

Table 2.1. Chromatographic analytical conditions for hydrocarbons analyses.

Thermal Desorption (TD)	
Equipment	Turbo Matrix
Trap	Cooling (-30°C)/ Heating (225°C)
Transfer line	200 °C
Split (inlet)	20 mL/min
Split (outlet)	20 mL/min
Time	10 minutes
Gas Chromatography	
Equipment	Ozone Precursor Analyzer System, Clarus500
Column	Ozone Precursor Column Set: 50 m x 0.22 mm x 1 µm dimethyl siloxane column and 50 m x 0.32 mm x 5 µm alumina/ Na ₂ SO ₄ PLOT column
Temperature	45 °C for 15 min, up 5 °C/ min to 170 °C, increasing 15 °C/ min to 200 °C for the last 6 minutes of running
Time	48 minutes
Detectors	Dual Flame Ionization Detectors at 250 °C
Carrier gas	He (45 mL/min)

For the identification and quantification of thirty-five HCs, a diluted standard gas mixture (C₆-C₁₁) (Ozone precursors mix standard® – Restek) at a concentration of 100 ppb was used, (chromatogram examples presented in figures 2.3 and 2.4). The standard gas is sampled in a TENAX TA tube for further GC analysis (following the same analytical conditions as the samples). When this standard was analyzed, the peaks registered in the chromatogram were related to each species of HCs that was identified by means of its retention time (RT) (Dominutti et al., 2016). The HCs were quantified by means of analytical curves with five dilution levels: 4 ppb, 5 ppb, 13 ppb, 19 ppb and 23 ppb and each dilution level was injected three times to evaluate the coefficient of variation, resulting in values up to 20%. The limits of detection (LOD) and quantification (LOQ) was calculated for each HC from the analytical curves (Table 2.3). Blanks of sorbent tubes were obtained for each sampling day at both sampling points. They were analysed together with the sampled tubes. In general, good results were obtained and in case of impurities observed, they were subtracted to the sampled tubes. A chromatogram of a blank tube is presented in the Figure 2.5.

2.2.2.1. Recovery test

The recovery (or recovery factor, R) is the ratio of analyte amount, existent or added in the test material which could be removed and subject to analysis and quantification. This test was performed with the purpose to know the efficiency of TENAX cartridges to absorb the analytes to be later desorbed and analysed by GC-FID. The recovery of most compounds was higher than 90% (Table 2.2), more details can be found in (Dominutti, 2016).

Table 2.2. Recovery values for each hydrocarbon on TENAX absorption test

Compound	Recovery (%)	Compound	Recovery (%)
<i>alkenes</i>		<i>alkanes</i>	
trans-2-hexene	100	n-hexane	90.96
cis-2-hexene	99.88	Methyl cyclopentane	98.89
<i>aromatics</i>		cyclohexane	90.14
benzene	99.69	2-methylhexane	100
toluene	99.71	3-methylhexane	100
ethylbenzene	99.82	2,2,4-trimethylpentane	70.44
p-xylene	99.58	n-heptane	100
m-xylene	100	methylcyclohexane	99.51
styrene	99.83	2,3,4-trimethylpentane	98.96
o-xylene	99.82	2-methylheptane	99.96
cumene	99.81	3-methylheptane	99.94
n-propylbenzene	99.8	n-octane	99.91
m-ethyltoluene	99.74	n-nonane	99.93
p-Ethyltoluene	99.84	n-Decane	99.93
1,3,5-trimethylbenzene	99.92	n-Undecane	99.73
o-Ethyltoluene	99.8		
1,2,4-trimethylbenzene	99.85		
1,2,3-trimethylbenzene	99.88		
m-Diethyl benzene	99.9		
p-Diethyl benzene	99.9		

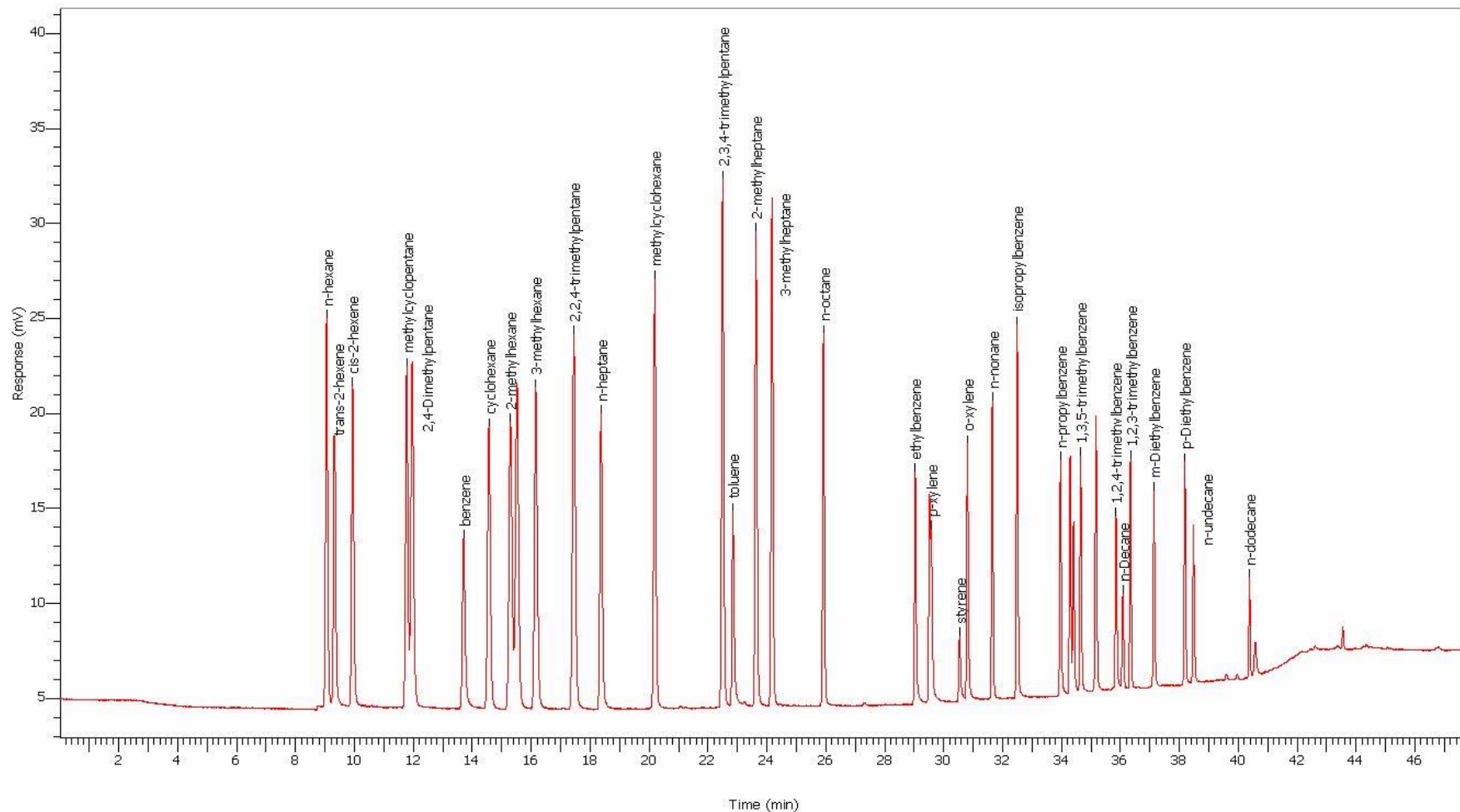


Figure 2.3. Standard gas mixture (Ozone precursor mix standard, Spectra Gases – Restek, concentration in average: 100 ppb) chromatogram for (C₆-C₁₂) eluted in the methyl silicone column. m,p-xylenes coeluted in this chromatographic system.

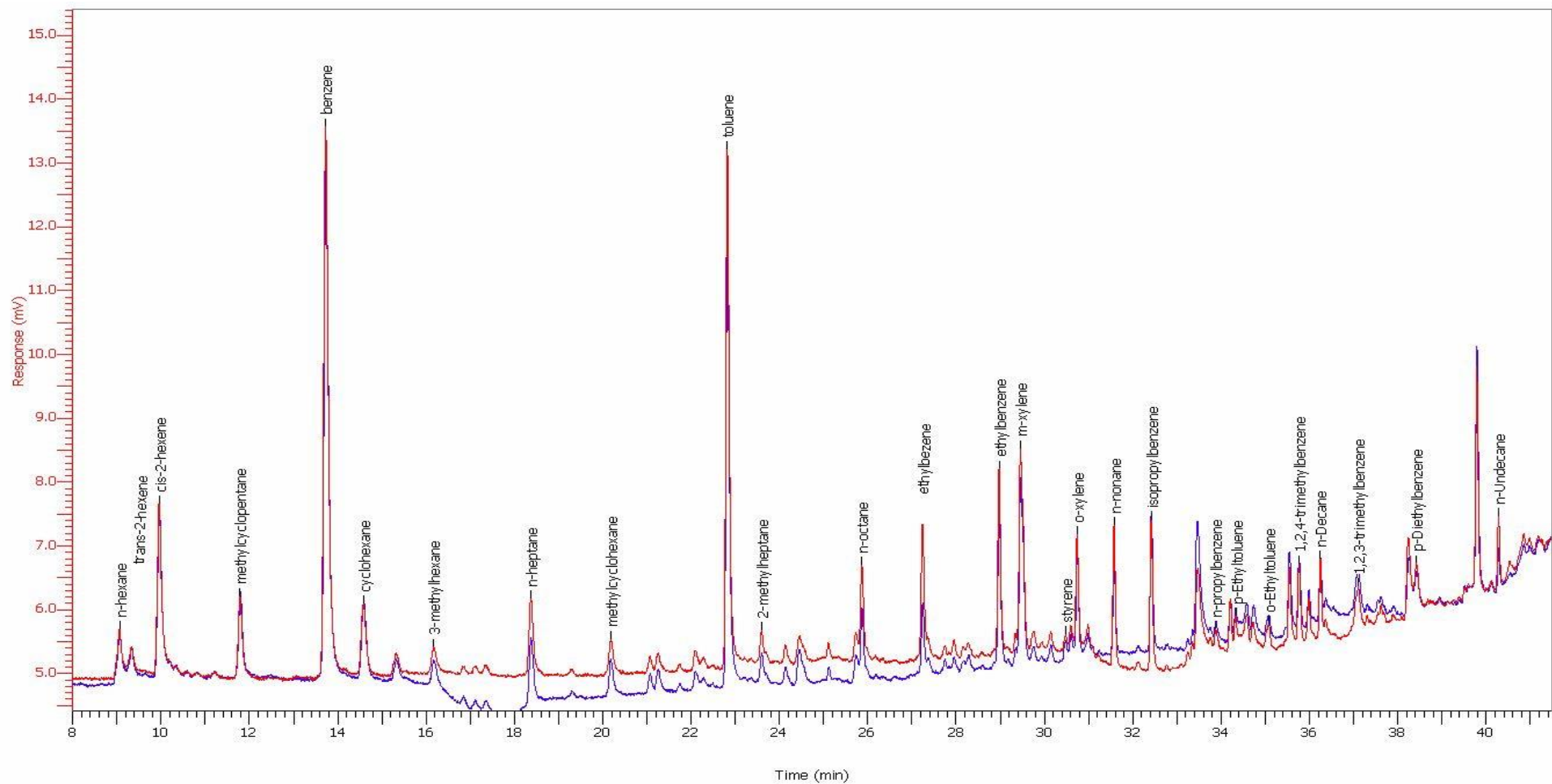


Figure 2.4. Chromatograms for (C₆-C₁₂) eluted in the methyl silicone column, obtained from a duplicate sample collected in BTP on July 14, 2017 (13:35 - 14:35 local time).

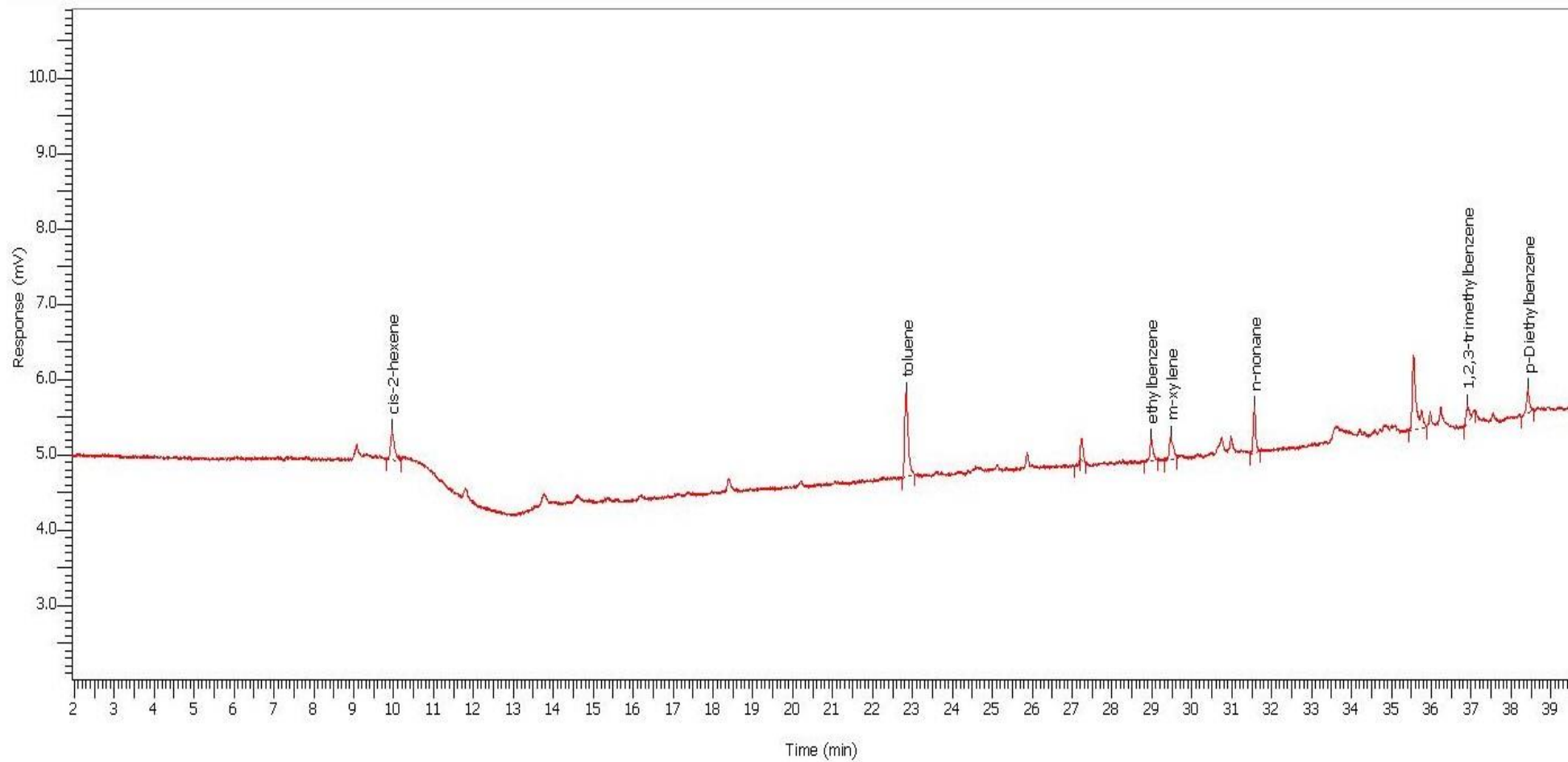


Figure 2.5. Chromatogram for (C₆-C₁₂) eluted in the methyl silicone column, obtained from analysis of blank from samples.

2.2.3. Estimating the formation of secondary pollutants

In order to estimate the potential effects that HCs measured in the PIC can have on the atmospheric chemistry, some metrics were applied. The maximum incremental reactivity (MIR), secondary organic aerosol potential (SOAP) and fractional aerosol coefficient (FAC) values used to calculate the potentials for some hydrocarbons sampled of this study are detailed in table 2.3.

The impact of HCs concentration on O₃ formation can be quantified using the MIR scale. The O₃ formation potential (OFP) was calculated from the mean concentrations of each HC quantified in this study, using the equation:

$$O_{3\text{formation potential}} = HC_i(\mu\text{g m}^{-3}) \times MIR_{HC_i} \quad \text{Eq. 1}$$

where HC_i is the concentration in $\mu\text{g m}^{-3}$; MIR_{HC_i} is the coefficient of each HC_i in $\text{g O}_3 \text{g VOC}^{-1}$.

In this study the applied method to estimate the SOA formation was proposed by Zhang et al. (2017). The potential for each HC was calculated using the equation:

$$SOA_{\text{formation potential}} = (HC_i(\mu\text{g m}^{-3}) \times SOAP_i) \div 100 \times FAC_{\text{toluene}} \quad \text{Eq. 2}$$

where HC_i is the concentration in $\mu\text{g m}^{-3}$; SOAP_i of respective HC_i, and FAC is the coefficient of toluene (%), being 5.4%, estimated by Zhang et al. (2017) This value reflects the propensity of each compound to form SOA. SOAP and FAC values were reported by Derwent et al. (2010) and Grosjean and Seinfeld (1989), respectively.

Table 2.3. Values of constant rate of reaction with respect to the hydroxyl radical (k_{OH}), Maximum Incremental Reactivity (MIR), Secondary Organic Aerosol Potentials (SOAP), Fractional Aerosol Coefficient (FAC) and Detection and Quantification limits (DL, QL) for some hydrocarbons sampled of the petrochemical and industrial complex in Metropolitan Area of São Paulo.

Compound	¹ k_{OH} at 298 K (10^{-12} cm ³ molecule ⁻¹ s ⁻¹)	² MIR g O ₃ / g HC	³ SOAP ug m ⁻³	⁴ FAC (%)	⁵ DL (ppt)	⁶ QL (ppt)
1,2,3-trimethylbenzene	32.5	8.87	20.6	1.7	141.9	430.1
1,2,4-trimethylbenzene	57	11.76	13.5	2.6	35.6	108.0
1,3,5-trimethylbenzene	8	1.26	-	0	3.3	10.0
2,2,4-trimethylpentane	3.68	1.2	-	-	2.5	7.5
2,3,4-trimethylpentane	3.68	0.97	-	-	2.8	8.4
2,3-dimethylpentane	5.1	1.25	0.4	-	1.5	4.6
2,4-dimethylpentane	5.7	2.05	-	-	2.1	6.3
2-methylheptane	5	1.07	-	0.5	3.1	9.4
2-methylhexane	6.9	1.19	-	0	4.2	12.6
3-methylheptane	8.6	1.24	-	0.5	3.0	9.0
3-methylhexane	5.1	1.61	-	0	3.8	11.4
benzene	1.23	0.72	92.9	2.6*	67.9	205.9
cis-2-hexene	63	8.31	1.3	-	14.6	44.1
cyclohexane	7.5	1.25	-	0.17	2.8	8.4
ethylbenzene	6.96	3.04	111.6	0.6	179.7	544.7
Isopropylbenzene (cumene)	6.6	2.52	95.5	0.7	1.8	5.4
m-Diethylbenzene	15	7.1	-	6.3	1.7	5.1
m-ethyltoluene	19	7.39	100.6	2.6	3.7	11.2
m+p-xylene	20.5	9.75	75.8	2.5	68.4	207.2
methylcyclohexane	10.3	1.7	-	1	2.9	8.9
methylcyclopentane	5.1	1.46	-	-	2.8	8.4
n-Decane	11.6	0.68	7	2	32.4	98.2
n-Undecane	13.2	0.61	16.2	2.5	0.1	0.3
n-hexane	5.6	1.24	0.1	0	2.7	8.2
n-heptane	7.2	1.07	0.1	0.06	43.6	132.0
n-nonane	10.2	0.78	1.9	1.5	33.4	101.2
n-octane	8.4	0.9	0.8	0.7	2.6	8.0
n-propylbenzene	5.8	2.03	109.7	0.7	2.5	7.7
o-Ethyltoluene	12	5.59	94.8	2.6	2.3	6.8
o-xylene	13.6	7.64	95.5	6.3	12.7	38.6
p-Diethylbenzene	10	4.43	-	6.3	307.8	932.7
p-Ethyltoluene	12	4.44	69.7	2.6	1.4	4.1
styrene	52	1.73	212.3	5.7 [†]	222.9	675.4
toluene	5.96	4	100	5.4 [‡]	21.8	66.0
trans-2-hexene	63	8.62	1.3	-	2.8	8.4

¹Wang et al. (2013)

²Carter (2013)

³Derwent et al. (2010)

⁴Grosjean; Seinfeld (1989)

[†]Zhang et al. (2017)

* Borrás and Tortajada-Genaro (2011)

[‡]Na et al. (2006)

⁵Detection limit

⁶Quantification limit

2.2.4. Risk assessment

The exposure risk was used to estimate the adverse effects of exposure on human health. For that, the Integrated Risk Information System (IRIS) method was applied (U.S. EPA, 2016). We calculated exposure concentration (EC):

$$EC = \frac{BTEX(\mu\text{g m}^{-3}) \times T \times F \times D}{AT} \quad \text{Eq. 3}$$

where BTEX is the concentration of each compound; T is the exposure time (8 hours); F is the exposure frequency (365 days year⁻¹); D is the exposure duration (70 years, assuming lifelong exposure) and AT is the averaging time (70 years x 365 days year⁻¹ x 24 hours day⁻¹).

Lifetime cancer risk (LCR) was calculated using the exposure concentration (EC) (equation above) and inhalation risk (IR) to estimate the cancer risk for benzene.

$$LCR = EC \times IR(\text{m}^3 \mu\text{g}^{-1}) \quad \text{Eq. 4}$$

Hazard quotient (HQ) was calculated using EC and continuous inhalation exposure reference (RFC) to estimate the non-cancer risk for BTEX. Hazard index (HI) is the sum of HQ of each compound and represents an accumulation hazard.

$$HQ = \frac{EC}{RFC(\mu\text{g m}^{-3})} \quad \text{Eq. 5}$$

$$HI = \sum HQ \quad \text{Eq. 6}$$

Table 2.5 presents the values of IR and RFC were obtained from U.S. EPA (IRIS) for each compound (U.S. EPA, 2016).

2.3. Results and discussions

2.3.1. Data overview

A total of 90 samples were collected in the two sampling sites, 44 at BTP and 46 at UFABC. It is important to note that all the samplings were performed during days with absence of precipitation and in weekdays. Among the thirty-four quantified hydrocarbons in our study, the most abundant ones, were toluene (1.5 ± 1.1 ppbv) and

cis-2-hexene (1.4 ± 1.9 ppbv) followed by benzene (0.55 ± 0.66 ppbv) and m+p-xylene (0.58 ± 0.3 ppbv), at both sites (Table 2.4). Figure 2.6 shows the average and standard deviation mixing ratios for the most abundant HCs at BTP and UFABC sampling sites. Other HCs presented average mixing ratios lower than 0.3 ppbv, with minimum and maximum ranging from 0.0024 to 13.5 ppbv, respectively.

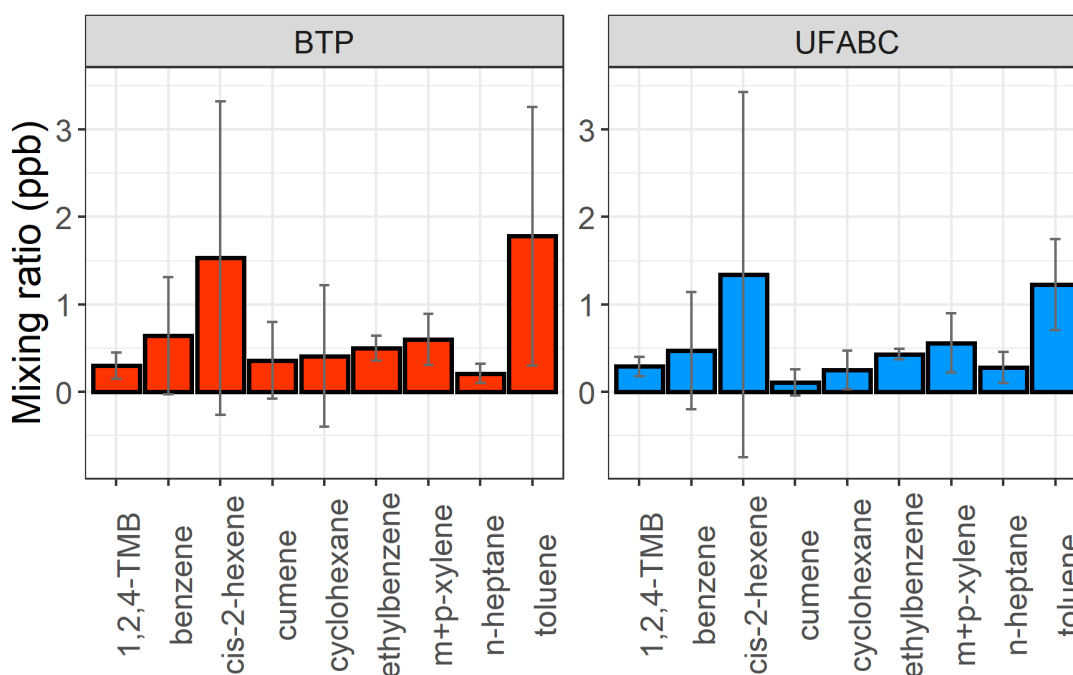


Figure 2.6. Average mixing ratios and standard deviation for the most abundant hydrocarbons at the BTP (left) and UFABC (right) sampling sites, for periods ranging from 8:00 a.m. to 6:00 p.m. during 2016-2017.

At both sites, the highest mixing ratios correspond to toluene and cis-2-hexene, while benzene presents a slight difference between the sites. In general, concentrations observed at BTP were higher than those at UFABC, by a factor of 2. Interestingly, the biggest difference was observed for the cumene 0.36 and 0.11 ppbv at BTP and UFABC, respectively. Cumene is not only a PIC product (ABC, 2017), but also it is present in fossil fuels and used in phenol and acetone manufacturing (Braskem, 2017). This fact can explain the different concentrations of this compound observed at both sites. To the contrary, 1,2,3-trimethylbenzene was the only compound with concentrations

below the LOQ at BTP site, although at UFABC, reaching average mixing ratios of 0.5 ppbv. Since this compound is known as a product of vehicular combustion emission, the location of UFABC site near traffic roads can explain its higher contribution.

BTEX concentrations were higher than the observed, by a factor ranged from 3.7 to 8.7, in previous study deployed at two sampling sites (UFABC and Sada Umeizawa school) in June 2013, collected for only two days in the morning period (8:00 to 11:00 am) (Boian et al., 2015). For example, benzene increased from 0.06 ppbv in 2013 to 0.55 ppbv in 2016-2017. Even though a similar sampling technique was used in both campaigns, the small number of samples in 2013 could include a bias uncovering the concentrations variability.

Petroleum refining, storage facilities, use and transport of solvents and fossil fuels combustion at production installations, are some examples of common emissions from petrochemical industries. Consequently, compounds like ethane, propane, benzene, toluene, and xylenes are the compounds usually emitted (Cetin et al., 2003; Baltrenas et al., 2011; Sharma et al., 2016; Wu et al., 2015). In the PIC area, the refinery performs a distillation of crude oil and production of by-products such as gasoline, diesel, and solvents (Petrobras, 2020), processes which could involve HCs fugitive emissions.

Table 2.4. Summary of statistical analysis for C6-C11 NMHCs hourly mixing ratios (ppbv) in the Metropolitan Area of São Paulo (MASP), for each sampling sites University Federal of ABC (UFABC) and Beneraldo de Toledo Piza school (BTP) for periods ranging from 8:00 a.m. to 6:00 p.m. during 2016-2017.

Compound (ppbv)	Mean	S.D. ¹	Max	Min	Median	1st. quartile	3th. quartile	N ²	site
1,2,3-trimethylbenzene	<QL	-	-	-	-	-	-	13	BTP
	0.50	0.50	2.46	<QL	0.30	0.19	0.64	29	UFABC
1,2,4-trimethylbenzene	0.30	0.15	0.76	<QL	0.27	0.22	0.35	44	BTP
	0.29	0.11	0.53	<QL	0.29	0.20	0.37	46	UFABC
1,3,5-trimethylbenzene	0.09	0.05	0.20	0.01	0.08	0.06	0.12	37	BTP
	0.10	0.05	0.22	<QL	0.10	0.06	0.14	39	UFABC
2,2,4-trimethylpentane	0.03	0.03	0.10	<QL	0.02	0.01	0.04	15	BTP
	0.05	0.10	0.46	<QL	0.01	0.01	0.04	21	UFABC
2,3,4-trimethylpentane	0.02	0.01	0.02	0.01	0.02	-	-	2	BTP
	0.03	0.00	0.03	0.03	0.03	-	-	2	UFABC
2,3-dimethylpentane	<DL								BTP
	0.11	0.03	0.15	0.06	0.11	0.07	0.14	4	UFABC
2,4-dimethylpentane	0.07	-	0.07	0.07	0.07	-	-	1	BTP
	<DL	-	-	-	-	-	-	-	UFABC
2-methylheptane	0.05	0.02	0.11	0.02	0.04	0.03	0.05	42	BTP
	0.06	0.03	0.12	0.01	0.05	0.03	0.07	43	UFABC
2-methylhexane	0.07	0.06	0.32	0.01	0.06	0.01	0.09	39	BTP
	0.14	0.12	0.55	0.01	0.11	0.05	0.21	41	UFABC
3-methylheptane	0.04	0.03	0.14	0.00	0.03	0.02	0.04	37	BTP
	0.06	0.04	0.16	0.01	0.04	0.03	0.08	38	UFABC
3-methylhexane	0.11	0.09	0.46	0.01	0.09	0.06	0.13	40	BTP
	0.20	0.19	0.90	0.01	0.14	0.08	0.28	42	UFABC
benzene	0.64	0.67	2.23	<QL	0.36	0.15	1.01	35	BTP
	0.47	0.67	2.98	<QL	0.22	0.12	0.40	34	UFABC
cis-2-hexene	1.53	1.79	9.25	<QL	0.82	0.50	1.93	44	BTP
	1.34	2.09	13.49	<QL	0.74	0.49	1.34	46	UFABC
cumene	0.36	0.44	1.70	0.01	0.17	0.03	0.51	26	BTP
	0.11	0.15	0.54	<QL	0.04	0.01	0.16	14	UFABC
cyclohexane	0.41	0.81	4.56	0.01	0.15	0.05	0.56	33	BTP
	0.25	0.22	0.70	0.02	0.20	0.06	0.39	37	UFABC
ethylbenzene	0.50	0.14	0.85	<QL	0.48	0.38	0.62	25	BTP
	0.43	0.06	0.63	<QL	0.42	0.40	0.45	18	UFABC
m+p-xylene	0.60	0.29	1.37	<QL	0.56	0.39	0.79	44	BTP
	0.56	0.34	1.82	<QL	0.51	0.33	0.71	46	UFABC

m-Diethylbenzene	0.26	0.29	0.58	0.01	0.18	0.01	0.58	3	BTP
	0.16	0.22	0.63	0.01	0.05	0.02	0.32	16	UFABC
methylcyclohexane	0.12	0.10	0.51	0.01	0.10	0.06	0.14	43	BTP
	0.10	0.08	0.36	0.01	0.08	0.05	0.13	45	UFABC
methylcyclopentane	0.29	0.22	0.88	0.03	0.20	0.15	0.32	41	BTP
	0.23	0.14	0.59	0.04	0.19	0.13	0.30	45	UFABC
m-ethyltoluene	0.14	0.08	0.38	0.03	0.12	0.09	0.18	44	BTP
	0.14	0.08	0.36	0.03	0.12	0.09	0.19	45	UFABC
n-Decane	0.16	0.09	0.50	0.07	0.15	0.10	0.22	44	BTP
	0.16	0.07	0.35	0.03	0.16	0.11	0.19	46	UFABC
n-heptane	0.21	0.11	0.59	<QL	0.19	0.14	0.25	43	BTP
	0.28	0.18	0.80	<QL	0.22	0.17	0.40	45	UFABC
n-hexane	0.21	0.13	0.71	0.04	0.18	0.14	0.25	44	BTP
	0.20	0.08	0.38	0.06	0.19	0.13	0.26	46	UFABC
n-nonane	0.18	0.07	0.37	<QL	0.17	0.14	0.23	44	BTP
	0.17	0.06	0.32	<QL	0.16	0.13	0.20	45	UFABC
n-octane	0.13	0.05	0.28	0.04	0.11	0.09	0.15	44	BTP
	0.14	0.07	0.31	0.02	0.13	0.10	0.19	46	UFABC
n-propylbenzene	0.05	0.03	0.11	0.01	0.04	0.03	0.06	36	BTP
	0.14	0.61	3.68	0.01	0.04	0.02	0.06	36	UFABC
n-Undecane	0.17	0.09	0.39	0.05	0.15	0.11	0.22	44	BTP
	0.19	0.22	1.55	0.03	0.14	0.10	0.18	46	UFABC
o-Ethyltoluene	0.08	0.04	0.20	0.01	0.08	0.05	0.10	39	BTP
	0.09	0.05	0.26	<QL	0.09	0.04	0.12	38	UFABC
o-xylene	0.23	0.11	0.56	0.04	0.21	0.16	0.32	44	BTP
	0.20	0.08	0.38	0.02	0.19	0.14	0.28	46	UFABC
p-Diethylbenzene	<DL	-	-	-	-	-	-	-	BTP
	<QL	-	-	-	-	-	-	1	UFABC
p-Ethyltoluene	0.08	0.05	0.24	<QL	0.07	0.05	0.11	42	BTP
	0.14	0.15	0.69	<QL	0.09	0.05	0.18	42	UFABC
styrene	<QL	-	-	-	-	-	-	5	BTP
	<QL	-	-	-	-	-	-	14	UFABC
toluene	1.78	1.48	9.05	0.40	1.40	0.88	2.03	44	BTP
	1.23	0.52	2.91	0.15	1.19	0.83	1.63	46	UFABC
trans-2-hexene	0.04	0.03	0.08	<QL	0.05	0.01	0.07	9	BTP
	0.04	0.04	0.09	<QL	0.01	0.00	0.09	5	UFABC

S.D.¹ standard deviation

N² number of samples for each site: BTP=44, UFABC=46 (total = 90)

2.3.2. Meteorological and air quality conditions

Figure 2.7 presents the meteorological and air quality conditions observed during the period under study. The average wind speed observed at Capuava station was 1.61 m/s with 7.5% of calm conditions (wind speed below 0.5 m/s) (Figure 2.7a). The dominant wind direction was from the south, but also with high frequencies from southeast and northeast directions. The most frequent and strongest winds (with around 10% between 2 and 5 m/s) were from the south and southeast, which are associated with the entrance of the sea breeze in the region (Vemado; Pereira Filho, 2016). The lowest monthly average temperature was observed in July (around 19 °C, winter) and the highest in February, (around 24 °, summer) (Figure 2.7b). The lowest monthly accumulated precipitation was observed in July 2017 (2.2 mm), followed by the same month in 2016 (7.4 mm). September (24.6 mm) and October (82.2 mm) 2016, presented accumulated values below climatologic average (85.9 and 125.7 mm, respectively), according to the reports of Climate Study Group (GREC/ USP, 2020). In summer, January presented an opposite anomaly (368.2 mm) with accumulated precipitation above the climatologic average (268.2 mm). The other months were according to the monthly climatologic averages.

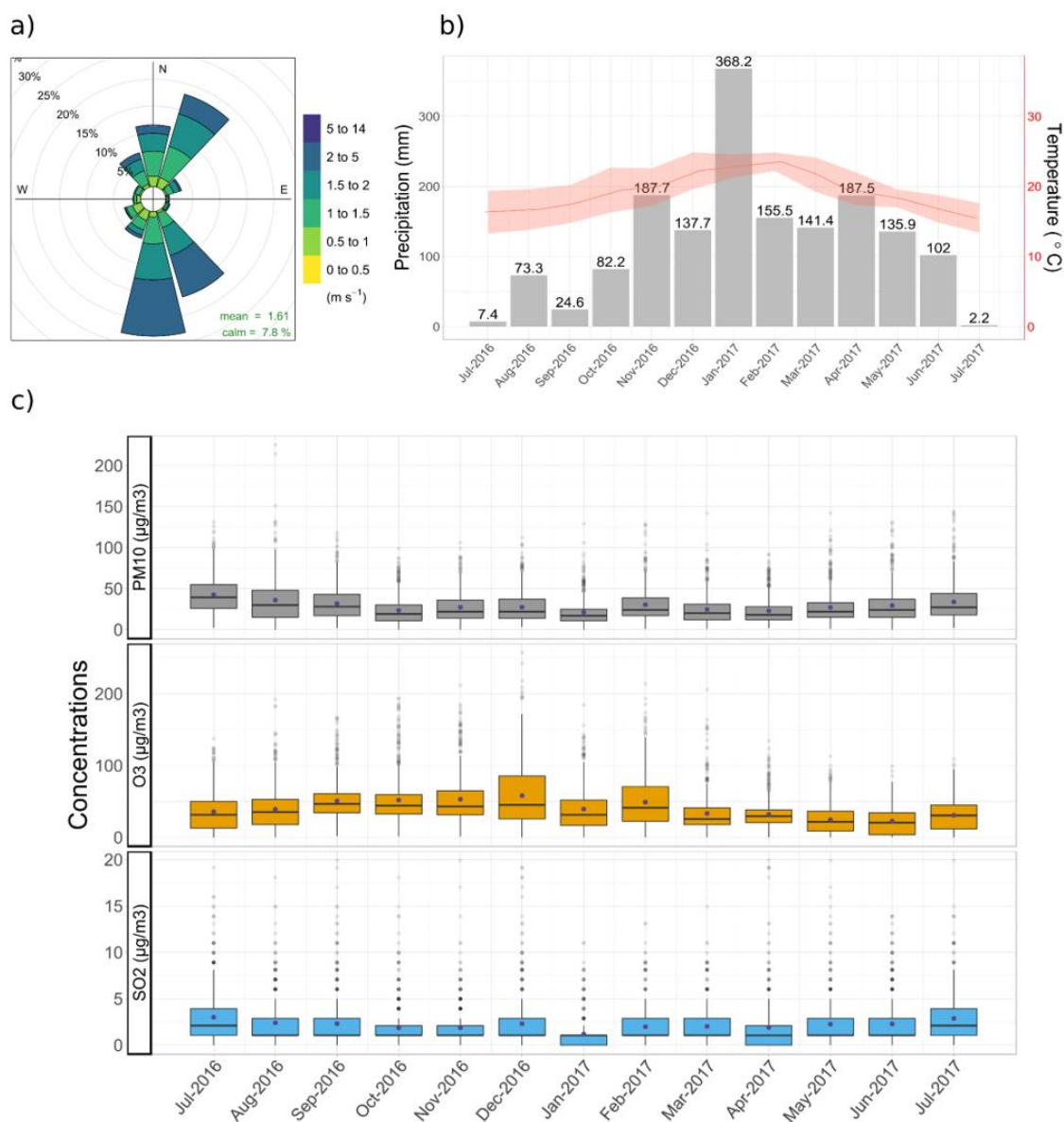


Figure 2.7. Monthly meteorological and pollutants variability for the period under study (July 2016 to July 2017) for: a) wind speed (m s⁻¹) and direction (°) (Capuava Station, CETESB, 2020); b) monthly accumulated precipitation (mm) and mean temperature (°C) (IAG/ USP Meteorological Station); c) monthly boxplots of air pollutant concentrations for PM₁₀, O₃ and SO₂ (µg m⁻³) (Capuava Station, CETESB, 2020). In boxplot width, the lower and upper hinges correspond to the first and third quartiles (the 25th and 75th percentiles). Lower whisker = smallest observation greater than or equal to lower hinge - 1.5 * IQR. Upper whisker = largest observation less than or equal to upper hinge + 1.5 * IQR. Middle is median, 50% quantile and the point is mean value. The circles point represents the arithmetic mean. Data beyond the end of the whiskers are called "outlying" points.

The CETESB air quality network has been monitoring CO, O₃, NO₂, SO₂, PM₁₀ and PM_{2.5} concentrations in the Great ABC region. These air pollutants are commonly associated with serious air pollution problems in urban and industrial areas, and their concentrations frequently exceed the air quality standard in the MASP (Andrade et al., 2017; CETESB, 2019). For 2016-2017, the maximum CO and O₃ values ranged from 2.8 to 6.3 ppm and 258 to 362 µg m⁻³ (8 hours mean), NO₂ from 87 to 189 µg m⁻³ (1 hour mean). SO₂, PM₁₀ and PM_{2.5} maximum values varied from 7 to 10 µg m⁻³, 61 to 77 µg m⁻³ and 36 to 44 µg m⁻³ (24 hours mean), respectively (CETESB, 2018). These concentrations exceeded the World Health Organization (WHO) guidelines, of 100 µg m⁻³ (8h mean) for O₃, 50 µg m⁻³ and 25 µg m⁻³ (24h mean) for PM₁₀ and PM_{2.5}, respectively (WHO, 2018). These exceedances show that secondary pollutants represent an air quality concern in the region. A previous study has indicated that the population of Great ABC region has been facing health degradation due to the pollution levels in the region. Statistically significant effects between PM₁₀ concentrations and hospitalizations of elderly patients were associated to congestive heart failure in Santo André city, part of Great ABC region (Evo et al., 2011).

Figure 2.7c shows the monthly concentrations and variability of PM₁₀, O₃ and SO₂ observed from July 2016 to July 2017, with the same period where HCs measurements were performed. Their average monthly concentrations at Capuava station vary from 21 to 42 µg m⁻³ for PM₁₀, from 24 to 58 µg m⁻³ for O₃ and from 1.18 to 3 µg m⁻³ for SO₂. Through the interquartile intervals between the first and second quartiles, it is possible to determine the variability of the data. Thus, the highest variability and concentration of SO₂ was present in July for both years (2016-2017, 3 and 2.8 µg m⁻³). The O₃, in comparison with the other pollutants, presented the highest monthly variability, which was also related the highest concentrations, mainly in December and February. Yet PM₁₀ presented the highest variability and average values in July and August (42 and 35 µg m⁻³).

The highest monthly variability and concentrations of PM₁₀ and SO₂ were observed in winter and early spring (from July to September) related to atmospheric stagnation episodes and less precipitation (2.2 and 73.3 mm), and, as a result, of less dispersion and wet removal. As for O₃, the highest amplitude and concentrations occurred in spring and summer (from September to February) related to the higher temperatures and radiation. The lower pollutants concentrations in January could be related to the accumulated precipitation (wet removal), the wide cloud cover and the less radiation incidence, is essential for O₃ formation (Chiquetto, 2008; Carvalho et al., 2015).

2.3.3. Seasonal and diurnal profiles

A seasonal variation was observed in the total measured HCs (sum of C₆-C₁₁), which averages were similar in winter (10.5 ± 0.3 ppbv) and autumn (10.4 ± 0.4 ppbv) followed by spring (7.2 ± 0.2 ppbv). HCs were not measured during summer. Our results somewhat agree with those in industrialized areas in China where higher contributions were also obtained in winter, followed by summer > spring > autumn (An et al., 2014). However, a dissimilar seasonal pattern was observed in Turkey where concentrations in summer were higher than in winter (Dumanoglu et al., 2014). Similarly, in Iran, HCs concentrations were higher in summer than in winter for benzene, toluene, xylenes and styrene, but not significantly different, except for toluene (Tohid et al., 2019). However, an absence of seasonal variation of total VOCs was observed in Korea, associated to the relatively constant emissions from the local industries (Kim et al., 2019). Therefore, it is difficult to generalize a seasonal variability for VOCs in industrial areas, due to specific meteorological conditions and emission sources characteristics in each region.

The diurnal profiles of HCs previously observed in the MASP were associated to traffic emissions, presenting higher concentrations during rush hours, with maximum values at 9:00 a.m. (Martins and Andrade, 2008; Brito et al., 2015; Dominutti et al., 2016). However, to the best of our knowledge, there are not previous studies

evaluating diurnal HCs profiles in industrial areas in the MASP. Figure 2.8 shows the diurnal profiles and the relative contribution by groups of compounds for the most abundant HCs (alkanes, alkenes and aromatics). Total HCs were higher at BTP ranging from 3.9 to 8.1 ppbv, with maximum values at 2:00 p.m. but without any considerable variation of total concentration along the day. Contrarily, at UFABC the mixing ratios ranged from 1.8 to 7 ppbv decreasing before 11 a.m. and increasing at 3 p.m., reaching maximum values at 6:00 p.m. Unlike the diurnal profile observed in BTP, UFABC presented a similar profile to the one already identified for the MASP (Martins and Andrade, 2008; Dominutti et al., 2016; Alvim et al., 2017), with higher mixing ratios during the rush hours (9:00 a.m. and after 6:00 p.m.). The diurnal variability of HCs in the MASP can be controlled by chemical removal processes (reaction with radical OH) and dilution in the diurnal boundary layer (Dominutti et al., 2016). For example, cis-2-hexene show a dissimilar trend at the two sampling sites but an increase in concentrations was observed after 2 p.m. and 4 p.m. for BTP and UFABC, respectively. It is important to highlight that cis-2-hexene is a very reactive compound towards OH radical ($k_{OH} = 63 \times 10^{-12} \text{ cm}^3 \text{ molecule}^{-1} \text{ s}^{-1}$), which might result in additional formation of O₃, enabling the photochemical production of other secondary pollutants.

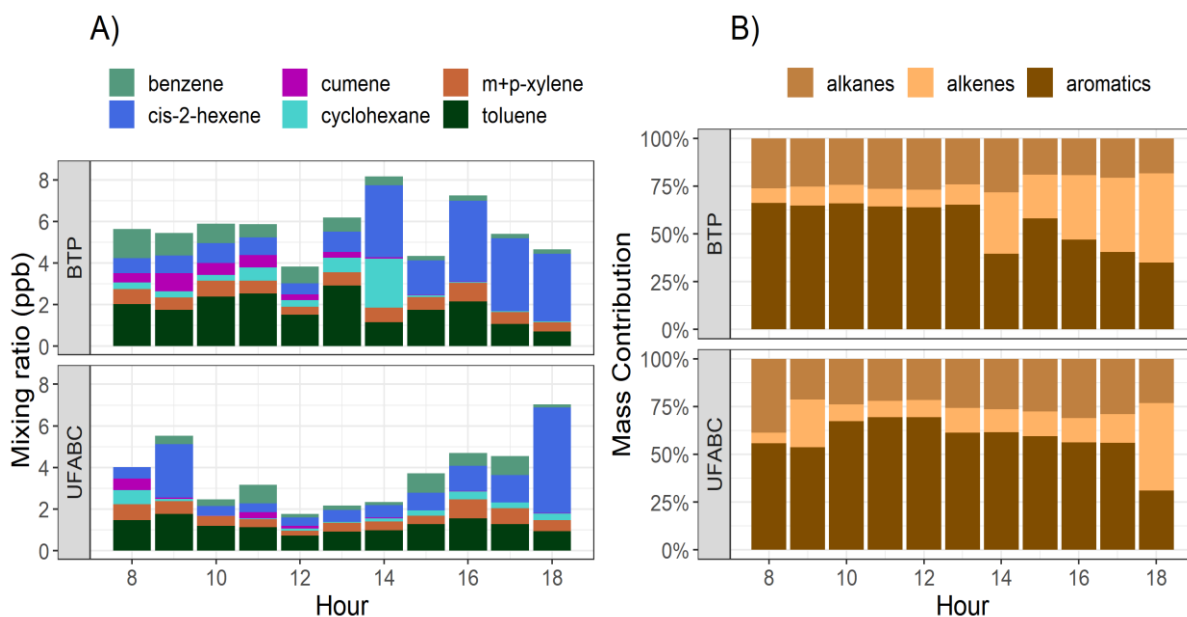


Figure 2.8. Average diurnal profiles of the most abundant hydrocarbons (A) and relative mass contribution for thirty-five hydrocarbons (B) grouped by alkanes (17), alkenes (2) and aromatics (16) at the BTP and UFABC sampling sites, during 2016-2017.

The compounds quantified in our study (C_6 - C_{11}) were integrated to calculate the relative mass contribution at each sampling site, being considered seventeen alkanes, two alkenes (cis/trans-2-hexene) and sixteen aromatics species. Aromatics are dominant fraction of HCs at BTP, by 70% on average, with higher contributions in the morning (Figure 2.8, top panel). Alkanes did not show a significant diurnal variation, presenting almost constant contribution all day long (20 to 25%). During the afternoon (from 2:00 p.m.), alkenes increased from 35% to 65% and, consequently, the aromatics decreased at BTP (Figure 2.8). The increase of alkenes during the afternoon could be associated to secondary formation processing due to the aging and chemical removal of primary emissions. On the opposite, alkenes contribution varied from 25% at 9:00 a.m. to 50% at 6:00 p.m. at UFABC (Figure 2.8, bottom panel), showing the influence of direct primary traffic emissions. Aromatic compounds also dominate the HCs contribution at UFABC site with some variations in the morning and the evening (52% and 30%, respectively). Alkanes did not show variations throughout the day (30 to 24%), except at 8:00 a.m., when they reached the highest percentual contribution (Figure 2.8).

2.3.3. BTEX mixing ratios comparison

In 2015, CETESB began the hourly automatic monitoring of benzene and toluene at five sites in different municipalities of São Paulo state. These different sites represent the influence of vehicular and industrial emissions in the MASP (CETESB, 2018). They are located in São José dos Campos – Vista Verde (SJC1) near the Henrique Lage Oil Refinery (REVAP); Paulínia station near the Paulínia Oil Refinery; Cubatão station near the Industrial Complex of Cubatão (petrochemical, steel and production of fertilizers); Pinheiros station close to one of the main traffic avenues in the MASP, São José dos Campos (SJC2) inside the urban area and Capuava station in vicinity of PIC (close to sampling sites of this study). This data provides an overview of the mixing ratios observed for the other industrial areas in São Paulo state. Therefore, a comparison with our measurements was performed to evaluate the differences and similarities among them.

Figure 2.9 shows the hourly average mixing ratios of toluene and benzene obtained during our study and those observed by CETESB in 2017 (CETESB, 2020). Toluene concentrations were higher than those observed for benzene in all the sites under analysis by a factor of 2.5 on average. Capuava showed the highest benzene mixing ratio (0.76 ± 1.2 ppbv), followed by BTP site (0.64 ± 0.67 ppbv), UFABC (0.47 ± 0.67 ppbv), Cubatão (0.45 ± 0.7 ppbv), SJC1 (0.42 ± 0.6 ppbv), Paulínia (0.34 ± 0.5 ppbv), Pinheiros (0.28 ± 0.3 ppbv) and SJC2 (0.09 ± 0.2 ppbv). An opposite trend is observed for toluene which presented the highest mixing ratios at BTP site (1.78 ± 1.48 ppbv), followed by Capuava (1.3 ± 1.2 ppbv), Pinheiros (1.2 ± 1.3 ppbv), UFABC (1.2 ± 0.52 ppbv), SJC1 (0.9 ± 1.3 ppbv), Paulínia (0.68 ± 0.9 ppbv), Cubatão (0.6 ± 1.2 ppbv) and SJC2 (0.3 ± 0.7 ppbv). Even though the slightly differences observed in the benzene and toluene concentrations at Capuava and BTP, there is a good agreement between both industrial sites.

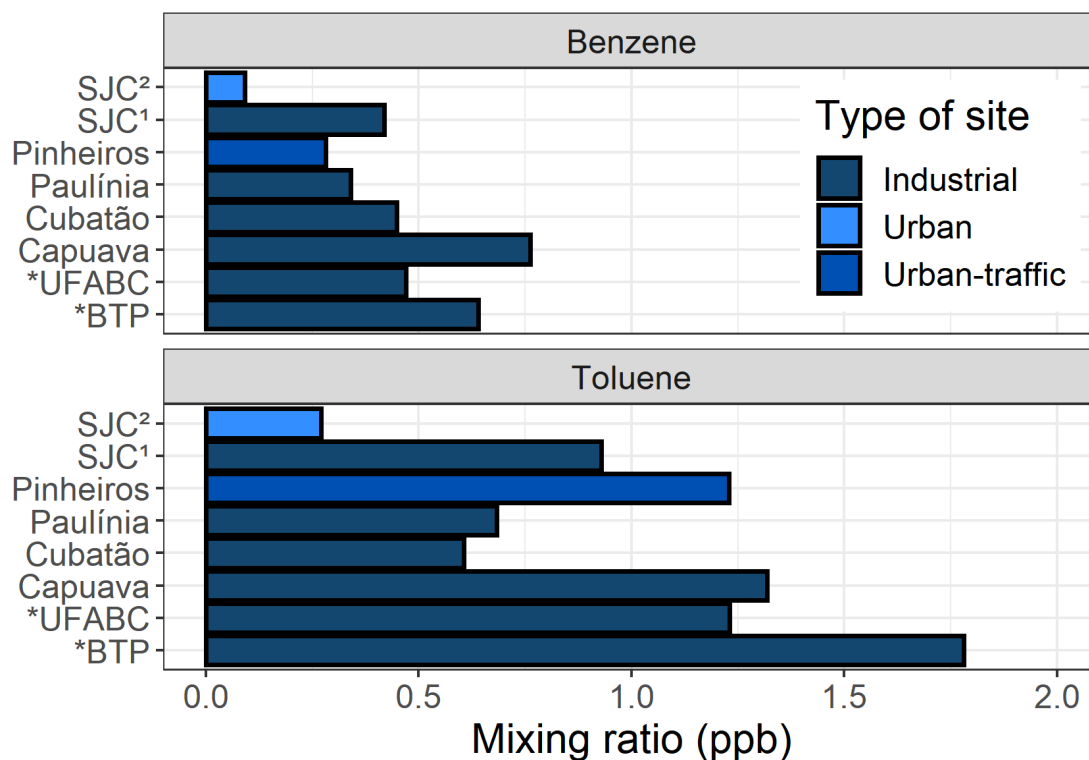


Figure 2.9. Hourly average mixing ratios of benzene and toluene obtained in the present study and those from CETESB Air Quality Monitoring Stations in São Paulo State, in 2017 (CETESB, 2018).¹SJC and ²SJC refers to São José dos Campos (Vista Verde) Station and São José dos Campos Station, respectively. *Sampling sites of Present study (UFABC and BTP).

In general, benzene presented higher mixing ratios at the sites located in industrialized areas (0.52 ± 0.5 ppbv), when compared to those close to urban (0.09 ppbv) and urban-traffic areas (0.3 ppbv). Nevertheless, a less clear profile is observed for toluene, which also presented high concentration in traffic-related sites. The higher contribution of benzene near the industrialized sites, highlight the influence that industrial HCs emissions can also have in a high-impacted traffic area like the MASP.

Aromatics, on average, were the predominant HCs fraction at BTP and UFABC (58.0 and 56.0%) followed by alkanes (23.6 and 28.5%) and alkenes (18.0 and 15.4%). BTEX contributed to 40.0 and 35.0% for the total HCs at BTP and UFABC, respectively. Previous worldwide studies in petrochemical and industrial areas have reported lower aromatics contributions compared to our study, ranged from 19 to 22% for the total VOCs in China (Wei et al., 2014; An et al., 2014). These observed differences may be related to the number of compounds that were integrated for each group. For example,

in the studies cited above, alkanes, such as ethane, propane, isobutane, n-butane and isopentane had the highest concentrations (Wei et al., 2014; An et al., 2014), but they were not quantified in the present study.

Figure 2.10 shows the average relative BTEX contribution observed at BTP and UFABC sites and those obtained in other studies performed at urban and industrialized areas worldwide. For most sites, toluene presented the highest contribution among the BTEX compounds (~ 50%), Rio de Janeiro, Brazil and China, showed the highest and lowest contribution (~60% and ~20%, respectively). Similarly, benzene mass contribution ranged from 10 to 17% in most places, except for China (~40%). Ethylbenzene and o-xylene presented the lowest mass contribution of BTEX, ranging from 7-15% and 3-10%, respectively. On average, the BTEX profile obtained in our study presented very similar relative contribution when compared to those observed in Yokohama, Japan and Texas, US (Figure 2.10, Tiwari et al., 2010; Leuchner; Rappenglück, 2010). However, the total BTEX absolute mixing ratios varied from 1.5 to 14.9 ppbv: Brazil (14.9 ± 3.5) > Korea (5.0 ± 0.69) > France (4.9 ± 0.96) > China (4.7 ± 0.61) > BTP site (3.7 ± 0.6) > UFABC site (2.9 ± 0.4) > Japan (2.0 ± 0.26) > United States (2.0 ± 0.25) > Canada (1.5 ± 0.26).

These results display the differences in the atmospheric composition among the places analyzed (Figure 2.10). The discrepancies could be related to the industrial processes associated to the BTEX emissions, but also to the type of measurements and the sampling time carried out in each study.

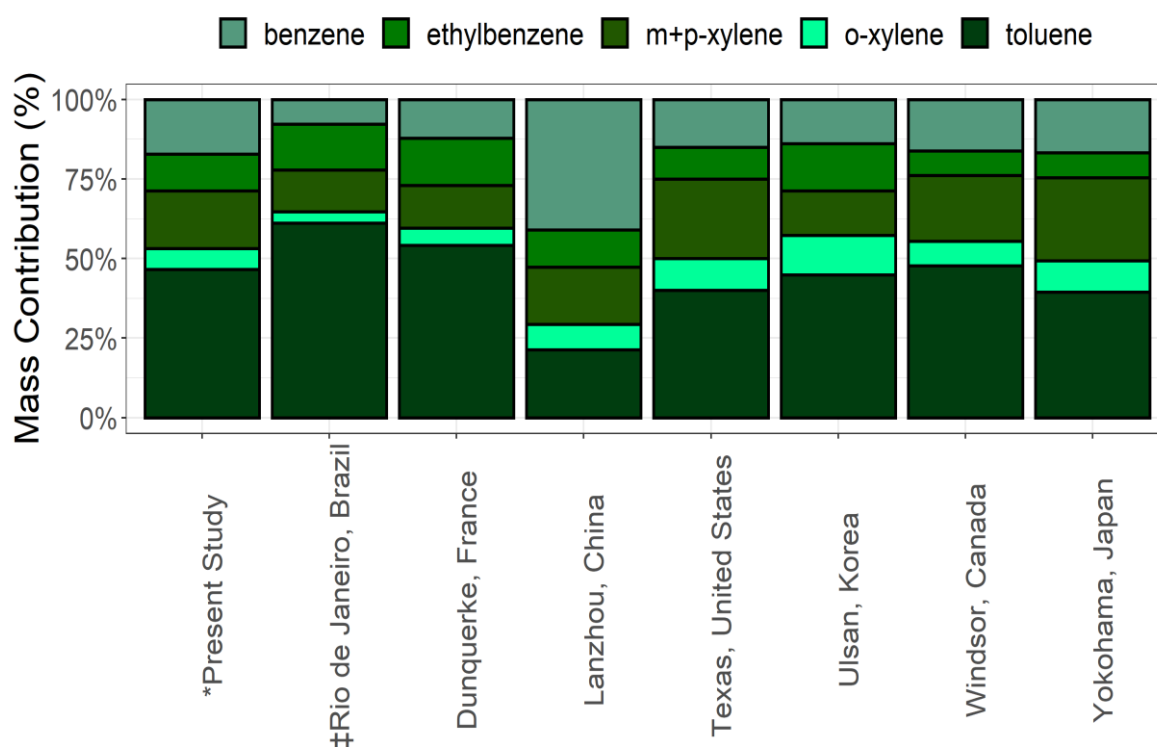


Figure 2.10. Comparison of relative BTEX mass contributions (%) observed in industrial and urban areas: Rio de Janeiro, Brazil (Silva et al., 2017), Dunquerque, France (Roukos et al., 2009), Lanzhou, China (Jia et al., 2016), Texas, United States (Leuchner and Rappenglück, 2010), Ulsan, Korea (Kim et al., 2019), Windsor, Canada (Miller et al., 2011), Yokohama, Japan (Tiwari et al., 2010). *Present study represents the averaged concentrations for both sampling sites. ‡Rio de Janeiro, Brazil represents the averaged concentrations for two sampling sites (Air Basins I and III) that represents industrialized urban areas.

2.3.4. Ratios and correlation between BTEX species

The ratios of benzene/toluene (B/T) and m+p-xylene/benzene (X/B) have been widely used to obtain preliminary information about sources and photochemical processing of emissions (Tiwari et al., 2010; Kumar et al., 2018). Benzene and toluene are emitted from vehicle fuel combustion at approximately ratio of 0.5 (Jiang et al., 2017), being ratios above this value indicative of other emission sources. Table 2.5 shows the comparison of ratio values among different countries, at urban and industrial areas. The B/T ratios ranged from 0.13 to 0.54, which indicates that the main source of HCs was fossil-fuel burning from vehicles (Table 2.5). Nevertheless, the B/T ratio at Lanzhou (China) was 1.92 indicating the influence of local industries, due to the mixing ratio of benzene (1.94 ppbv) higher than toluene (1.01 ppbv) (Jia et al., 2016). Our sampling sites showed B/T ratios of 0.36 and 0.43 for BTP and UFABC (Table 2.5),

respectively, highlighting the influence of vehicular combustion emissions, despite the presence of PIC in the region.

Table 2.5. Comparison of ratios (B/T and X/B) observed indifferent countries and areas (industrial and urban).

City, Country (Year of sample)	Type of site	Ratio		Reference
		B/T	X/B	
*BTP (2016/2017)	Industrial	0.36	0.94	Present Study
*UFABC (2016/2017)	Urban	0.43	1.19	Present Study
Ulsan, Korea (2014)	Industrial	0.31	1.00	Kim et al (2019)
MASP, Brazil (two days, 2013)	Urban/ Industrial	0.3	2.5	Boian et al (2015)
MASP, Brazil (2013)	Urban	0.54	0.69	Dominutti et al (2016)
Lanzhou, China (2013)	Industrial	1.92	0.44	Jia et al (2016)
Rio de Janeiro, Brazil (2015)	Urban/ Industrial	0.13	1.69	Silva et al (2017)
Paulínia, Brazil (2008/2009)	Industrial	0.25	-	Ueda and Tomaz (2011)
Yokohama, Japan (2008)	Industrial	0.43	1.56	Tiwari et al (2010)
MASP, Brazil (2008)	Urban	0.18	2.53	Alvim et al (2017)
Dunquerque, France (2007)	Industrial	0.22	1.10	Roukos et al (2009)
Houston, Texas (2006)	Industrial	0.38	1.67	Leuchner and Rappengluck (2010)
Windsor, Canada (2005)	Industrial	0.34	1.28	Miller et al (2011)

The constant rate with OH radical indicates that benzene ($k_{OH} 1.23 \times 10^{-12} \text{ cm}^3 \text{ molecule}^{-1} \text{ s}^{-1}$) is less reactive than xylenes ($k_{OH} 20.5 \times 10^{-12} \text{ cm}^3 \text{ molecule}^{-1} \text{ s}^{-1}$) (Atkinson, 2000; Wang et al., 2013). In this way, evidence of the air masses transport and photochemical aging can be inferred from the X/B ratios (Kumar et al., 2018; Tiwari et al., 2010). High values indicate a fresh air masses and the influence of local sources and low values indicate transported aged air mass which results from the diffusion or dispersion processes of the pollutants (Tiwari et al., 2010; Kumar et al., 2018; Tohid et al., 2019). The X/B ratios obtained were 0.94 and 1.19 for BTP and UFABC, respectively, suggesting the influence of aged air mass (Kumar et al., 2018). These values were lower than those observed in a previous study for the PIC area (X/B: 2.5, for samples of two-days, Boian et al., 2015), at an urban traffic site in the MASP (X/B: 2.53, Alvim et al., 2017) and industrial sites at Canada, Japan, Texas and urban/ industrial area of Rio de Janeiro, Brazil (X/B: 1.28, 1.56, 1.67 and 1.69, respectively (Miller et al., 2011; Tiwari et al., 2010; Leuchner and Rappenglück, 2010; Silva et al., 2017). The lower X/B observed in our study can be explained by the higher mixing ratios of benzene in relation to m+p-xylene, mainly at the BTP site. A similar scenario was observed at industrial sites

for China, Korea and France (X/B: 0.44, 1.0 and 1.10, respectively, Jia et al., 2016; Kim et al., 2019; Roukos et al., 2009) and urban site in the MASP (X/B: 0.69, Dominutti et al., 2016). In addition to local emissions, possibly these areas are under the influence of air masses transported from other places, for example at our study, a highly traffic avenue near the BTP site in the south (wind direction dominant frequency), could be a probable influence in the benzene concentrations.

Figure 2.11 presents the scatter plots and linear correlations between BTEX species at both sampling sites, BTP and UFABC. The linear regression between HCs has been analyzed in order to evaluate the contribution from similar emission sources (Parrish et al., 1998; Ait-Helal et al., 2014). Hydrocarbons mixing ratios could be directly influenced not only by emissions and atmospheric transport, but also by chemical reactions due to the reactivity of these compounds. The correlation between xylenes and ethylbenzene showed a strong positive correlation ($r > 0.70$), mainly at BTP site (Figure 2.11). This result indicates that these three compounds may have originated from the same emission sources, for example, vehicular emissions (Shao et al., 2016; Tiwari et al., 2010). For toluene, the correlations with m+p-xylene, ethylbenzene and o-xylene ranged from 0.46 to 0.75 (Figure 2.11). This suggests that these four compounds may have been emitted preferably by vehicular combustion.

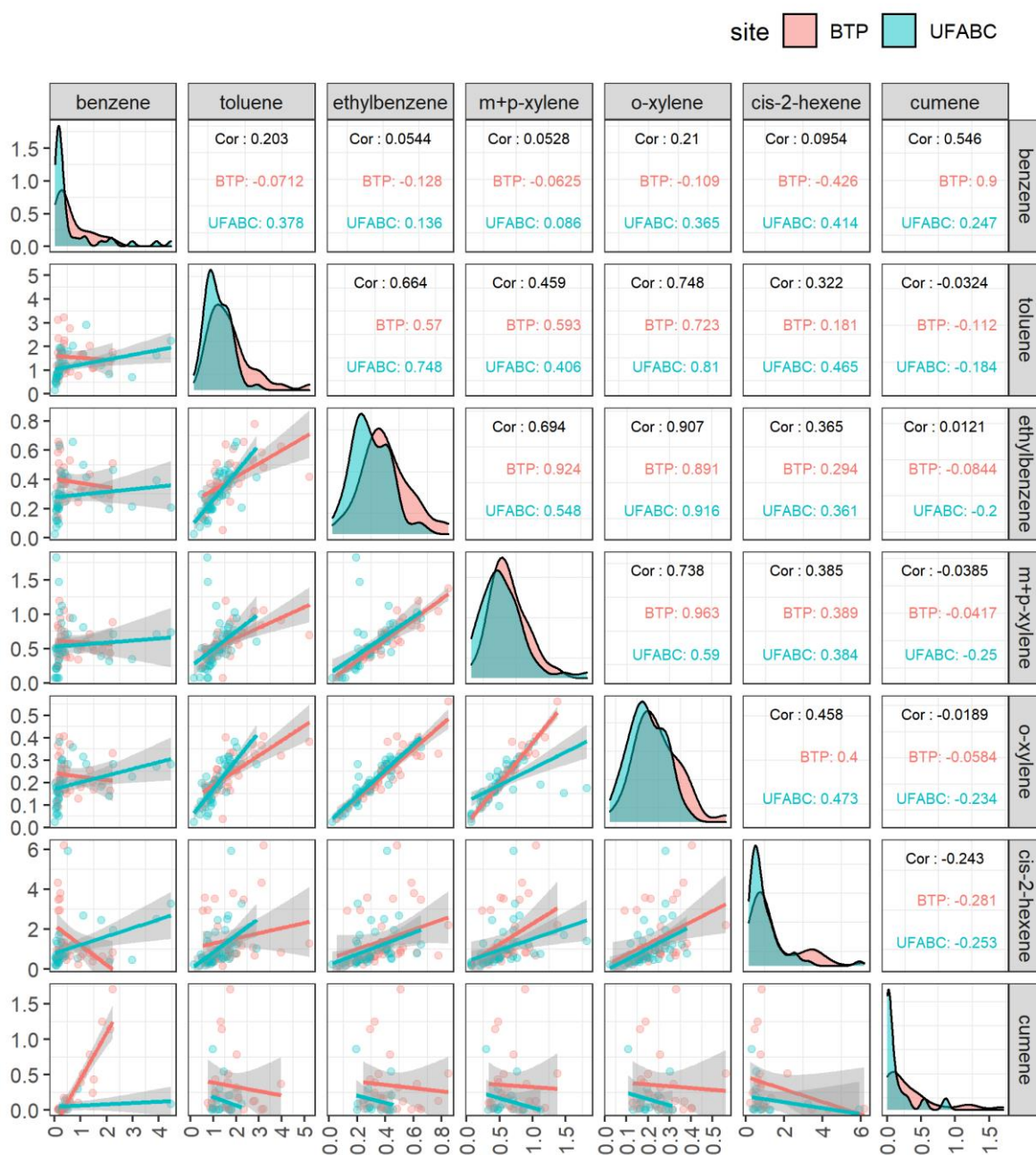


Figure 2.11. Scatter plots and respective linear regression for BTEX at the two sampling sites, BTP (red) and UFABC (blue). Cor is the correlation coefficient (Pearson) and the curves represent the mixing ratios distribution at both sites (in ppb).

Benzene did not present significant correlations with other BTEX species, at UFABC ($r= 0.08$ to 0.38) and at BTP sampling sites ($r = -0.06$ to -0.13). These findings were comparable to those obtained in previous studies at industrial areas (Ueda, 2010; Tiwari et al., 2010). Thus, our results suggest that benzene may have been either emitted or influenced by other sources, such as local industrial activities. When we

examine the correlations obtained for cumene, which has no significant correlations, except for benzene, were 0.9 and 0.25 for BTP and UFABC, respectively. This suggests that cumene and benzene are probably released from the same emission source (industrial). In addition, the negative correlation for cis-2-hexene with benzene (-0.4 to 0.4) and cumene (-0.3 to 0.2), suggests the photochemical production of cis-2-hexene especially at BTP site. This is in agreement with our observations in the diurnal profiles.

2.3.5. O₃ and SOA formation potentials (OFP and SOAFP)

Secondary pollutants formation metrics were applied to evaluate the potential impacts that HCs concentrations in the PIC area might imply on the local atmosphere. Figure 2.12 shows the results of the OFP and SOAFP applied to the most abundant compounds observed in our study to estimate the ozone and SOA formation potentials. In general, BTP site depicted higher potentials than UFABC for both OFP and SOAFP metrics. The OFP results showed that cis-2-hexene (47.7; 41.8 $\mu\text{g m}^{-3}$), toluene (29.3; 20.2 $\mu\text{g m}^{-3}$) and m+p-xylene (27.7; 25.9 $\mu\text{g m}^{-3}$) presented the higher contribution at BTP and UFABC, respectively (Figure 2.12). Additionally, toluene (39.5; 27.3 $\mu\text{g m}^{-3}$) and m+p-xylene (11.6; 10.9 $\mu\text{g m}^{-3}$) presented the higher contribution to the SOAFP estimation, followed by benzene (11.2; 8.2 $\mu\text{g m}^{-3}$), at BTP and UFABC, respectively (Figure 2.12).

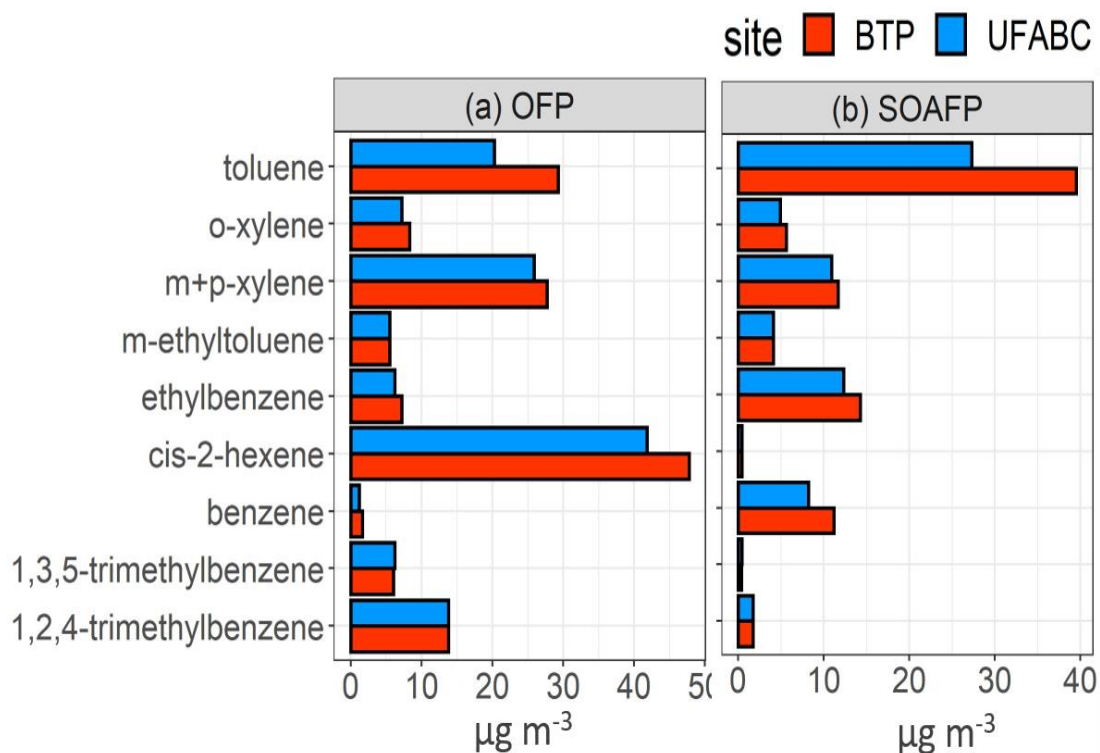


Figure 2.12. (a) Ozone Formation Potential (OFP) and (b) Secondary Organic Aerosol Formation Potential (SOAFP) estimation for most abundant compounds, at BTP (red) and UFABC (blue) sampling sites.

Even though other HCs have higher MIR values, the most abundant compounds (toluene, cis-2-hexene and m+p-xylene), present the highest OFP since the OFP is directly influence by the mixing ratio of each compound (Figure 2.12). For instance, 1,3,5-trimethylbenzene has a MIR of 11.76 and a reaction rate of $k_{\text{OH}} 57.0 \times 10^{-12} \text{ cm}^3 \text{ molecule}^{-1} \text{ s}^{-1}$ (Wang et al., 2013), but despite its significant reactivity, it does not present a large OFP ($6.1 \mu\text{g m}^{-3}$).

In the present study, aromatics represent a 64.6% of the OFP estimated for both sites, followed by alkenes and alkanes (32.6% and 2.8%, respectively). Studies carried out in industrialized areas have observed the contribution of alkenes, alkanes and aromatics as the main precursors of O_3 (An et al., 2014; Yuan et al., 2010). Additionally, alkylbenzenes and alkenes accounting for ~68% of the calculated potential for anthropogenic origin (Wu et al., 2017). Previous studies performed in the MASP showed that O_3 formation has been limited by VOCs, suggesting that control and reduction of VOCs emissions could be more effective to decrease O_3 concentrations

(Martins, 2006; Chiquetto, 2008; Alvim et al., 2011). Moreover, the main O₃ precursors in the MASP have been associated to alkenes, aldehydes, and aromatics from vehicular emission sources (Alvim et al., 2011; Dominutti et al., 2016). Nevertheless, these previous studies did not consider the potential effects from local industries emissions. In our estimation, aromatics represent 98% of the total SOA formation potential (Figure 2.12). A previous study in an industrialized area of China has predicted that alkenes and aromatics were the main responsible for SOA formation ranging from 10 to 30% and from 90 to 70%, respectively (Zhang et al., 2017).

In general, the ability to form SOA is also related to the one to form O₃. This pattern is commonly observed for toluene and m+p-xylene, which have previously been reported as compounds that mostly individually contributed to both SOA and O₃ formation (Wu et al., 2017). In accordance with this, our results show that m+p-xylene and toluene have a significant contribution in the formation of both secondary pollutants (Figure 2.12). Nonetheless, cis-2-hexene (due to its reactivity, $k_{OH} 63 \times 10^{-12} \text{ cm}^3 \text{ molecule}^{-1} \text{ s}^{-1}$) showed a dissimilar behaviour, with high contribution to O₃ formation ($45 \mu\text{g m}^{-3}$), and low to SOA formation ($0.4 \mu\text{g m}^{-3}$) at both sites.

2.3.6. Exposure risk

We provide here an estimation of non-cancer and cancer risk to analyze the hazard of BTEX inhalation for people who live, work, or circulate daily on the Great ABC region, especially in the vicinity of the PIC. Table 2.6 shows the estimated factors for each site. EC ranges from 0.32 to $2.43 \mu\text{g m}^{-3}$ with higher values for BTP than UFABC site (Table 2.6). HQ values less than 1 imply that there are not health effects expected, because the exposure is below the reference limit (Miri et al., 2016; Tohid et al., 2019; Ly et al., 2020). The values obtained during our study ranged from 0.0003 to 0.025 for the BTEX at the sampling sites do not exceed the U.S. EPA recommendation (<1) (Table 2.6), and the cumulative non-cancer hazard index (HI) was 0.07, suggesting

that HQ was negligible. Our results are in agreement with previous study at an industrial area, where HQ values ranged from 0.001 to 0.11 (Tohid et al., 2019).

Table 2.6. Calculated values of exposure concentration (EC), lifetime cancer risk (LCR), hazard quotient (HQ) and hazard index (HI) for the sampling sites of the present study. Inhalation exposure reference (RFC) and inhalation risk (IR) were obtained from U.S. EPA (IRIS) for each compound.

	Site	RFC ($\mu\text{g m}^{-3}$)	IR ($\mu\text{g m}^{-3}$)	EC	LCR	HQ	HI
Benzene	BTP	30	7.8×10^{-6}	0.74	5.75×10^{-6}	0.0246	0.07
	UFABC			0.55	4.25×10^{-6}	0.0182	
Toluene	BTP	5000		2.43		0.0024	
	UFABC			1.68		0.0017	
Ethylbenzene	BTP	1000		0.79		0.0002	
	UFABC			0.68		0.0001	
m,p-xylene	BTP	100		0.95		0.0095	
	UFABC			0.89		0.0089	
o-xylene	BTP	100		0.37		0.0037	
	UFABC			0.32		0.0032	
EPA recommendation					$<1 \times 10^{-6}$	<1	

The values for LCR less than 1×10^{-6} represent an acceptable risk, between 1×10^{-5} and 1×10^{-6} indicates a possible risk, between 1×10^{-4} and 1×10^{-5} a probable risk, and more than 1×10^{-4} can be defined as a definite risk (Hadei et al., 2018; Tohid et al., 2019; Ly et al., 2020). In the present study the LCR for benzene were 4.25×10^{-6} and 5.75×10^{-6} for UFABC and BTP, respectively, indicating a probable cancer risk. The LCR obtained from our results was higher than those reported for industrialized areas of Taiwan and Iran (3.68×10^{-7} and 7.82×10^{-6} , respectively, Tsai et al., 2019; Tohid et al., 2019) and in an urban area in Mexico ($1.09 - 5.28 \times 10^{-6}$, Bretón et al., 2020). However, our LCR values are lower than those estimated at urban areas for Beijing (4.19×10^{-5}) and Hanoi (3.56×10^{-5}) (Zhang et al., 2012; Ly et al., 2020).

2.4. Conclusions

Thirty-four hydrocarbons (C₆ - C₁₁) were quantified in MASP, specifically in the Great ABC Region, close to an extensive petrochemical area. Our observations depicted higher hydrocarbon concentrations at BTP than UFABC site (industrial and traffic sites, respectively). Among them, the most abundant HCs were aromatics, with higher contributions of toluene, benzene, xylenes and cumene. The total HCs concentrations at BTP site were less abundant than those observed at previous studies in MASP, by a factor ranging from 5.6 to 16.4 (Alvim et al., 2011, 2017, 2018; Dominutti et al., 2016) and 1.4 for BTEX + cumene (Dominutti et al., 2016). A possible explanation in these differences in the concentrations could be the VOC emission control strategies applied in MASP and a smaller contribution of vehicle emissions in the PIC area.

A similar BTEX profile was obtained when compared to those observed in Japan and United States. However, the mixing ratios observed at our sampling sites were higher, especially for BTP. The diurnal profiles did not show significant variation at BTP site. Nonetheless, the UFABC profile presented maximum values at rush hours, similar to the HCs diurnal variation already identified in MASP. The correlations between BTEX species suggested that benzene did not have similar emission sources to other BTEX compounds. A good correlation for benzene with cumene, especially at BTP site, indicated the potential influence of PIC activities in the emission of these compounds. However, despite the contribution of PIC, B/T ratios indicated that the main sources of HCs were related to vehicle emissions, while X/B ratios highlighted that this area might have been under the influence of air masses transported from other places, by the analysis of dominant wind direction frequency.

Our evaluation of potential health impacts and risks bring to light the effects that HCs concentrations near industrial areas can affect the population. Although the non-cancer hazard for BTEX was negligible, the lifetime cancer risk value calculated for BTP site was six times higher than the value recommended by U.S. EPA, indicating a probable cancer risk due to exposure to benzene.

Regarding secondary pollutants formation, cis-2-hexene presented mixing ratios increasing along the day, indicating the influence of its secondary photochemical production. Moreover, this compound has a high estimated potential to form O₃ (44.7 μg m⁻³), indicating a potential impact in the formation of secondary pollutants over the area. In addition, toluene and m+p-xylene showed high contributions on the ozone and SOA potential formation at both sites, reaching up to 103.1 μg m⁻³ and 89.3 μg m⁻³ of SOA.

Frequent exceedances of WHO guidelines for ozone and PM_{2.5} have been commonly observed in the PIC area, suggesting that additional efforts are needed to better understand the sources of their precursors and the implications on air quality degradation in the MASP atmosphere.

Chapter 3. Air Quality Impact Estimation Due to Uncontrolled Emissions from Capuava Petrochemical Complex in the Metropolitan Area of São Paulo (MASP), Brazil.

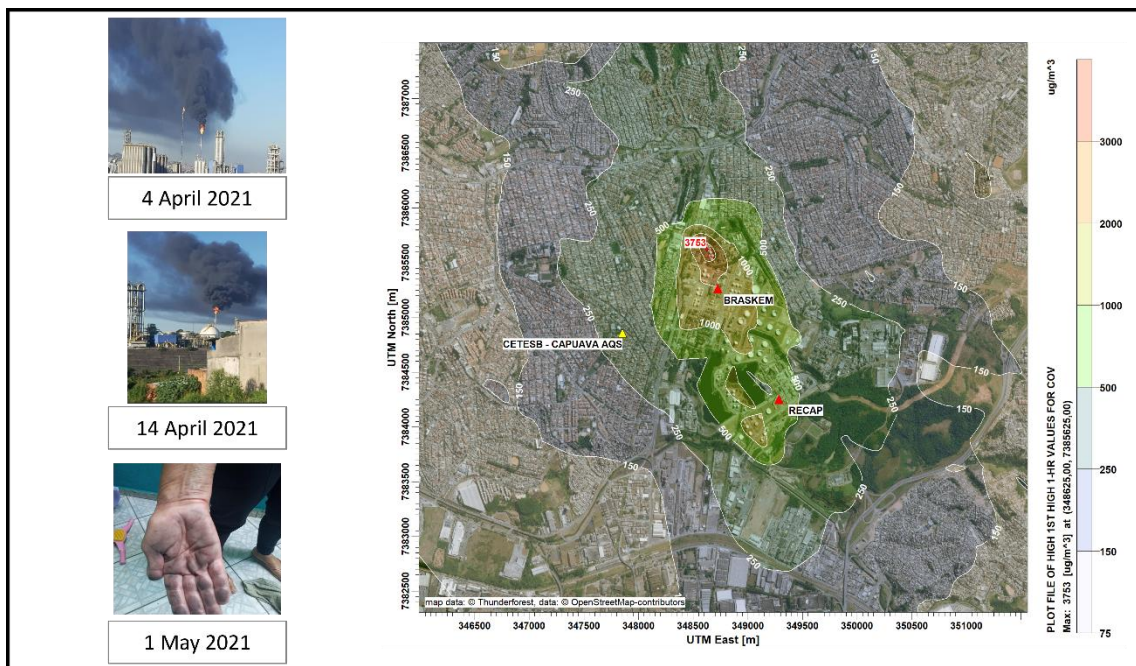


Article

Air Quality Impact Estimation Due to Uncontrolled Emissions from Capuava Petrochemical Complex in the Metropolitan Area of São Paulo (MASP), Brazil

Monique Silva Coelho ^{*}, Daniel Constantino Zacharias, Tayná Silva de Paulo, Rita Yuri Ynoue and Adalgiza Fornaro

GRAPHICAL ABSTRACT



3.1. Introduction

The metropolitan area of São Paulo (MASP) is among the largest urban agglomerations in the world with more than 22 million inhabitants. The official inventory of air pollutant sources showed that more than 7 million vehicles were responsible for the emission of 24.9 (72.8%), 48.3 (64.9%), and 1.22 (40%) kton per year

of hydrocarbons (HC) and particulate matter (PM), respectively, in 2020 (CETESB, 2022). On the other hand, despite being less intense, industrial sources and fuel-based storage were responsible for the emission of 9.3 (27.2%) and 3.6 (10%) kton per year of HC and PM, respectively (CETESB, 2021). In the southeast region of MASP there are seven important municipalities, known as the ABC region, with more than 2.8 million inhabitants; this is where Capuava Petrochemical Complex (CPC), the most important industrial complex of MASP, is located.

The CPC (lat. -23.6404, lon. -46.4843, Figure 3.1, in ABC region) stands out among the industrial emissions, contributing to the deterioration of air quality in that region (Coelho et al., 2021; Evo et al., 2011; Saiki et al., 2007). The CPC is composed of the Capuava Oil Refinery (RECAP), Braskem S.A. and other industries, in a range of ~8.5 km² inside a densely populated (~3400 inhabitants/km²) urban area.

This complex produces gasoline, diesel (S-10), liquefied petroleum gas (LPG) ethylene, propylene, and polyethylene from the distillation of naphtha, as well as fertilizers and various intermediates with the capacity to process about 53,000 barrels of oil per day (Saiki et al., 2007; Petrobras, 2020). Braskem S.A. and RECAP are close (~1.0 km) to the Capuava Air Quality Station (AQS) (Figure 3.1) that has been monitoring benzene and toluene since 2017, and they are representative of the urban air measurement, including the presence of the CPC (CETESB, 2022).

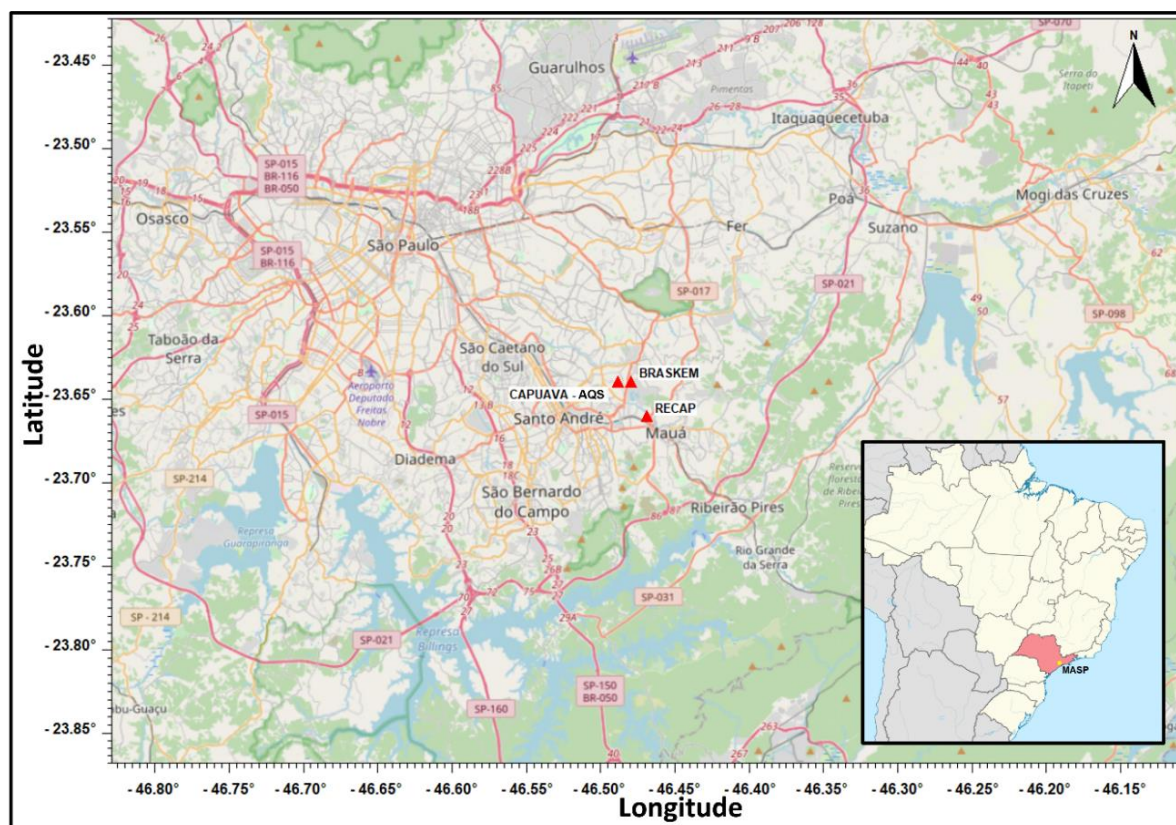


Figure 3.1. Metropolitan area of São Paulo (MASP) with Braskem and RECAP industries, and the CETESB, Capuava Air Quality Station, and AQS (identified by the red triangles). Source: Open-StreetMap.

On 14 April 2021, the Environmental Agency of São Paulo State (CETESB) announced that the companies Braskem S.A. and Capuava Refinery (RECAP), located inside the CPC, were fined for improper emissions that reached several neighborhoods, causing discomfort and hundreds of public complaints (CETESB, 2021). This was a consequence of general maintenance; for instance, the flare had been turned off for cleanup during April and May 2021 (approximately 50 days), causing the most acute period of odorous substance emission from 4 to 11 April 2021 (Diário do ABC, 2021). The effects registered, such as headaches and nausea, reported by residents correspond to the classical knowledge of exposure to VOCs (Otto et al., 1990; Sekar et al., 2019).

VOCs can be emitted directly into the atmosphere, in urban areas, by vehicle exhausts, fuel evaporation, solvent use, emissions of natural gas, and industrial processes. PM is emitted by vehicle exhausts, mainly those powered by diesel,

industrial processes, and re-suspended soil dust, in addition to that produced in the atmosphere by photo-chemical reactions (Evo et al., 2011; Sekar et al., 2019). VOCs have been widely studied around the world, both to assess their role in the formation of secondary pollutants, such as ozone (O₃) and secondary organic aerosol (SOA), and to determine health and environmental risks, due to their toxicity (Dominutti et al., 2020; Zhang et al., 2021; Mao et al., 2021; Xu et al., 2021; Liu et al., 2021; Harrison et al., 2021; Gao et al., 2021). PM₁₀ and PM_{2.5} concentrations higher than those of the World Health Organization (WHO) guidelines have been observed worldwide, as well as in MASP. Additionally, the human exposure to these particles has been evaluated as one of the top ten environmental health risk factors (Andrade et al., 2017; Bali et al., 2021; WHO, 2021).

A recent study has provided a detailed analysis of 35 non-methane hydrocarbons (NMHC) measured near the CPC area (Coelho et al., 2021), including alkanes (C₆-C₁₁), aromatics (C₆-C₁₀), and alkenes (cis/trans-2-hexene). The field campaign, which took place from 2016 to 2017, depicted the most abundant compounds near CPC as being toluene (1.5 ± 1.1 ppbv), cis-2-hexene (1.4 ± 1.9 ppbv), benzene (0.55 ± 0.66 ppbv), and m+p-xylene (0.58 ± 0.3 ppbv). Furthermore, the observations showed higher NMHC concentrations (by a factor of 2) at the site near the industrial complex when compared to the one located at the University Federal of the ABC (UFABC), where vehicular traffic dominates the pollutant emissions. The aromatics were the most abundant, reaching 56–58% among the evaluated hydrocarbons (Coelho et al., 2021). The evaluation of correlations and ratios of benzene, toluene, ethylbenzene, and xylenes (BTEX), all aromatic hydrocarbons that represent a significant fraction of VOCs (Lee et al., 2002), showed that in addition to the industrial influence around CPC, vehicular contributions were also observed (Coelho et al., 2021). The comparison with other industrial areas worldwide showed a similar NMHC profile as that in Japan and the United States of America (USA),

suggesting the presence of similar emission sources (Coelho et al., 2021; Tiwari et al., 2010; Leuchner et al., 2010).

The lifetime cancer risk for Capuava was estimated by comparing the risk among BTEX compounds. Benzene presented the highest probability of cancer risk, six times higher than the value recommended by the United States Environmental Protection Agency (US EPA) for people who spend most of their time at work or who live in Santo André and Mauá, especially in the CPC's vicinity (Coelho et al., 2021).

The biomonitoring of air pollution in Santo André city has evidenced the highest concentrations of pollutants in the vicinity of CPC, in comparison to the areas which are not under the influence of the industries (Saiki et al., 2007). In the same place, one study identified statistically significant effects between PM₁₀ levels and hospitalizations of elderly patients associated with congestive heart failure (Evo et al., 2011). Another study investigated the air pollution relationship with blood pressure alterations and concluded that traffic controllers working outdoor shifts in Santo André presented higher blood pressure during exposure to local pollutants (Chiarelli et al., 2011). In addition, atmospheric pollutants in the CPC area seem to be the highest risk factor for primary hypothyroidism in children and adults, but a considerable increase in the incidence of this disease was observed in residents in the proximity of CPC (Zaccarelli-Marino 2012; Zaccarelli-Marino et al., 2016 and 2019).

Since the 1990s, the CETESB AQS has been monitoring O₃, nitrogen dioxide (NO₂), sulfur dioxide (SO₂), inhalable particles (PM₁₀), fine particulate matter (PM_{2.5}), and carbon monoxide (CO) concentrations in MASP. Frequent exceedances of WHO guidelines (WHO, 2021) for O₃ and PM_{2.5} have been reported in the CPC area. In 2017, CETESB began the automatic hourly monitoring of benzene and toluene at Capuava AQS, which is the only station that monitors these compounds in this area, representing the influence of industrial emissions in the region.

Capuava had the highest annual average concentrations for benzene when compared with the CETESB AQS in the other large industrial areas such as the cities

of Cubatão and Paulínia. The benzene annual averages in recent years were as follows: 2017: 2.8 $\mu\text{g m}^{-3}$; 2018: 1.6 $\mu\text{g m}^{-3}$; 2019: 2.8 $\mu\text{g m}^{-3}$; and 2020: 2.6 $\mu\text{g m}^{-3}$, and toluene annual averages were as follows: 2017: 5.7 $\mu\text{g m}^{-3}$; 2018: 5.0 $\mu\text{g m}^{-3}$; 2019: 5.0 $\mu\text{g m}^{-3}$; and 2020: 3.9 $\mu\text{g m}^{-3}$ at Capuava AQS (CETESB, 2022). At the same station, for 2020, aldehydes were also monitored. The averages observed for formaldehyde and acetaldehyde were 4.3 and 3.2 $\mu\text{g m}^{-3}$, respectively, and their maximum values were 21.9 and 15.3 $\mu\text{g m}^{-3}$, respectively (CETESB, 2022).

The health effects caused by the presence of industrial emissions in the region have already been demonstrated in previous studies (Evo et al., 2011; Saiki et al., 2007; Chiarelli et al., 2011; Zaccarelli-Marino 2012; Zaccarelli-Marino et al., 2016 and 2019), and air quality stations have been showing that pollutant concentrations constantly exceed the Brazilian air quality standards (CETESB, 2022). In MASP, where vehicular emissions have been decreasing in recent decades (Andrade et al., 2017), it is necessary to evaluate other sources of air pollution, such as industrial emissions and their implications in air quality degradation, mainly in acute episodes, as we discuss in the present study.

Despite the few studies developed in the great ABC region, the evidence of the air pollution health effects, and the fact that local industrial emissions are an additional source of VOCs in MASP, little is known about CPC emissions that result in odor and soot episodes denounced by the media in that neighborhood. In this paper, we provide a detailed analysis of the benzene, toluene, and PM_{10} concentrations measured in the Capuava AQS from 2017 to 2022. We provide statistical analyses from these Capuava AQS hourly data and near-field plume modeling (AERMOD) results, improving the knowledge about the contribution of uncontrolled emissions from CPC during the episode and their environmental impacts.

3.2. Materials and Methods

3.2.1. Gaussian Plume Model (AERMOD)

In the state of the art of regulatory models, AERMOD (steady-state plume model) is recommended for short-range impact, <50 km (US EPA, 2022). On the other hand, CALPUFF (California Puff: non-steady-state puff dispersion model) (US EPA, 2022) and FLEXPART (flexible particle dispersion model) (US EPA, 2022) are suggested for longer ranges (>50 km), while CMAQ (community multiscale air quality) (US EPA, 2022) is developed for photochemistry modeling, and HYSPLIT (hybrid single-particle Lagrangian integrated trajectory) is designed for complex dispersion and deposition simulation (Bihalowicz et al., 2021).

AERMOD is a Gaussian plume model used to simulate nearfield pollutant dispersion from industrial sources. It is based on the planetary boundary layer turbulence structure from Monin–Obukhov similarity theory, and it includes the treatment of both surface and elevated sources, as well as simple and complex terrain (Venkatram et al., 2001). AERMOD has been tested in several arrangements: industrial and agricultural facilities, with high-resolution land use modeling episodes, or multiple years spent conducting environmental impact assessments. It has been estimating the levels of exposure to gases and PM of the population living close to the installations (Cerqueira et al. 2019, Macêdo and Ramos, 2020, Kelleghan et al., 2021, Pirhalla et al. 2021, Tyovenda et al. 2021, Pecha et al. 2021; Cimorelli et al., 2005; Motalebi and Guo, 2021). In the regulatory applications as environmental impact assessments (EIAs), AERMOD simulations cover the most recent 5-year period of atmospheric data. A worst case scenario was applied, estimating the highest concentrations that can be found in an area, with five years of recurrence (Kelleghan et al., 2021).

Different studies have been developed using this model, such as the dispersion of pollutants from thermal power plants (Cerqueira et al. 2019) and the evaluation of atmospheric vehicle pollution (Macêdo and Ramos, 2020); atmospheric dispersion and

the deposition of ammonia (Kelleghan et al., 2021); laboratory dispersion experiments to improve dispersion model performance (Pirhalla et al. 2021); modeling CO₂ and NO₂ emission from an industrial stack (Tyovenda et al. 2021), and oil refinery odor emission rates estimated via reverse dispersion modeling (Motalebi and Guo, 2021).

The substantial simulation period (five years) helps to ensure the inclusion of the worst case scenario in the modeling period (Kelleghan et al., 2021). However, situations with loss of emission control, as occurred in Capuava in 2021, are not provided in the EIAs and can generate higher concentrations, causing harmful acute effects among the population health.

The Lakes Environmental © AERMOD v. 10.0.1 was used to model the dispersion of CPC emission of pollutants (VOC and PM) for the episode period to predict ground-level pollutant concentrations in the stable boundary layer (SBL) and in a horizontal direction in the convective boundary layer (CBL) (Cimorelli et al., 2005). AERMOD requires source data (source geometry, pollutant emission rates, emitted gas stream temperature, and flow rate (Table 3.1)), topographical data for sources and receptors, and meteorological data (Table 3.2) as inputs and outputs of ambient pollutant concentrations at receptors. Two preprocessors called AERMAP and AERMET convert raw topographical and meteorological data to the readable format for AERMOD through two separate runs before dispersion modeling runs (Motalebi and Guo, 2020; Hennig et al., 2001).

Table 3.1. Summary of AERMOD input data extracted from Environmental Licenses of Braskem and RECAP.

BRASKEM STACK	COORDINATES (m)		FLOW RATE (Nm ³ /s)	POLLUTANTS (mg/Nm ³)	
	UTM X	UTM Y		PM	
1	348568	7384835	17.372		91.820
2	348568	7384835	17.927		24.780
3	348588	7384829	19.936		31.410
4	348611	7384825	14.572		11.030
5	348580	7384809	16.846		30.670
6	348562	7384812	18.149		12.410
7	348604	7384802	18.740		13.860
8	348595	7384773	18.140		80.240
9	348572	7384778	6.923		99.560
10	348623	7384797	8.607		44.380
11	348642	7384784	2.195		23.240
12	348532	7384771	18.033		11.450
13	348527	7384775	16.853		0.000
14	348443	7384959	2.534		0.000
15	348443	7384949	0.975		0.000
16	348446	7384972	5.194		0.000
17	348487	7385054	3.497		0.000
18	348478	7385023	1.003		0.000
19	348490	7385064	11.804		0.000
20	348552	7384838	12.148		0.000
21	348546	7384818	12.148		0.000
22	348475	7384810	86.027		17.800
23	348759	7385190	30.920		8.820
24	348756	7385208	20.900		5.360
25	348581	7384731	56.192		0.000
26	348557	7384736	56.192		0.000
27	348595	7384740	54.290		0.000
28	348570	7384746	54.290		0.000

RECAP STACK	COORDINATES (m)		FLOW RATE (Nm ³ /s)	POLLUTANTS (mg/Nm ³)	
	UTM X	UTM Y		VOC	PM
1	7384480	349130	12.500		31.340
2	7384470	349140	12.500		42.650
3	7384450	349150	12.500		33.620
4	7384400	349290	61.111		45.690
5	7384390	349270	12.500		94.580
6	7384330	349340	13.889		37.710
7	7384500	349180	1.111		211.480
8	7384510	349230	1.667	0.01	0.010
9	7384150	349840	1.667	0.01	0.010
10	7384447	349377	1.667	0.001	36.660

11	7384319	349508	1.667	0.001	39.07
12	7384331	349517	1.667	0.001	39.07
13	7384283	349456	8.333	0.04	0.320
14	7384414	349580	25.000		38.300
15	7384362	349371	1.389		188.900

Table 3.2. Summary of statistical analysis of AERMET input data.

	Temperature	Relative humidity	Atmospheric pressure	Wind direction	Wind speed	Cloud coverage level	Cloud height level
	(° C)	(%)	(hPa)	(°)	(m.s ⁻¹)		
Availability (%)	99.9	99.9	100.0	99.8	100.0	100.0	100.0
Mín.	11.6	18.0	919.4	0.0	0.0	0.0	0.0
Mean	19.4	71.4	927.0	134.8	1.3	4.5	4882.9
Máx.	30.2	93.0	934.8	360.0	3.2	10.0	9999.0
S.D.	3.6	16.1	2.6	93.6	0.6	3.9	4011.3

The terrain was pre-processed using AERMAP and SRTM1/SRTM3 data. The Shuttle Radar Topography Mission (SRTM, (Hennig et al., 2001)) digital elevation data are part of an international research effort that obtained digital elevation models on a near global scale, provided by National Aeronautics and Space Administration (NASA) at a resolution of 1 arc second (approximately 30 m). The land use was pre-processed using NLCD 2001–2016 land use codes (National Land Cover Database, Wickham et al., 2021) with 1 km GLCC data (global land cover characterization). GLCC is a series of global land cover classification datasets that are based primarily on the unsupervised classification of 1 km AVHRR (advanced very-high-resolution radiometer) and 10-day NDVI (normalized difference vegetation index) composites (USGS, 2021). GLCC data were post-processed using 2021 Google Earth satellite images and WebLakes Land User Creator to increase the horizontal resolution until 1 arc second (approximately 30 m).

Emission rates, buildings, stacks, and industrial maps were obtained via the EIA and environmental licenses from CETESB (Braskem process number 16/01562/04, license 16011156, dated 15 March 2021, and RECAP process number 16/01566/04, license 16011084, dated 4 January 2021) due to the law on access to information,

privacy, and health research in Brazil (Federal Law n. 12.527/2011). In addition, using the industrial map, we visually identified the tanks in order to insert an estimation of fugitive emissions. We made the following considerations: height and diameter of each tank and VOC flow rate of 0.5 m s^{-1} . Braskem and RECAP's EIA were used in the industrial tridimensional modeling (Figure 3.2).



Figure 3.2. Braskem and RECAP industrial plants on tridimensional modeling. In blue are the buildings or tanks, in red are the point sources (stacks/flare). Source: Google Earth (accessed on 11 March 2023)

3.2.2. Air Quality Data Analysis

The available data of hourly pollutants (PM_{10} , benzene, and toluene), wind direction, and wind speed from Capuava (<https://cetesb.sp.gov.br/ar/qualar/>. Accessed on 10 January 2023) were analyzed from 2017 to 2022. Statistical analyses of data were performed using R statistical software—open air package (<https://www.r-project.org/>. Accessed on 18 June 2022. (Carlaw and Ropkins, 2012))—which has been used extensively in different studies, such as elements inside $\text{PM}_{2.5}$ in urban areas (Ciu et al., 2020), the analysis of air pollution on a roadside (Kamara et al., 2021), air pollution and biomass burning (Squizzato et al., 2021), and the study of different VOC sources (Dominutti et al., 2016; Dominutti et al., 2020; Vestenius et al., 2021).

The normalization in the diurnal profiles enables the comparison among variables on contrasting scales. The variables were divided by their mean values, which helped compare the diurnal trends for the compounds evaluated in the present study (Cui et al., 2020; Chang and Hanna, 2004). Additionally, pollutant concentrations with values higher than $(\text{mean} + 3 \times (\text{standard deviation}))$ were considered to be outliers in the data validation and were excluded from boxplot analyses. To identify potential contributions from the sources, we used the polar annulus function, which is a graphical resource that provides temporal variation in concentrations for each compound according to wind direction. The code and major information are available in the open air package manual (Carslaw and Ropkins, 2012).

The Pearson correlation coefficient between modeled data (AERMOD) and Capuava AQS data was analyzed to provide a statistical evaluation for the AERMOD performance (Chang and Hanna, 2004). The Pearson correlation is normally used to reflect the linear correlation and it demonstrates the contribution from similar emission sources (Parrish et al., 1998; Mao et al., 2021).

3.3. Results and Discussions

3.3.1. Air Quality Data

The episode period of uncontrolled emissions (April–May 2021) was statistically analyzed by comparing the previous (2017–2020) and the subsequent (2021–2022) periods (Figure 3.3 and Table 3.3). The annual averages at Capuava AQS varied from $21.6 \mu\text{g m}^{-3}$ to $29.4 \mu\text{g m}^{-3}$ for PM_{10} , from $1.5 \mu\text{g m}^{-3}$ to $4.2 \mu\text{g m}^{-3}$ for benzene, and from $3.7 \mu\text{g m}^{-3}$ to $5.9 \mu\text{g m}^{-3}$ for toluene (Figure 3.3 and Table 3.3). It is possible to determine the variability of the data through the interquartile intervals between the first and third quartile. Thus, the highest variability and values of PM_{10} , benzene, and toluene happened with the highest amplitude, as well as the average concentrations reaching $29.3 \mu\text{g m}^{-3}$ (PM_{10}), $4.6 \mu\text{g m}^{-3}$ (benzene), and $7.1 \mu\text{g m}^{-3}$ (toluene) in this episode period (Figure 3.3 and Table 3.3).

Table 3.3. Summary of statistical analysis for hourly concentrations ($\mu\text{g m}^{-3}$) in the Capuava AQS, during 2017-2022 and modeled data provided by AERMOD.

BENZENE								
Year	Mean	S.D.	Max.	Min.	Median	1 st quartile	3 th quartile	N
2017	2.70	3.98	52.6	0.1	1.2	0.54	2.92	8277
2018	1.55	2.6	46.2	0.1	0.62	0.32	1.63	6561
2019	2.70	4.25	74.5	0.1	1.3	0.58	2.95	7567
2020	2.48	4.19	52.2	0.1	0.91	0.48	2.42	1630
Episode	4.60	8.73	79.1	0.02	1.45	0.64	4.26	1141
2021	4.19	7.1	77.7	0.1	1.6	0.75	4.38	4878
2022	3.06	4.93	49.4	0.1	1.3	0.6	3.3	3154
TOLUENE								
2017	5.37	4.89	44.7	0.14	4.1	1.94	7.16	8291
2018	4.74	4.8	55.3	0.15	3.34	1.63	6.17	6562
2019	4.71	5.29	64.6	0.1	3.26	1.45	6.18	7564
2020	3.74	3.96	48.2	0.14	2.7	1.21	5.1	1628
Episode	7.10	7.34	58.7	0.3	5.07	2.04	9.4	1154
2021	5.97	6.4	69.4	0.1	4.1	1.64	7.83	4867
2022	5.55	6.25	72.8	0.1	3.7	1.30	7.5	3153
PM₁₀								
2017	26.0	21.5	184	1.0	21.0	12.0	35.0	8585
2018	24.6	20.7	192	1.0	19.0	11.0	33.0	8305
2019	21.6	17.3	222	1.0	18.0	9.0	29.0	7951
2020	21.7	19.8	171	1.0	16.0	8.0	28.0	7221
Episode	29.3	25.5	174	1.0	21.0	11.0	39.0	1450
2021	28.1	22.8	201	1.0	22.0	13.0	36.0	7021
2022	29.4	21.4	185	1.0	25.0	15.0	38.0	4321
Modeled data - April and May, 2021								
PM	5.8	13.9	119.1	0.03	0.81	0.24	3.81	1464
VOC	27.84	61.0	433.8	0.3	4.2	2.1	9.94	1464

When we compare the mean concentrations between the previous period (2017–2020) and episode (April–May 2021), an increase by a factor of 1.95, 1.53, and 1.25 was observed for benzene, toluene, and PM₁₀, respectively. However, a small increase in the average values in 2021 and 2022 was observed when compared to the previous period (2017–2020) by a factor of 1.54, 1.24, and 1.22 for benzene, toluene, and PM₁₀, respectively.

It is important to highlight that these higher concentrations that continued to be observed after the episode (Figure 3.3 and Table 3.3) may have characterized a change not only in the episode but also in the internal protocols of these companies. However, reports or references presenting information about this have not been found. Yet, these variations for the period after this episode still cannot be fully explained. Nevertheless, it is worth highlighting that the subsequent period corresponds to the post-pandemic period. Additionally, the available data of 2022 correspond only to a half year, from January to June.

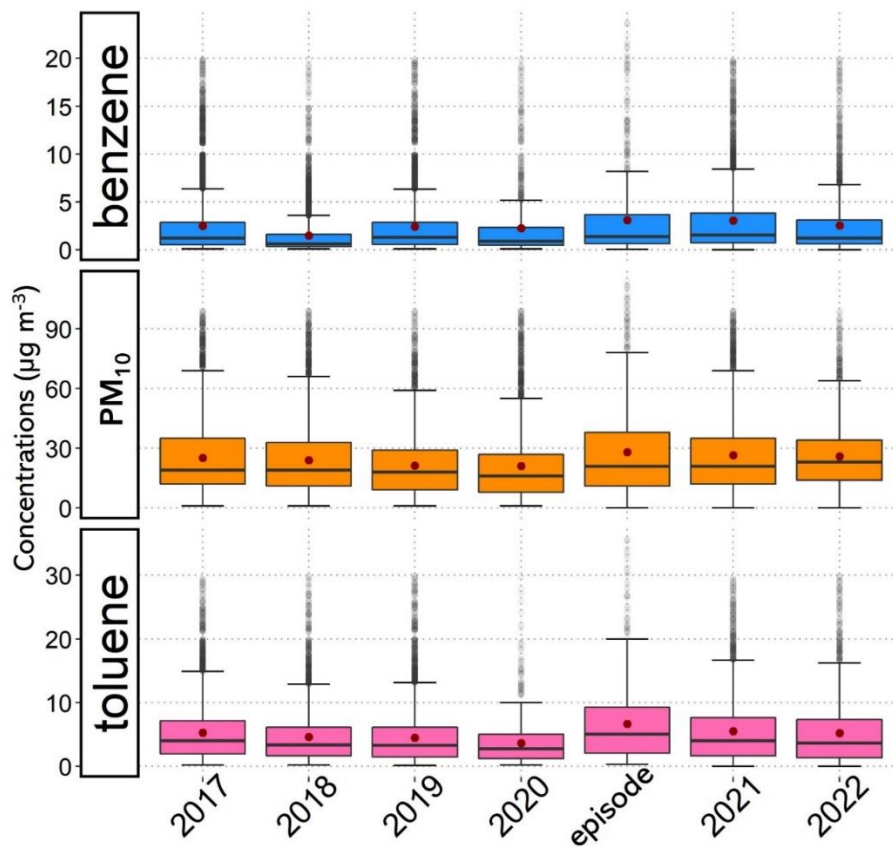


Figure 3.3. Annual boxplots of 1 h concentrations ($\mu\text{g m}^{-3}$) for PM10, benzene, and toluene at Capuava AQS, from 2017 to 2022, and for each episode. Boxplot width and the lower and upper hinges correspond to the first and third quartiles (the 25th and 75th percentiles). Lower whisker: smallest observation greater than or equal to lower hinge - $1.5 * \text{IQR}$ (interquartile range), above 75th percentile. Upper whisker: largest observation less than or equal to upper hinge + $1.5 * \text{IQR}$, below 25th percentile. The middle is the median (50% quantile), and the red point is the mean value. Points beyond the end of the whiskers are “outliers”, which correspond to values > 1.5 and < 3 times the standard deviation (sd). The data were presented on the Y axis with an appropriate scale for good visualization of the percentiles and the mean in relation to the median. Obs.: The episode corresponds to April–May of 2021, 2021 corresponds to the other months of this year, the data available for 2020 were only from January to March, and 2022 was only from January to June.

The normalized concentrations in relation to the mean value profiles of PM₁₀, benzene, and toluene from April to May for each year from 2017 to 2022 are presented in Figure 3.4. PM₁₀ shows higher concentrations at night, showing peaks after 9 pm, especially in 2017, 2018, 2019, and 2020 (Figure 3.4). The minimum values of PM₁₀ observed in 2020 may have been the consequence not only of the pandemic situation, but also of the influence of meteorological parameters. For instance, in this year, the number of unfavorable days (planetary boundary layer < 400 m) to the dispersion of pollutants was lower in comparison with the last ten years (CETESB, 2022). The diurnal cycles observed in the present study for PM₁₀ agreed with the previous studies in MASP and the Great ABC Region (Carvalho et al., 2015; Valverde et al., 2020).

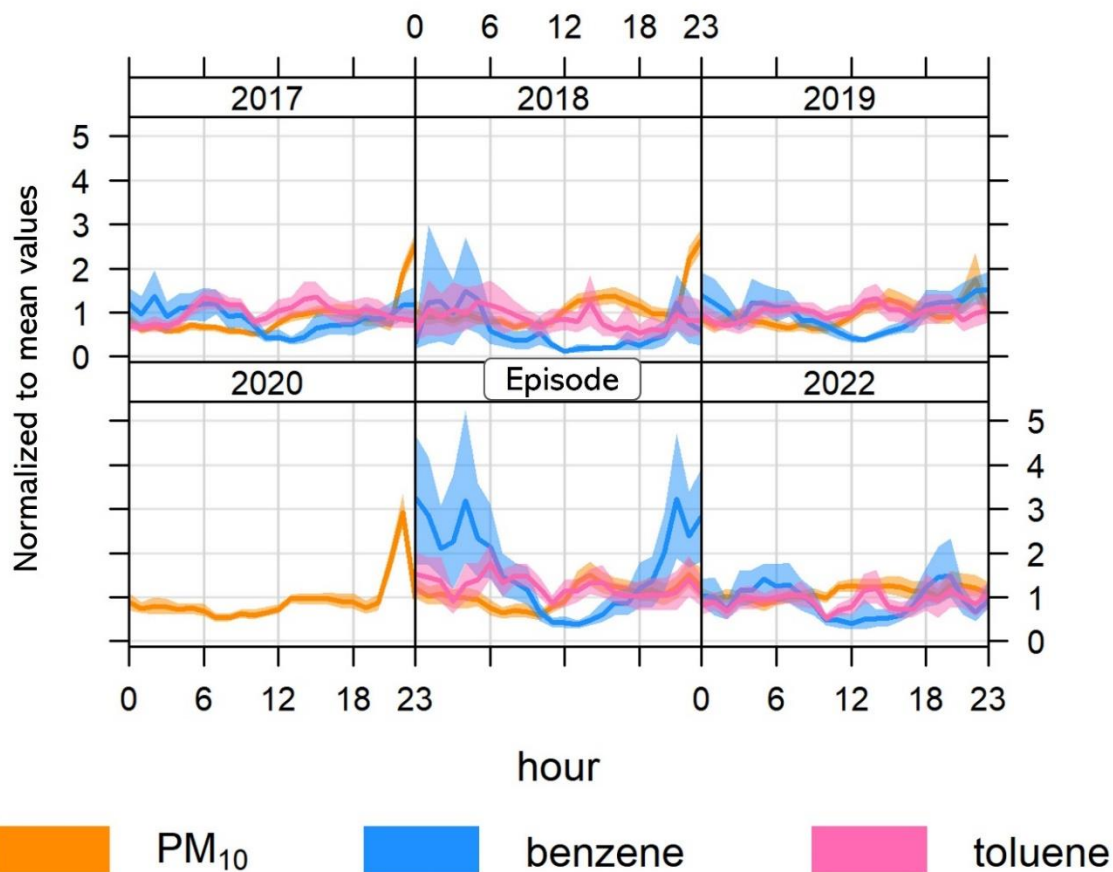


Figure 3.4. Normalized concentrations in relation to the mean value profiles for PM₁₀, benzene, and toluene at Capuava AQS, from April to May for each year from 2017 to 2022. Episode represents the 2021 concentrations.

For benzene and toluene, there are no data available for 2020 to compare with other years. Benzene shows a profile with higher concentrations from 6 p.m. to 6 a.m. (Figure 3.4). Despite fugitive emissions from RECAP and Braskem that remained almost constant during the 24 h period, it was possible to observe a decrease in the benzene concentrations during the afternoon. Toluene showed a divergent profile concerning the other pollutants evaluated (Figure 3.4). Although higher values were observed during the day, a peak in concentrations could be seen twice, at 6 a.m. and 2 p.m. (Figure 3.4). It is probable that the first peak was a result of local traffic emission, considering that toluene is commonly emitted by vehicular fleets (CETESB, 2022; Jiang et al., 2017). A possible explanation for the diurnal peak is the more intense emission of toluene by some point source, such as CPC industrial emissions (Coelho et al., 2021; Simpsons et al., 2010).

Toluene is around five times more reactive than benzene (Ragothaman et al., 2017), especially during hours with intense solar radiation. The constant rates with OH radical for toluene and benzene are $k_{OH} 5.96 \times 10^{-12} \text{ cm}^3 \text{ molecule}^{-1} \text{ s}^{-1}$ and $k_{OH} 1.23 \times 10^{-12} \text{ cm}^3 \text{ molecule}^{-1} \text{ s}^{-1}$, respectively (Ragothaman et al., 2017; Atkinson et al., 2003). Toluene is expected to have a decreasing concentration profile compared to benzene at times of higher photochemistry action. Considering these different profiles between benzene and toluene, one might think that toluene presented more intense emissions than all of the working atmospheric removal processes.

The previous study in the CPC region demonstrated a poor correlation of benzene with other aromatic HCs (toluene, ethylbenzene, m,p, and o-xylenes) and a strong correlation with cumene (CPC product (Coelho et al., 2021; Braskem, 2020; ABC do ABC, 2021). This indicates that benzene might be related to industrial sources (Coelho et al., 2021). Due to the fact that toluene is commonly emitted by vehicles, the result from the present study indicates that the CPC is an important emission source for this pollutant. For the episode period, the profiles of pollutants generally presented

a similar variation, even though an increase in the mean concentrations was observed via a 2-time factor for PM₁₀, benzene, and toluene.

The effect of the wind directions for pollutant concentration variations can indicate the CPC contributions during the day (Figure 3.5). Benzene showed higher concentrations ($\geq 10 \mu\text{g m}^{-3}$) from 11 p.m. to 8 a.m., during northeast wind directions, while values below $2 \mu\text{g m}^{-3}$ were observed in other orientations. For the episode period, the highest concentrations remained with the northeast winds, reaching values above $15 \mu\text{g m}^{-3}$ at dawn (Figure 3.5).

Toluene and PM₁₀ showed similar distributions regarding all wind directions during the day. Toluene presented higher values from northeast winds, with a peak in the late hours of the day, reaching values higher than $20 \mu\text{g m}^{-3}$ during the episode. PM₁₀ showed concentrations above $40 \mu\text{g m}^{-3}$ from all wind directions during the previous period in the first hours of the day, and contributions from southeast to northeast with concentrations between $30 \mu\text{g m}^{-3}$ and $45 \mu\text{g m}^{-3}$ from 6 p.m. to 10 p.m. (Figure 3.5).

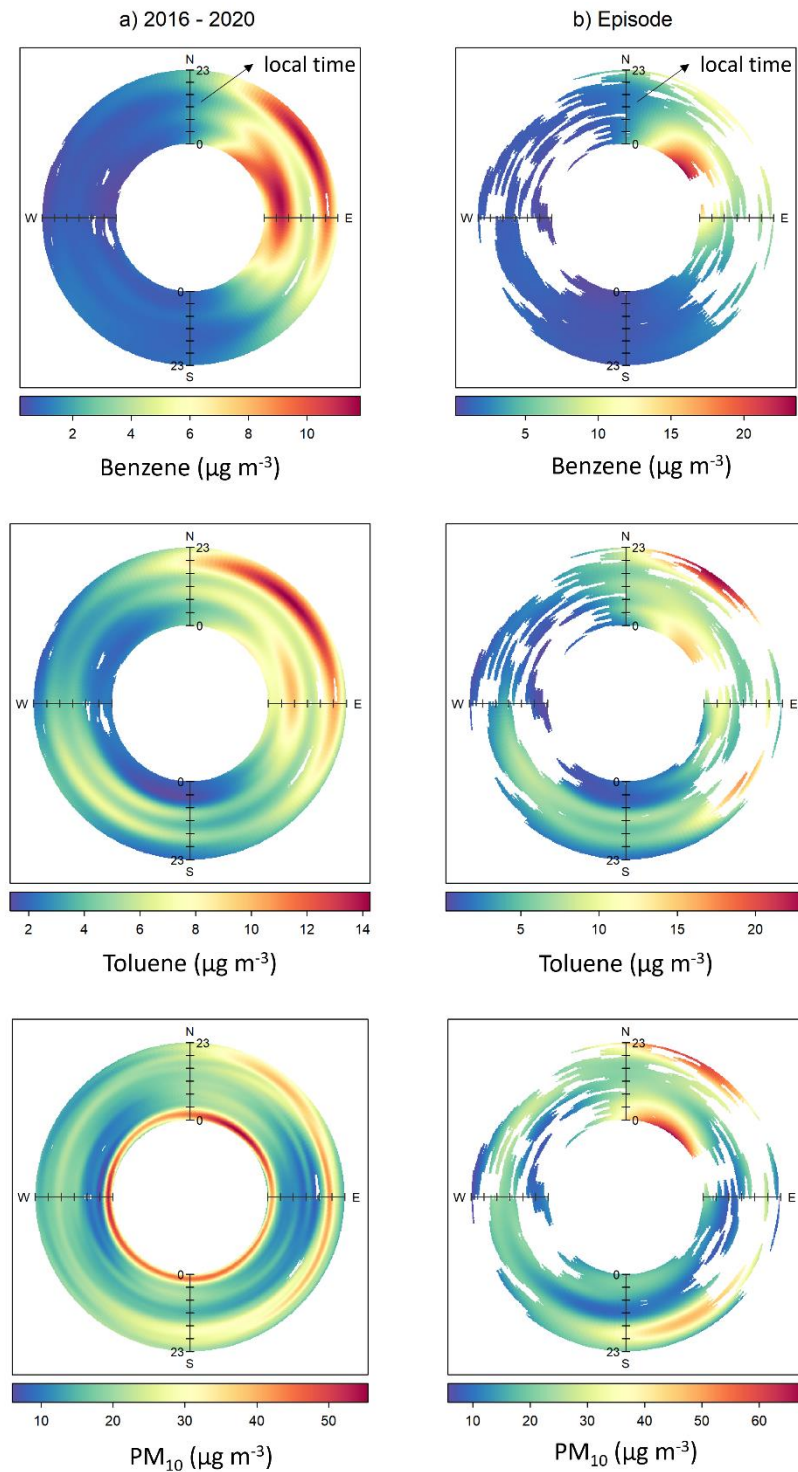


Figure 3.5. Changes in benzene, toluene and PM₁₀ mean hourly concentrations at Capuava station, depending on wind directions. a) Polar annulus plots from 2017 – 2020 and b) Polar annulus plots for episode from April to May 2021. Color scale represents concentrations ($\mu\text{g m}^{-3}$), the thickness in the circle represents the hour of the day: 00:00 inside to 11:00 p.m. outside. Blank spaces are missing values.

For the episode, values between $30 \mu\text{g m}^{-3}$ and $50 \mu\text{g m}^{-3}$ were observed from the southeast, and concentrations were $\geq 50 \mu\text{g m}^{-3}$ from the northeast, from 10 p.m. to 4 a.m. A clear pattern can be observed for these pollutants (PM_{10} , benzene, and toluene) in the previous period as well as in the episode, and the major contribution for the highest concentrations comes from the CPC direction.

Data from Capuava AQS station presented PM_{10} $29.3 \pm 25.5 \mu\text{g m}^{-3}$ average concentrations with minimum and maximum values varying from 1.0 to $174.0 \mu\text{g m}^{-3}$, respectively, with maximum values being between 1 a.m. and 4 a.m. (Figure 3.6). In the first half of April, a sequence of PM_{10} peaks was observed at the same scheduled time (1 a.m.) associated with the periodic use of the flares, with the maximum values ranging from 60 to $100 \mu\text{g m}^{-3}$ on average (Figure 3.6). After the main flare shutdown for cleaning and maintenance, there was a change in the behavior of the PM_{10} nocturnal peaks (from 17 April). In early May, the main flare was restarted and high concentrations of PM_{10} , varying from 100 to $174 \mu\text{g m}^{-3}$, were again noticed (Figure 3.6).

The PM_{10} concentrations observed in Figure 3.6 cannot be explained by special meteorological events, and not even by the behavior of a typical profile of traffic emissions in this area. Therefore, flare emissions could have been the leading source of the concentrations observed in Capuava's AQS. This possibility was reinforced by the constant reports of a deposition of greasy soot in the houses (ABC, 2021). The chemical composition of a mixed deposition has been evaluated in a previous study, in the vicinity of CPC, where it showed the highest contribution of heavy metals, such as lead, and strong acids (sulfuric and nitric). This study has identified emission sources such as the oil refinery and the surrounding traffic routes (Valverde et al., 2020).

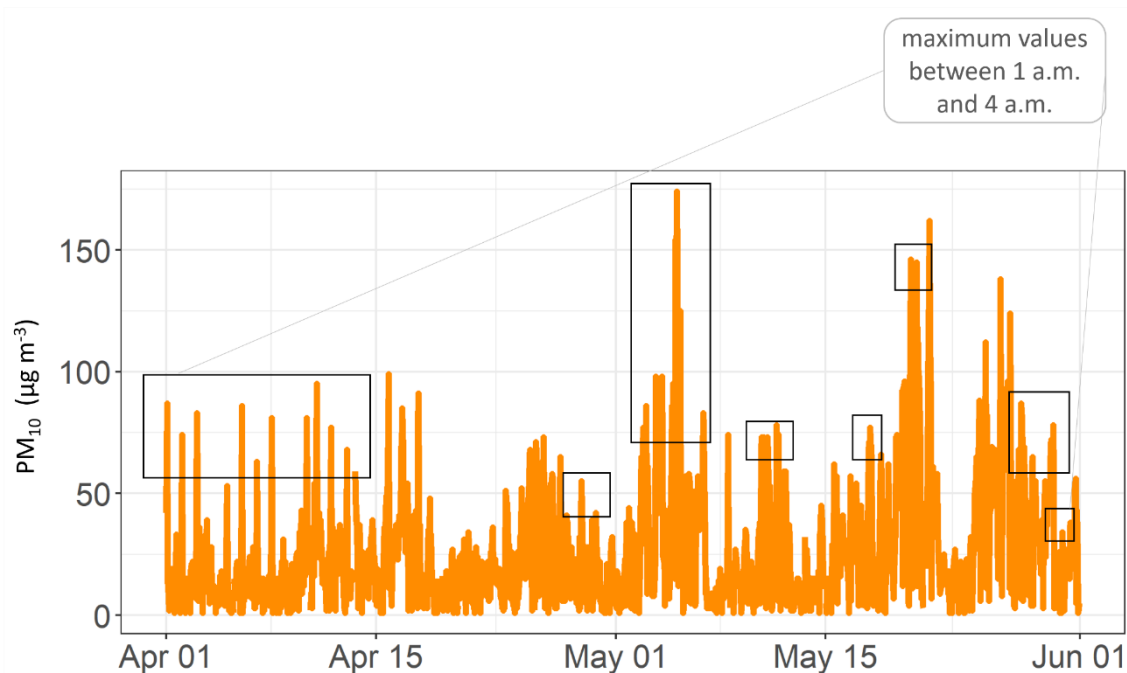


Figure 3.6. Hourly concentrations of PM10 at Capuava AQS, during the episode (April to May 2021). Rectangles represent the peaks observed from 1:00 a.m. to 4:00 a.m.

3.3.2. Air Quality Modeling

The AERMOD model gives a 1 h average for PM and VOC concentrations providing temporal series that were compared with the data of benzene, toluene, and PM10 from Capuava AQS (Figure 3.7a). For this purpose, the data were filtered by the wind direction, considering only hourly data when the wind direction was in the preferred quadrant for CPC emissions (0° – 180°) (Figure 3.7b). The comparison between PM and VOC provided by AERMOD and PM10, benzene, and toluene was provided. In general, the minimum and maximum values coincided with the AERMOD data versus the Capuava AQS data. These results also indicate that the AQS is well located and has a significant representative area.

Positive correlations were observed between VOC–AERMOD and benzene–AQS ($r = 0.62$), and for VOC–AERMOD and toluene–AQS ($r = 0.26$). A linear correlation indicates that CPC could be responsible for more than 60% of benzene behavior in the Capuava AQS. Considering all of the limitations of the Gaussian plume model in a

complex urban atmosphere, this is a satisfactory result (Figure 3.7a), although toluene showed poor levels of linear correlation ($r = 0.26$).

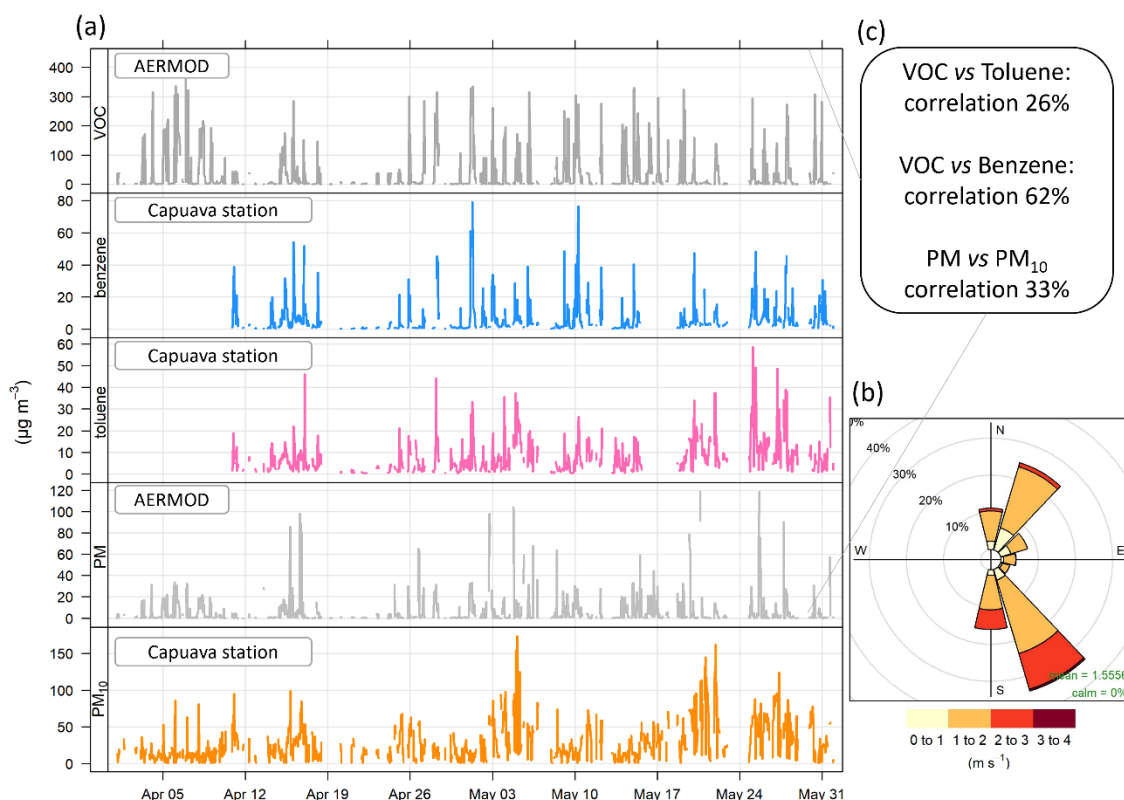


Figure 3.7. (a) Hourly mean concentrations for benzene, toluene, and PM₁₀ at Capuava AQS, VOC, and PM (AERMOD: modeled data) during the episode (April to May 2021), white spaces are missing values. (b) The wind rose shows the wind speed (m s^{-1}) and wind direction ($^{\circ}$), data were filtered by the preferential wind direction from the Capuava Petrochemical Complex (0° to 180°) (c) “Correlation” is the correlation coefficient of Pearson.

The linear correlation between benzene and toluene measurements from the Capuava AQS was less than 50% ($r = 0.49$). From the observations of the diurnal profile (Figure 3.4), we can consider that pollutants were emitted by the same sources, as discussed earlier. However, a possible explanation for the low correlation between them is that toluene emissions were more intense than for benzene. These findings, along with our observations here, lead us to some possible explanations, such as that the emission of benzene was not as constant as that of toluene. Benzene emissions can

result either from a less-used product or from the activation of a sporadic production line, resulting in fewer emissions.

The low level of the PM linear correlation that followed (PM–AERMOD and PM₁₀-AQS ($r = 0.33$)) was an unexpected result. The simulation conditions (industrial sources, near-field model, very close weather station, and good description of building downwash) were appropriate for modeling a pollutant such as PM₁₀. This poorer result of linear correlation ($r = 0.33$) makes it evident that local traffic has an important role in the emissions of particulate matter. However, vehicle and truck traffic could not explain the behavior of early morning peaks, or the soot layers observed on the houses. Therefore, it is quite possible that the emissions inventory used in the EIA is incomplete or underestimated.

In operational conditions, PM emission rates around 2 g s^{-1} are acceptable; however, in poor burning conditions, this value may be an order of magnitude higher (Johnson et al., 2011; McEwen et al., 2012). Flaring is the common practice of burning unwanted, flammable gases via combustion in an open atmosphere, usually to avoid system overload. Although flares are a security system to prevent explosions and to ensure the operational integrity of the refinery (CETESB, 2017), using them is not an effective emission control system as a combustion chamber (CETESB, 2017). The frequent use of the flare can be interpreted as an under dimensioning of the atmospheric emission treatment system (combustion chamber, gas scrubber, etc.), resulting in an unnecessary level of exposure of the surrounding population to PM.

The pollutants' dispersion provided by AERMOD is shown in Figures 7 and 8. The maximum concentration of the 1 h average of VOC ($3.753 \mu\text{g m}^{-3}$, $23^{\circ}37'58.59'' \text{ S}$, $46^{\circ}29'2.37'' \text{ W}$) is highlighted in Figure 3.8, during April and May of 2021. It is very important to observe that this highest VOC value modeled by AERMOD happened, practically, inside the CPC area. Therefore, when observing the dispersion of the plume, it could be verified that the residential area was exposed to concentrations that varied from 75 to $500 \mu\text{g m}^{-3}$ (areas in different shades of blue in Figure 3.8). These

values are consistent with the event observed by official air quality monitoring (CETESB, 2022) and are compatible with the levels of odor perception (Gutiérrez et al., 2023). The plume of $75 \mu\text{g m}^{-3}$ concentration reached areas from 8 to 19 km away from the complex, and the plume ranging from 250 to $1000 \mu\text{g m}^{-3}$ reached the nearest areas, about 3 km away.

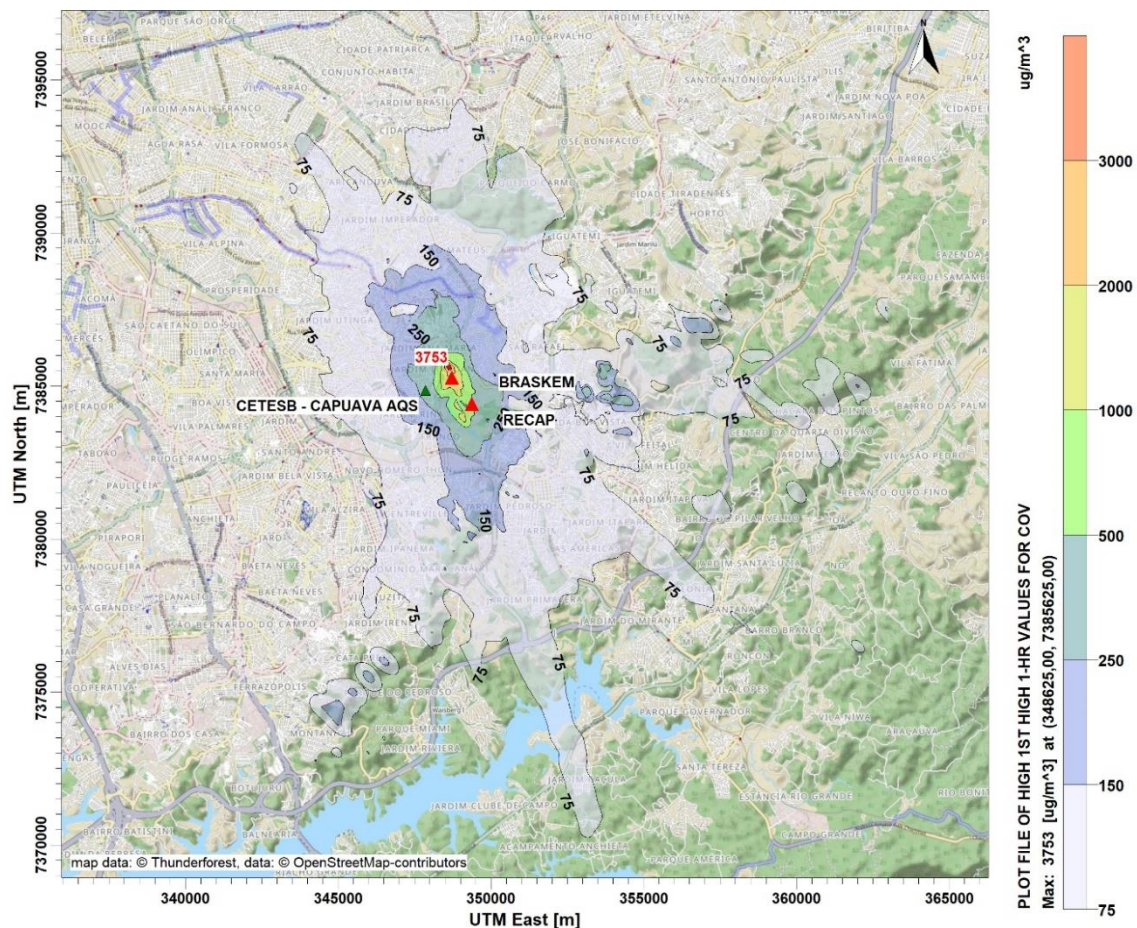


Figure 3.8. The maximum concentration of 1 h average ($\mu\text{g m}^{-3}$) of VOC in the affected area during the CPC maintenance period.

This aspect of concentration isolines (centered at the source, with low dilution rates) is typical of industries whose fugitive emissions (tanks, valves, and pipes) are predominant. Whenever the odorous substances were emitted from fugitive sources, the plume tended to remain close to the ground (near the urban canopy) with low dilution rates (or high concentration levels) which would explain the fact that closer residents reported large discomfort (ABC, 2021). The VOC result modeling was consistent with the areas where odor reports occurred. However, the simulated

concentrations were too low to generate odor discomfort as reported by local people. However, higher concentrations were registered by Capuava AQS, indicating that the odor might have been generated by uncontrolled emissions that were higher than the values established by the environmental licenses. The reports obtained from local people mentioned slightly sweet unpleasant odors, headaches, and nausea, whereby these descriptions are consistent with benzene contamination (Sekar et al., 2019). While most countries have different and long term (between 5 and 10 $\mu\text{g m}^{-3}$ according to annual average) standards for benzene, Brazil does not define the air quality standard for it. The few short-term air quality standards for benzene are as follows: 300 $\mu\text{g m}^{-3}$ (20-min, Russia); 22 $\mu\text{g m}^{-3}$ (1 h, Vietnam); 5 $\mu\text{g m}^{-3}$ (8 h, Albania); and 3.9 $\mu\text{g m}^{-3}$ (24 h, Israel) (Sekar et al., 2019). Comparing 1 h Capuava AQS data (Figures 3 and 4) with the Vietnam air quality standard (22 $\mu\text{g m}^{-3}$, 1 h) (Sekar et al., 2019), some exceedances of the air quality standard could be observed during the April/May 2021 episode, which did not occur in the previous years, evidencing possible higher uncontrolled emissions of VOC.

The PM isolines showed the 396 $\mu\text{g m}^{-3}$ maximum 24 h average concentration, (23°43'26.30" S, 46°31'31.37" W) which occurred 10 km southwest from CPC (Figure 3.9). The plume ranging from 100 to 200 $\mu\text{g m}^{-3}$, with second maximum concentration of the 300 $\mu\text{g m}^{-3}$, reached areas closer to the sources, about 2 km away.

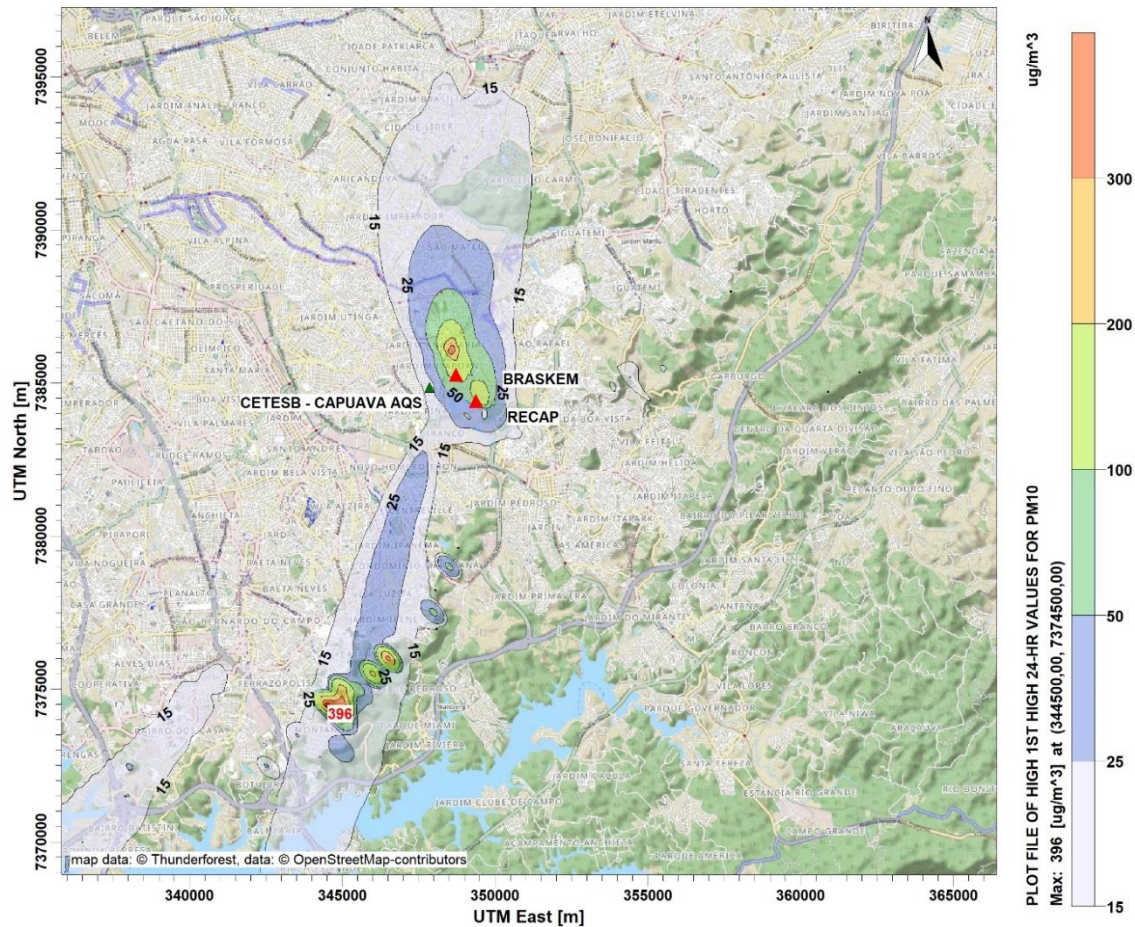


Figure 3.9. The maximum concentration of 24 h average ($\mu\text{g m}^{-3}$) of PM in the affected area during the CPC maintenance period.

These extended distances of PM happened when the releases from the source had enough energy to reach the higher parts of the boundary layer and carried out the advection process more intensively. The CPC flare launched the PM from 110 m high and at temperatures above 1000 °C. These conditions allowed the pollutants to reach the top of the boundary layer effortlessly, keeping the pollutants in suspension for a longer time, suffering slow dry depletion and resulting in layers of soot on the houses, as noted by several residents (ABC, 2021). The secondary maximum area occurrence (≥ 200 and $\leq 350 \mu\text{g m}^{-3}$) was the outcome of the building downwash effect in low wind and stable atmosphere (or a low height of the boundary layer). This result may have indicated that CPC emissions produced high PM concentrations in the vicinity, which to a certain extent can explain the early morning peaks observed in the Capuava AQS (Figure 3.6).

3.4. Conclusions

CPC carried out a 50-day scheduled shutdown for the maintenance, resulting in severe uncontrolled emissions of PM and VOCs in a densely populated and residential area (~3400 inhabitants/km²). The absence of information about the release of odorous gas and soot into the atmosphere makes it impossible to carry out more accurate analyses. However, by using existing AQS data and the dispersion model, it was possible to estimate the impact on the air quality from these emissions in MASP, especially in the ABC region.

The episode period of uncontrolled emissions (April–May 2021) was statistically analyzed by comparing the previous (2017–2020) and the subsequent (2021–2022) periods. When we compared annual 1 h concentrations and the diurnal profiles from the four previous years, an increase in the mean concentrations was observed by a factor of 2 for PM₁₀, benzene, and toluene, reaching maximum values during the episode: 174 µg m⁻³ (PM₁₀), 79.1 µg m⁻³ (benzene), and 58.7 µg m⁻³ (toluene). The description of the odor and symptoms presented by the local population, in the same period, were compatible with the presence of benzene and other volatile substances. The reports of soot deposition in the houses can be explained by PM₁₀ which showed unexpected peaks that could not be associated with special meteorological events or typical profiles of traffic emissions in that area. These reports by the population were compatible with the Braskem and RECAP public declarations about the more intense use of the flare before and after the maintenance period.

Meanwhile, these higher concentrations continued to be observed after the episode, but their variation cannot be fully explained yet. However, it is worth highlighting that this corresponds to the post-pandemic period and the 2022 data also correspond to the period from January to June, that is, they do not represent the annual variation.

Additionally, the estimation by the AERMOD model showed that the VOC plume could potentially reach a large part of the Mauá and Santo André municipalities

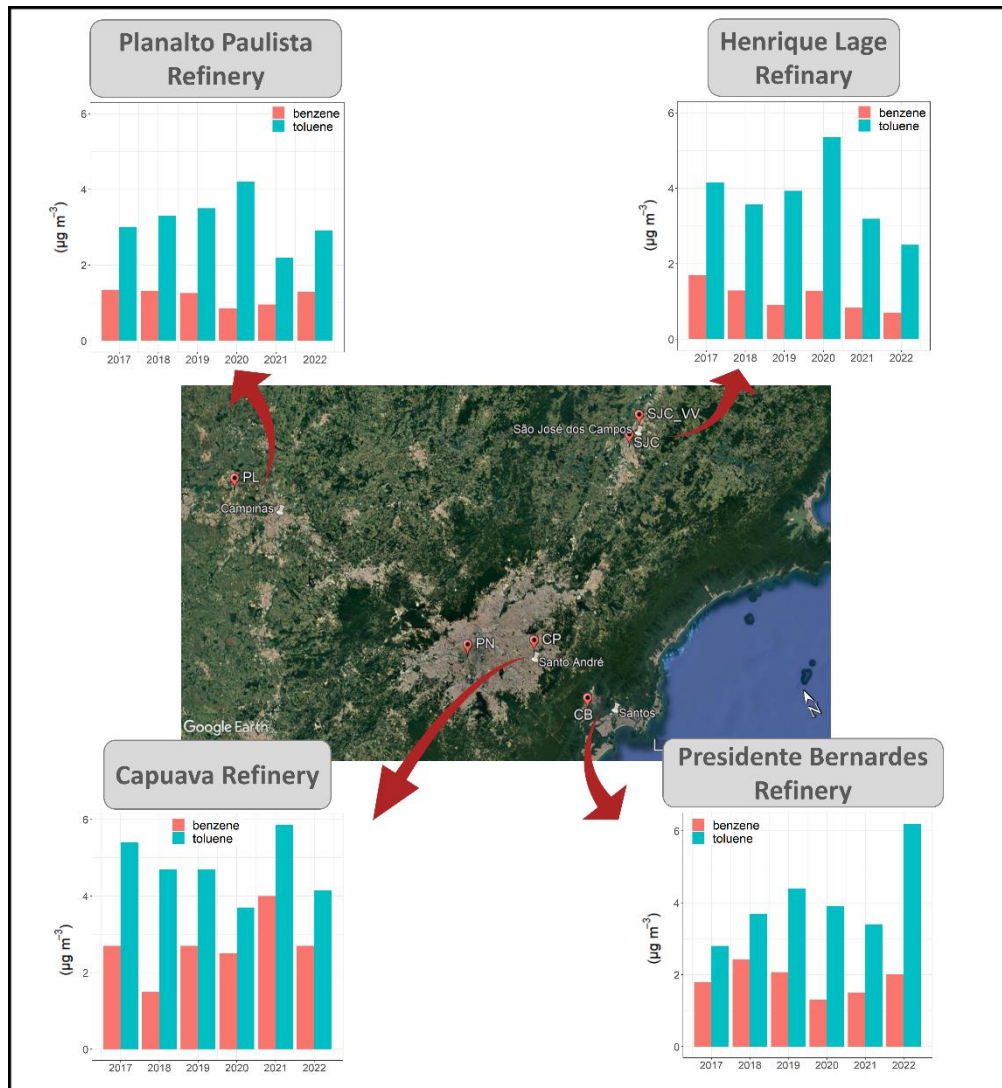
and the east side of São Paulo city. A linear correlation indicated that CPC could be responsible for more than 60% of benzene concentrations in the Capuava AQS. In this case, we could consider the Capuava AQS to be well-positioned regarding these pollutants' concentrations, resulting from CPC emissions with good spatial representation for this type of source, with most of them being fugitives and near-canopy advection.

The maximum concentration of PM was observed far from the CPC area (~10 km) in São Bernardo do Campo municipality, increasing the amount of people exposed to these emissions, which can explain the poor correlation between modeled versus AQS data ($r = 0.33$). In this way, AQS probably cannot perform accurate PM measurements, or they are being underestimated, considering the height of the sources (stacks and flares), presenting a plume that reaches a larger area. Additionally, it is quite possible that the emissions inventory used in the EIA is incomplete or underestimated. However, the several reports of soot on houses in the neighborhoods close to the CPC, associated with the turned-on flares and early morning peaks of PM₁₀ in Capuava AQS, indicate the local impact of these industrial activities.

Many studies around the world are aiming to evaluate some industrial source types and current discussions about their effects on air quality have been developed in different places (Lin et al., 2021; Parveen et al., 2021; Arulprakasajothi et al., 2020; Bergstra et al., 2021; Michalik et al., 2022). However, in Brazil, few studies address this topic as little is known about the emissions inventory, VOC speciation, or PM chemical composition for industrial emissions (Coelho et al., 2021; Cerqueira et al., 2018; Macêdo et al., 2020; Tadano et al., 2010; Kawashima et al., 2020). To conclude, our results provide significantly important information on the effects of airborne emissions from the CPC on air quality in a densely urbanized area, analyzing data from an official AQS and modeled results (AERMOD) for a special episode of air contamination in Brazil.

Chapter 4. Six years (2017-2022) of benzene and toluene monitoring: Trends and impacts for São Paulo state, Brazil.

GRAPHICAL ABSTRACT



4.1. Introduction

The metropolitan area of São Paulo (MASP) is among the largest urban agglomerations in the world with more than 22 million inhabitants. The official inventory of air pollutant sources showed that more than 7 million vehicles were responsible for the emission of 24.9 (72.8%), 48.3 (64.9%), and 1.22 (40%) kton per year of hydrocarbons (HC) and particulate matter (PM), respectively, in 2020 (CETESB,

2022). On the other hand, despite being less intense, industrial sources and fuel-based storage were responsible for the emission of 9.3 (27.2%) and 3.6 (10%) kton per year of HC and PM, respectively (CETESB, 2022).

In urban atmospheres, BTEX (benzene, toluene, ethylbenzene, m+p- and o-xylenes) represent a significant fraction of VOCs, reaching up to 50% of total VOCs (Lee et al. 2002). Crude oil consists of 94% in weight of HCs, being 30% alkanes, 49% cycloalkanes, and 15% aromatics (Simpson et al. 2010). In addition, fossil fuels or solvents containing aromatic compounds with less than 15 carbons can easily evaporate into the air due to their high vapor pressures and low boiling points (Rajabi et al. 2020). However, the relative importance of different VOC emission sources in urban areas remains under discussion, as it varies according to each region (Yuan et al. 2013; Salameh et al. 2015; Andrade et al. 2017; Ly et al. 2020).

In 2015, CETESB began the hourly automatic monitoring of benzene and toluene at five sites in different municipalities of São Paulo state. These different sites of Air Quality Monitoring Stations (AQS) represent the influence of vehicular and industrial emissions in the MASP (CETESB, 2018). They are located in Cubatão (CB) near the Industrial Complex of Cubatão (petrochemical, steel, and production of fertilizers); Capuava (CP) in vicinity of industrial complex of Capuava; Paulínia (PL) near the Paulínia Oil Refinery; Pinheiros (PN) close to one of the main traffic avenues in the MASP; São José dos Campos (SJC) inside the urban area and São José dos Campos–Vista Verde (SJC-VV) near the Henrique Lage Oil Refinery (REVAP). This data provides an overview of the concentrations observed for different industrial areas in São Paulo state.

In this study, we provide a detailed analysis of the concentrations for benzene and toluene at six AQS during the period of 2017 to 2022. Here, we analyze the daily profiles, seasonal trends and exploring the correlation between species for emission sources evaluation. The potential impacts that these compounds could have on

atmospheric chemistry and health of population, with estimations of secondary pollutants formation (O_3 and SOA) and potential cancer risk.

4.2. Materials and Methods

The data of six AQS distributed in municipalities of São Paulo state were evaluated during the period from 2017 to 2022. Hourly concentration for benzene and toluene were considered for this study (<https://cetesb.sp.gov.br/ar/qualar/>). These different sites represent the influence of vehicular and industrial emissions (CETESB, 2022). MASP has two stations: Pinheiros (PN) close to one of the main traffic avenues in the region and Capuava station (CP), in the vicinity of Capuava Refinery (RECAP); Outside MASP area: Two stations at São José dos Campos (SJC and SJC_VV) near the Henrique Lage Refinery (REVAP); Paulínia station (PL) near the Planalto Paulista Refinery (REPLAN) and Cubatão station (CB) near the Presidente Bernardes Refinery (RPBC) (Figure 4.1).

Statistical analyses of data were performed using R statistical software—open-air package (<https://www.r-project.org/>. (Carslaw et al., 2012))—which has been used extensively in different studies (Dominutti et al., 2016; Cui et al., 2020; Vestenius et al., 2021; Harrison et al., 2021; Squizzato et al., 2021). Concentrations with values higher than ($\text{mean} + 3 \times (\text{standard deviation})$) were considered to be outliers in the data validation and were excluded from box-plot analyses. To identify potential contributions from the sources, we used the polar annulus function, which is a graphical resource that provides temporal variation in concentrations for each compound according to wind direction. The code and major information are available in the open-air package manual (Carslaw et al., 2012).

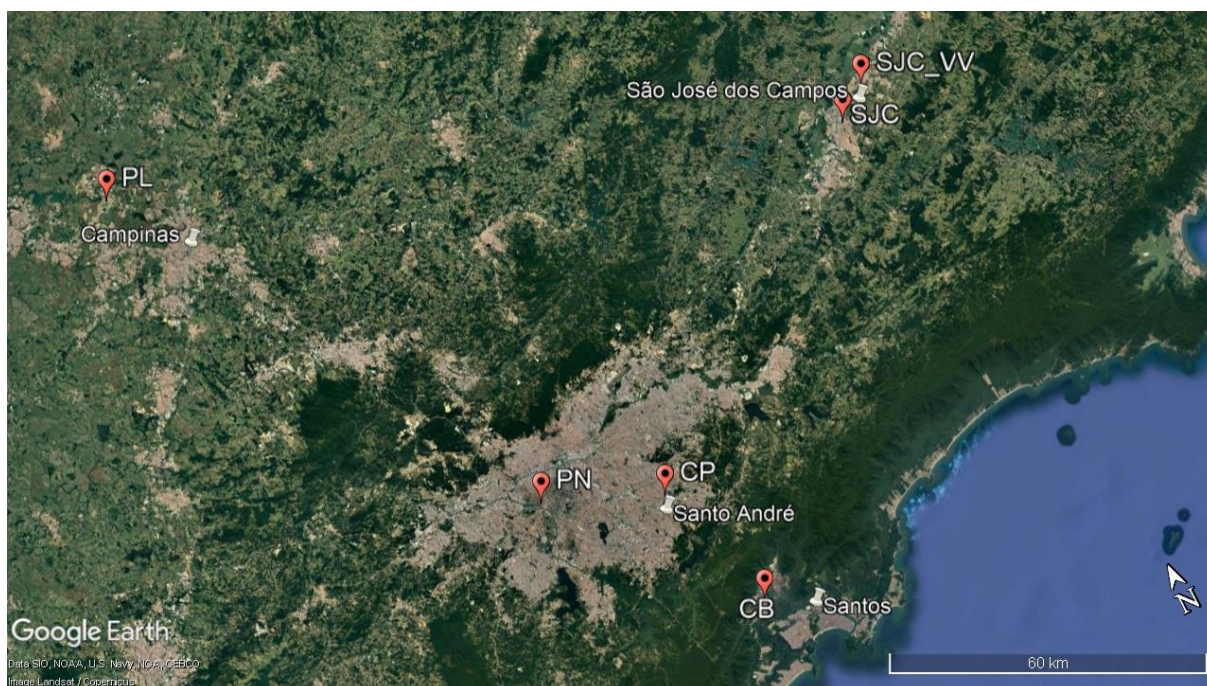


Figure 4.1. Part of São Paulo State with the demarcations of CETESB Air Quality Station (AQS) (identified by the red pins) and the respective municipality of each station (with pins). Source: Google Earth.

4.2.1. Estimating the formation of secondary pollutants

In order to estimate the potential effects that benzene and toluene can have on the atmospheric chemistry, some metrics were applied. The maximum incremental reactivity (MIR), secondary organic aerosol potential (SOAP) and fractional aerosol coefficient (FAC) values used to calculate the potentials, more details can be found in Coelho et al. (2021).

4.2.2. Risk assessment

The exposure risk was used to estimate the adverse effects of exposure on human health. For that, the Integrated Risk Information System (IRIS) method was applied (U.S. EPA, 2016). We calculated exposure concentration (EC), hazard quotient (HQ) and lifetime cancer risk (LCR) to estimate the cancer risk for benzene, more details can be found in Coelho et al. (2021).

4.3. Results and discussion

4.3.1. Air quality station characteristics

4.3.1.1. Cubatão (CB)

Figure 4.2 shows the localization of Presidente Bernardes Refinery in relation to AQS, about 1 km. The preferential wind directions from the refinery were southwest to northwest (quadrant: 180° to 360°).



Figure 4.2. Cubatão (CB) Air Quality Station (AQS) (red pin) and the respective distance of industrial area (~1 km) of Presidente Bernardes Refinery (RPBC) (with arrow). Source: Google Earth.

The effect of the wind directions for pollutant concentration variations can indicate the industrial contributions during the day (Figure 4.3). Benzene showed higher concentrations ($\geq 4 \mu\text{g m}^{-3}$), during the years of 2018, 2019 and 2021, while values below $3 \mu\text{g m}^{-3}$ were observed in other orientations during the other years of monitoring. Toluene showed dissimilar distributions regarding all wind directions during the day with values ranged from 2 to $6 \mu\text{g m}^{-3}$. Higher values from southwest,

south, and southeast winds, was observed in 2022, reaching values higher than $14 \mu\text{g m}^{-3}$ during the year.

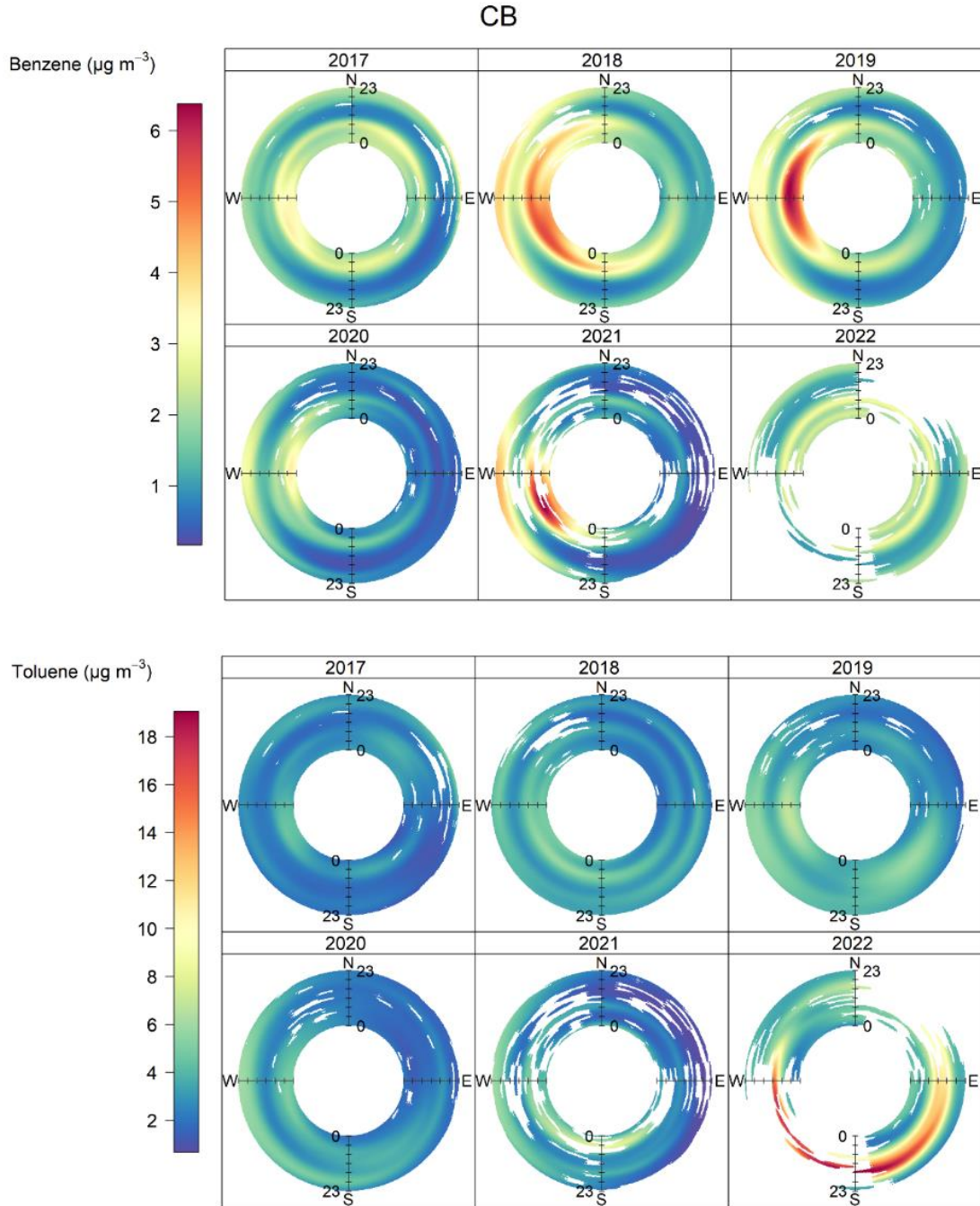


Figure 4.3. Changes in benzene and toluene mean hourly concentrations at Cubatão station, depending on wind directions. Polar annulus plots from 2017 – 2022. Color scale represents concentrations ($\mu\text{g m}^{-3}$), the thickness in the circle represents the hour of the day: 00:00 inside to 11:00 p.m. outside. Blank spaces are missing values.

4.3.1.2. Capuava (CP)

Figure 4.4 shows the localization of Capuava Refinery in relation to AQS, about 0.5 km. The preferential wind directions from the refinery were from north to south (quadrant: 0° to 180°).

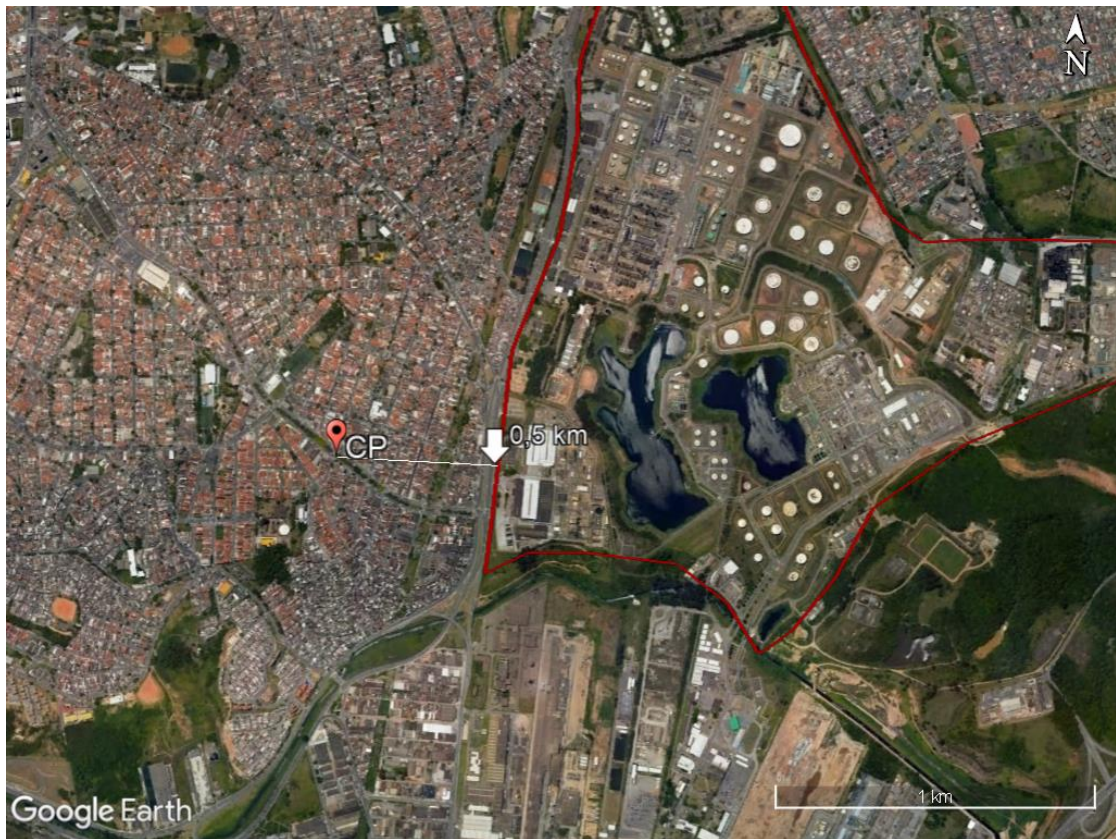


Figure 4.4. Capuava (CP) Air Quality Station (AQS) (red pin) and the respective distance of industrial area (~0.5 km) of Capuava Refinery (RPBC) (with arrow). Source: Google Earth.

Figure 4.5 shows the wind directions for pollutant concentration variations during the day. Benzene showed higher concentrations ($\geq 10 \mu\text{g m}^{-3}$), for all years of monitoring, from northeast, while values below $5 \mu\text{g m}^{-3}$ were observed in other orientations during the period. Toluene showed distributions regarding all wind directions during the day with values ranged from 5 to $10 \mu\text{g m}^{-3}$. Higher values from northeast winds, was observed for 2018 and 2021, reaching values higher than $15 \mu\text{g m}^{-3}$.

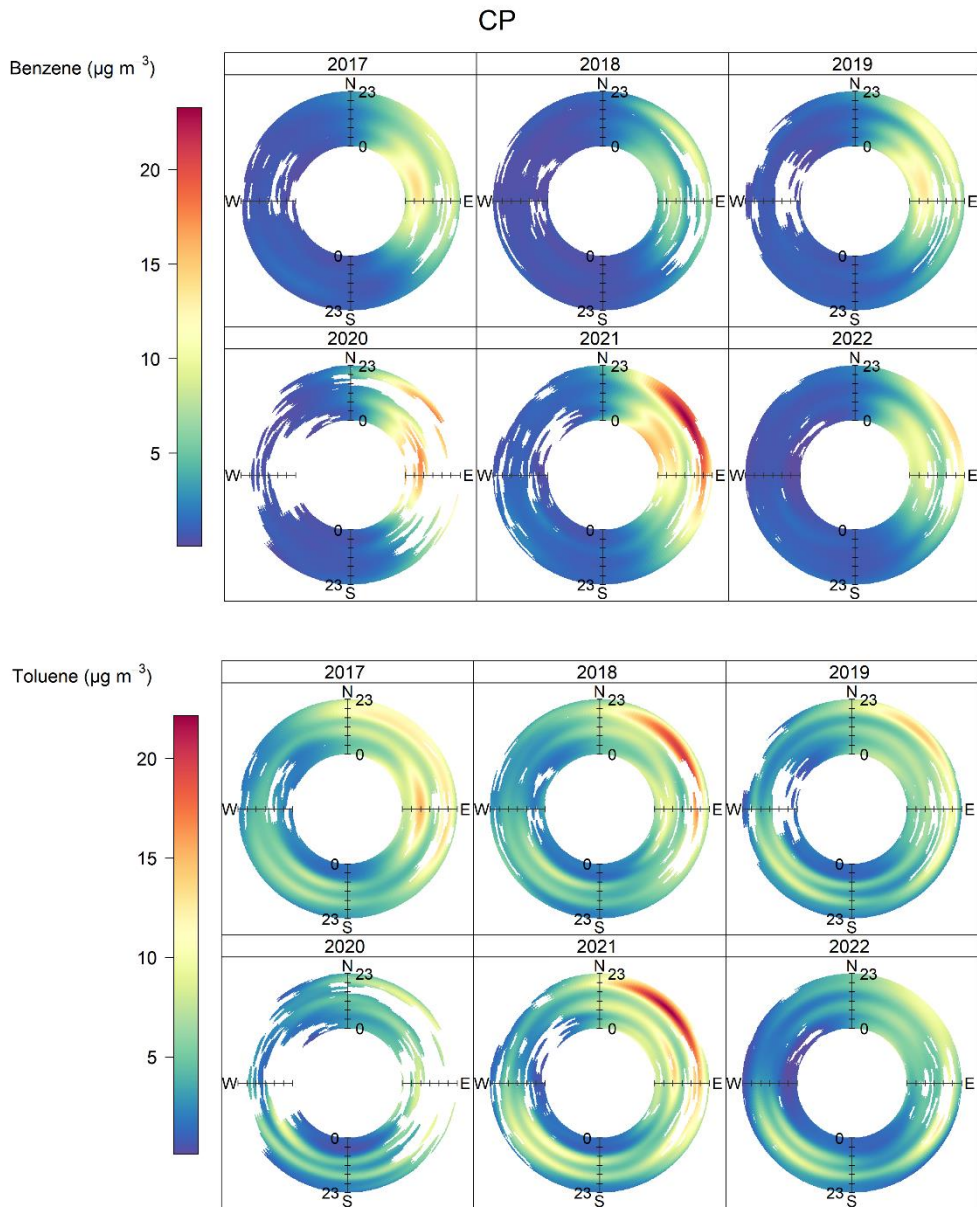


Figure 4.5. Changes in benzene and toluene mean hourly concentrations at Capuava station, depending on wind directions. Polar annulus plots from 2017 – 2022. Color scale represents concentrations ($\mu\text{g m}^{-3}$), the thickness in the circle represents the hour of the day: 00:00 inside to 11:00 p.m. outside. Blank spaces are missing values.

4.3.1.3. Paulínia (PL)

Figure 4.6 shows the localization of Planalto Paulista Refinery (REPLAN) in relation to AQS, about 2 km. The preferential wind directions from the refinery were from northwest to northeast (quadrant: 270° to 90°).



Figure 4.6. Paulínia (PL) Air Quality Station (AQS) (red pin) and the respective distance of industrial area (~2 km) of Planalto Paulista Refinery (REPLAN) (with arrow). Source: Google Earth.

Figure 4.7 shows the wind directions for pollutant concentration variations during the day. Benzene showed higher concentrations ($\geq 3 \mu\text{g m}^{-3}$), for all years of monitoring from northwest and northeast, while values below $1 \mu\text{g m}^{-3}$ were observed in other orientations during the period. Toluene showed distributions regarding all wind directions during the day with values ranged from 2 to $6 \mu\text{g m}^{-3}$. Higher values from southwest winds, was observed for 2017, 2018 and 2019, reaching values higher than $10 \mu\text{g m}^{-3}$.

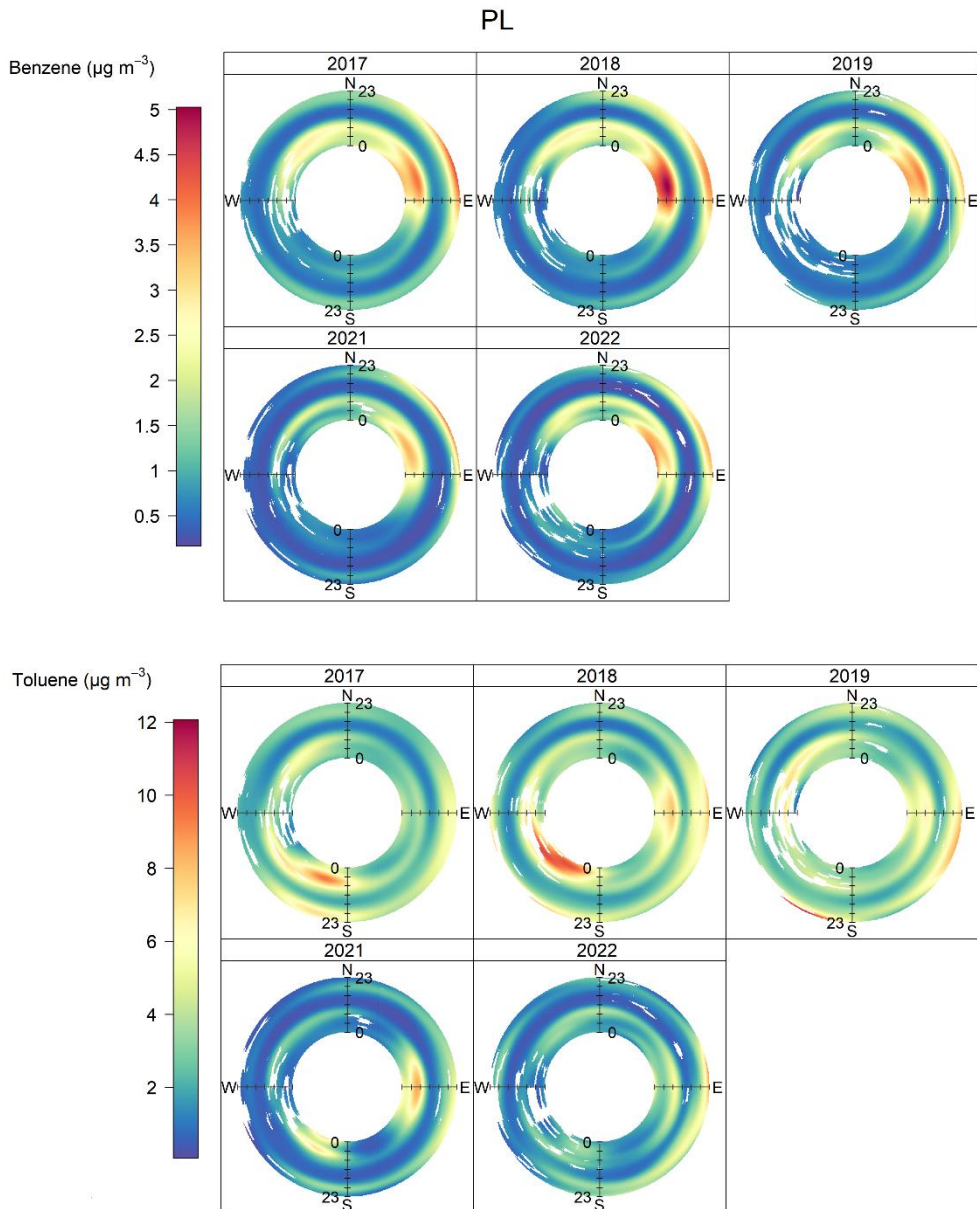


Figure 4.7. Changes in benzene and toluene mean hourly concentrations at Paulínia station, depending on wind directions. Polar annulus plots from 2017 – 2022 (insufficient number of measurements for 2020). Color scale represents concentrations ($\mu\text{g m}^{-3}$), the thickness in the circle represents the hour of the day: 00:00 inside to 11:00 p.m. outside. Blank spaces are missing values.

4.3.1.4. Pinheiros (PN)

Figure 4.8 shows the localization of Pinheiros AQS, about 0.2 km of the Marginal Pinheiros. This is one of the main traffic routes in the MASP, being the second route with the highest circulation of vehicles during the day (CET, 2018). Approximately 9.784 vehicles in the morning (rush from 7:15 a.m. to 8:15 a.m.) and in the afternoon 9.336 vehicles (rush from 6:30 p.m. to 7:30 p.m.) (CET, 2018).

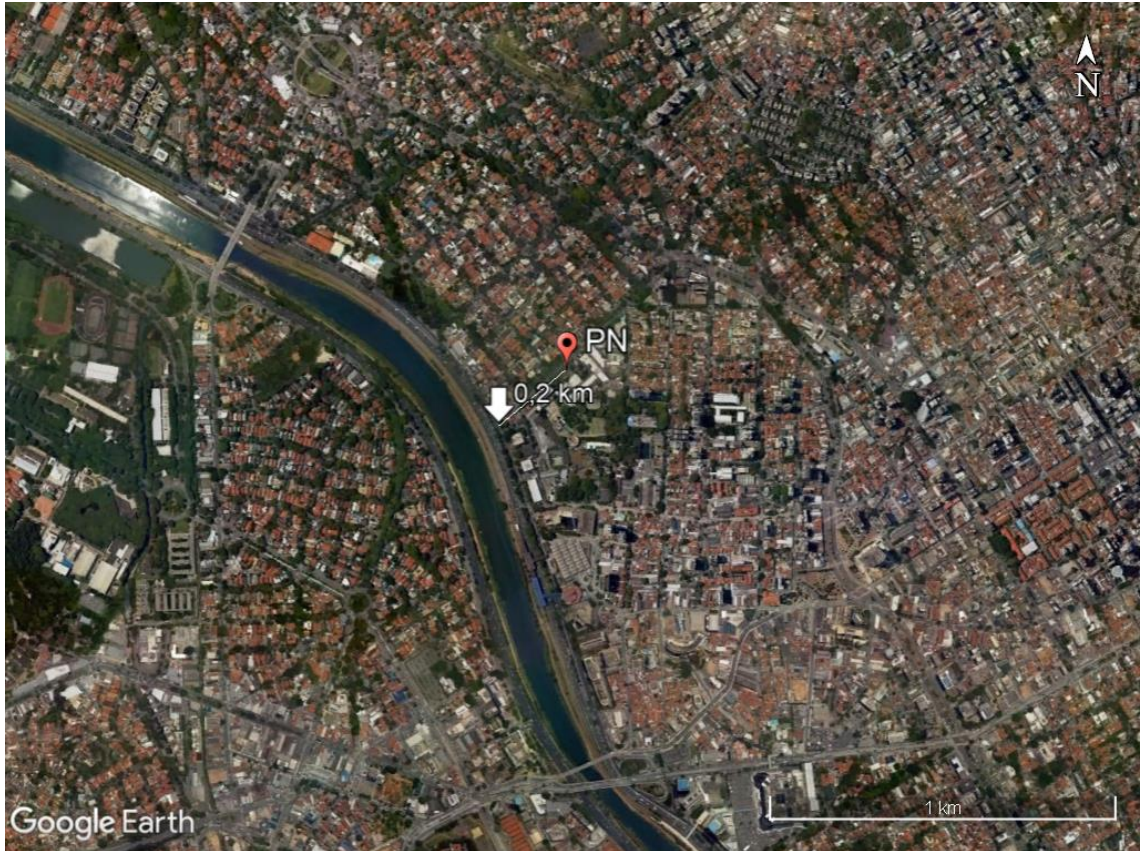


Figure 4.8. Pinheiros (PN) Air Quality Station (AQS) (red pin) and the respective distance of Marginal Pinheiros (~0.2 km) (with arrow). Source: Google Earth.

Figure 4.9 shows the wind directions for pollutant concentration variations during the day. Benzene showed higher concentrations ($\geq 4 \mu\text{g m}^{-3}$), for 2018 only, for other years of monitoring values below $1.5 \mu\text{g m}^{-3}$ were observed. Toluene showed distributions regarding all wind directions during the day with values ranged from 2 to $10 \mu\text{g m}^{-3}$. Higher values from northeast winds, was observed for 2018, 2020 and 2021, reaching values higher than $14 \mu\text{g m}^{-3}$.

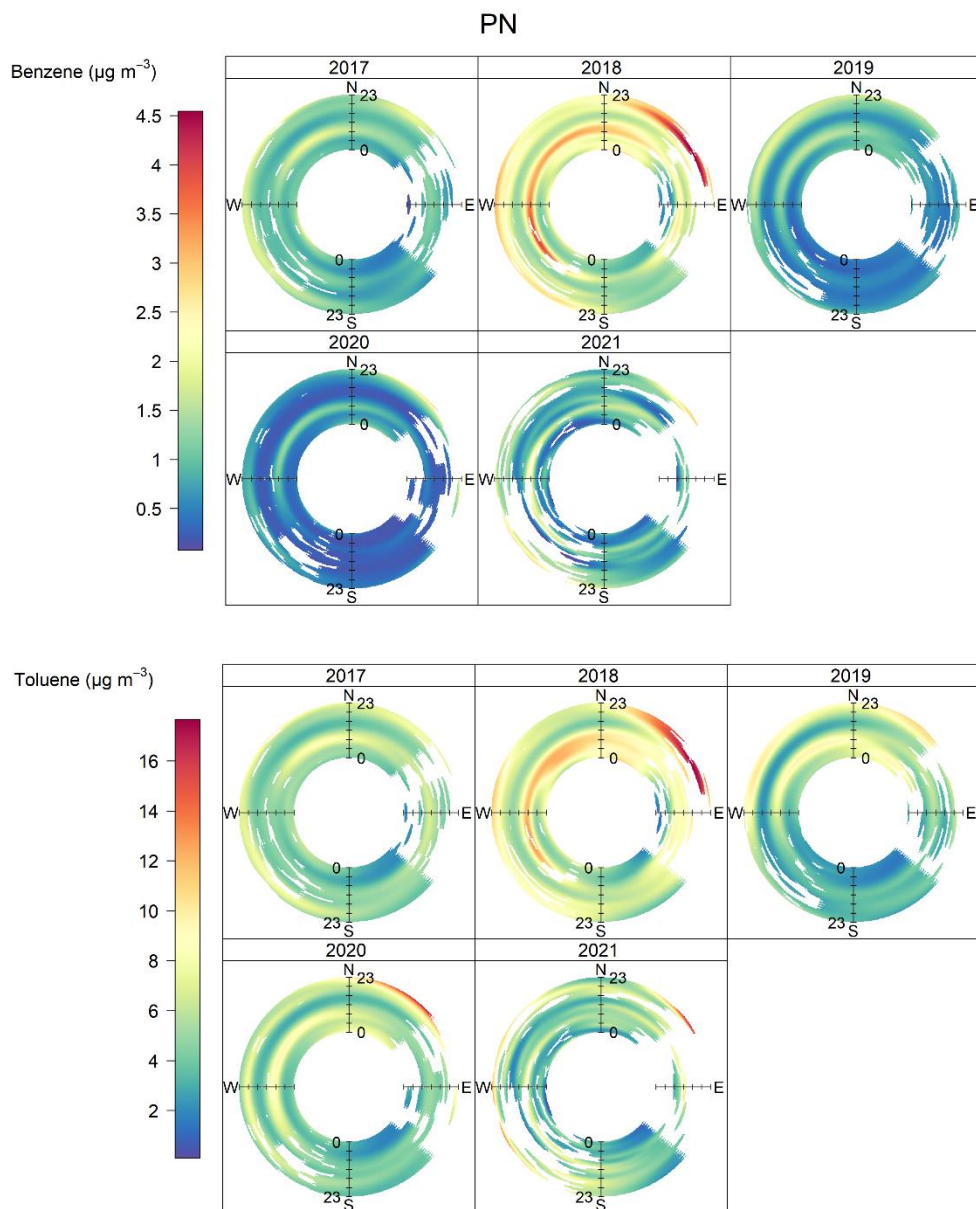


Figure 4.9. Changes in benzene and toluene mean hourly concentrations at Pinheiros station, depending on wind directions. Polar annulus plots from 2017 – 2021 (there is no valid data for 2022). Color scale represents concentrations ($\mu\text{g m}^{-3}$), the thickness in the circle represents the hour of the day: 00:00 inside to 11:00 p.m. outside. Blank spaces are missing values.

4.3.1.5. São José dos Campos (SJC) and São José dos Campos – Vista Verde (SJC-VV)

Figure 4.10 shows the localization of Henrique Lage Oil Refinery (REVAP) in relation to AQS, about 0.3 km and 6 km for SJC and SJC-VV, respectively. The preferential wind directions from the refinery for SJC were from east to west (quadrant: 90° to 270°).



Figure 4.10. São José dos Campos (SJC) and São José dos Campos – Vista Verde (SJC-VV) Air Quality Stations (AQS) (red pins) and the respective distance of industrial area of Henrique Lage Oil Refinery (REVAP) (with arrow). Source: Google Earth.

Figure 4.11 shows the wind directions for pollutant concentration variations during the day at São José dos Campos AQS. Benzene showed higher concentrations ($\geq 1.4 \mu\text{g m}^{-3}$), from southwest wind for 2018, 2021 and 2022. For other years of monitoring values below $1 \mu\text{g m}^{-3}$ were observed. Toluene showed distributions regarding all wind directions during the day with values below $5 \mu\text{g m}^{-3}$ during 2017 to 2019. For 2020 and 2021 highest values were observed, from south/ southwest directions, with concentrations above of $15 \mu\text{g m}^{-3}$.

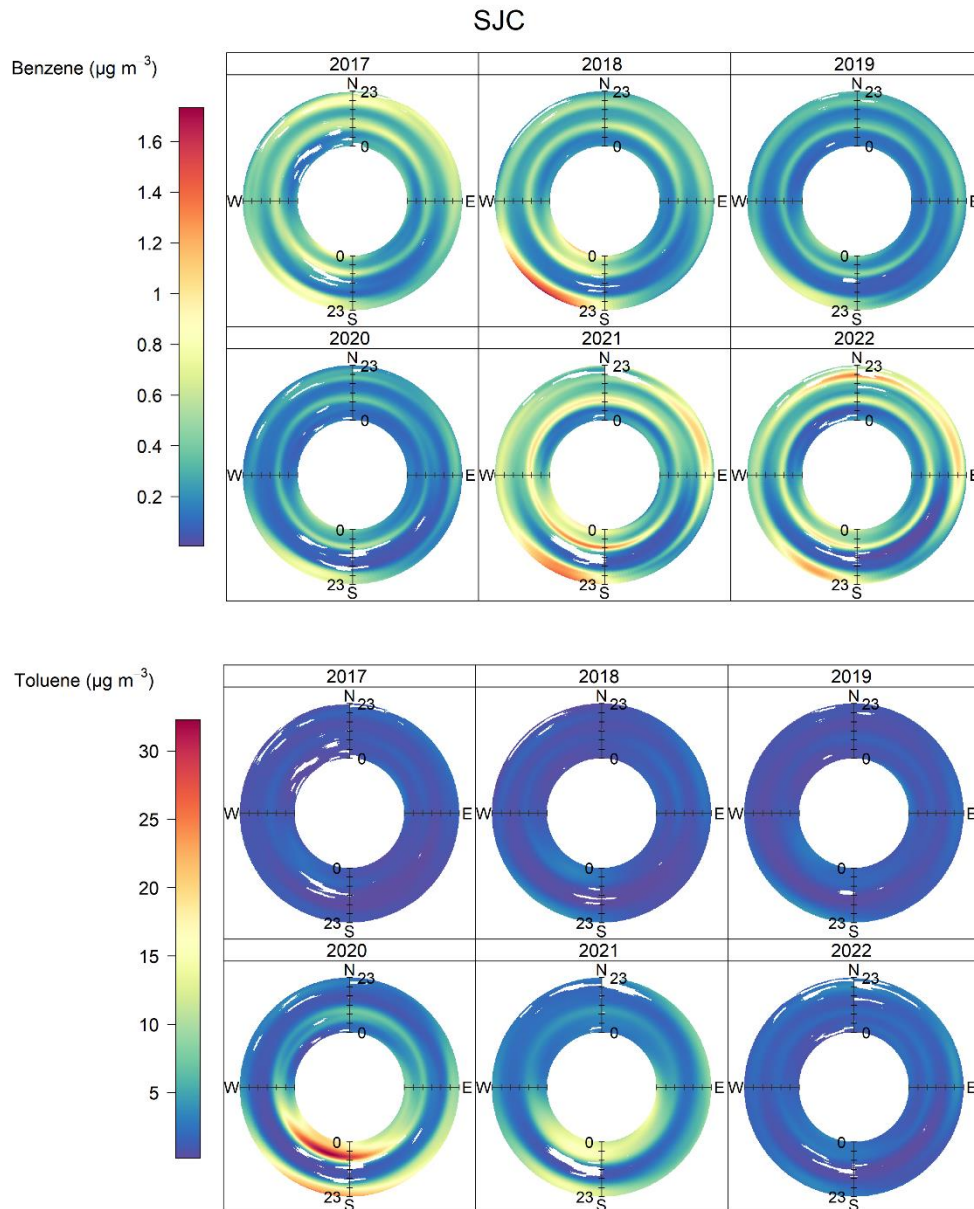


Figure 4.11. Changes in benzene and toluene mean hourly concentrations at São José dos Campos station, depending on wind directions. Polar annulus plots from 2017 – 2022. Color scale represents concentrations ($\mu\text{g m}^{-3}$), the thickness in the circle represents the hour of the day: 00:00 inside to 11:00 p.m. outside. Blank spaces are missing values.

Figure 4.12 shows the wind directions for pollutant concentration variations during the day. Benzene showed higher concentrations ($\geq 3 \mu\text{g m}^{-3}$), for all years of monitoring from southwest, while values below $2 \mu\text{g m}^{-3}$ were observed in other orientations during the period. Toluene showed distributions regarding all wind directions during the day with values ranged from 2 to $8 \mu\text{g m}^{-3}$. Higher values from

southwest winds, was observed for 2017, 2018, 2019 and 2020, reaching values higher than $10 \mu\text{g m}^{-3}$.

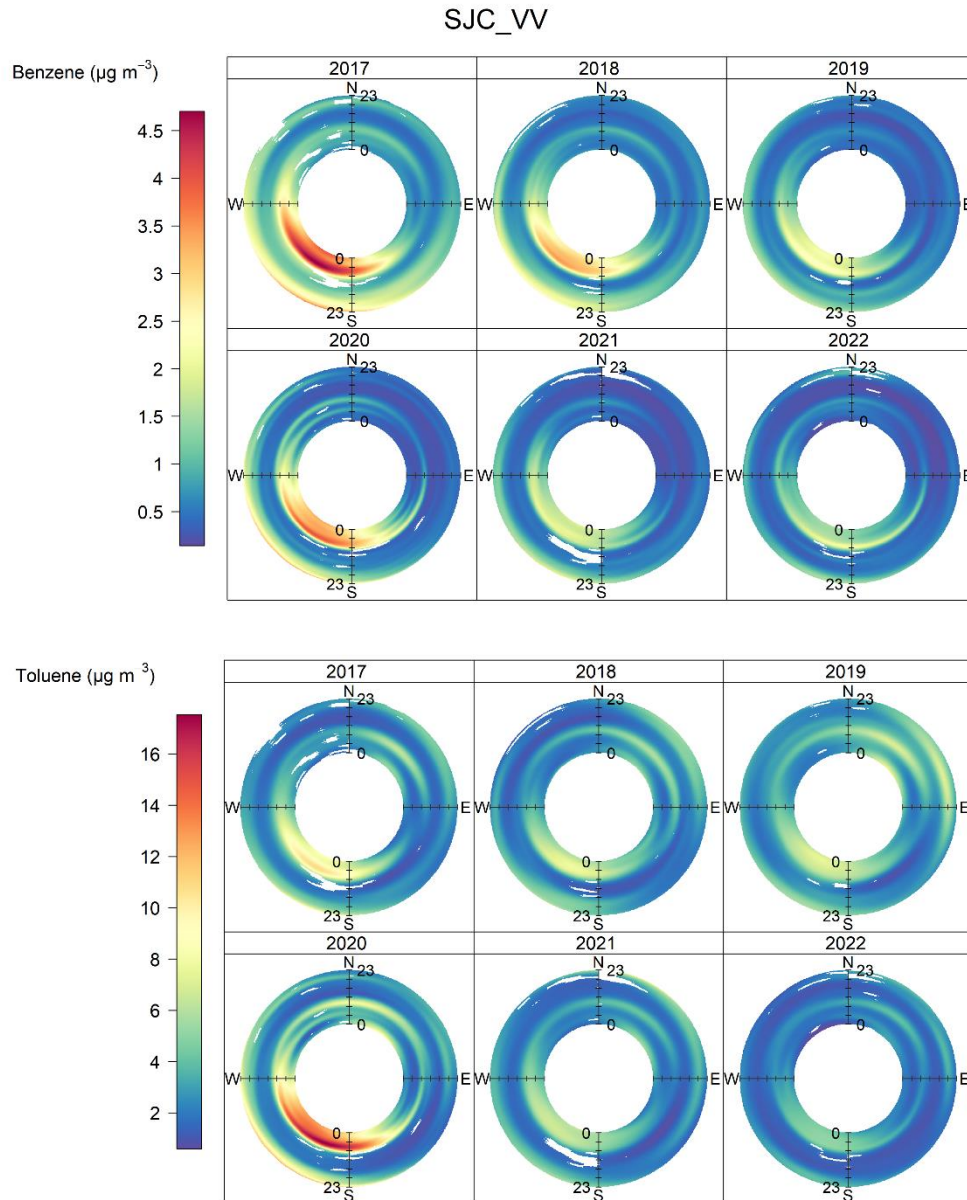


Figure 4.12. Changes in benzene and toluene mean hourly concentrations at São José dos Campos – Vista Verde station, depending on wind directions. Polar annulus plots from 2017 – 2022. Color scale represents concentrations ($\mu\text{g m}^{-3}$), the thickness in the circle represents the hour of the day: 00:00 inside to 11:00 p.m. outside. Blank spaces are missing values.

4.3.2. Data overview

Among the six years of data evaluated here, for the period (2017-2022) (Table 4.1), toluene monitored by CETESB AQS, presented higher annual mean concentrations at all sites in comparison to benzene. The annual averages at CB AQS ranged from 2.8 to 6.2 $\mu\text{g m}^{-3}$ for toluene and from 1.3 to 2.4 $\mu\text{g m}^{-3}$ for benzene; CP AQS: 4.1 to 5.8 $\mu\text{g m}^{-3}$ for toluene and 1.5 to 4.0 $\mu\text{g m}^{-3}$ for benzene; PL AQS: 2.2 to 4.2 $\mu\text{g m}^{-3}$ for toluene and 0.8 to 1.3 $\mu\text{g m}^{-3}$ for benzene; PN AQS: 4.2 to 6.7 $\mu\text{g m}^{-3}$ for toluene and 0.9 to 1.9 $\mu\text{g m}^{-3}$ for benzene; SJC AQS: 1.3 to 7.0 $\mu\text{g m}^{-3}$ for toluene and 0.4 to 0.8 $\mu\text{g m}^{-3}$ for benzene; SJC-VV AQS: 2.5 to 5.3 $\mu\text{g m}^{-3}$ for toluene and 0.7 to 1.7 $\mu\text{g m}^{-3}$ for benzene.

Table 4.1. Summary of statistical analysis for hourly concentrations ($\mu\text{g m}^{-3}$), for all sites, during 2017-2022. Years in bold represent data without annual representation.

Cubatão (CB)								
Benzene								
year	N	Mean	S.D.	Min.	Max.	Median	1 st quartile	3 th quartile
2017	7549	1.80	2.26	0.1	34.26	1.00	0.48	2.23
2018	8564	2.42	3.33	0.1	94.82	1.35	0.58	2.88
2019	7142	2.07	2.50	0.1	31.48	1.21	0.51	2.66
2020	5440	1.31	1.69	0.1	18.12	0.68	0.34	1.59
2021	8117	1.50	2.04	0.1	23.56	0.72	0.33	1.76
2022	2907	2.01	2.84	0.1	45.90	1.00	0.40	2.50
Toluene								
year	N	Mean	S.D.	Min.	Max.	Median	1 st quartile	3 th quartile
2017	7593	2.77	4.88	0.10	117.98	1.34	0.59	2.95
2018	8624	3.73	5.89	0.10	79.76	1.83	0.83	3.99
2019	7467	4.36	6.34	0.11	122.83	2.54	1.36	5.13
2020	5683	3.87	7.26	0.10	121.91	1.70	0.75	3.87
2021	8214	3.42	7.46	0.10	129.22	1.43	0.61	3.42
2022	2914	6.20	13.55	0.10	171.50	2.30	1.00	5.70
Capuava (CP)								
Benzene								
year	N	Mean	S.D.	Min.	Max.	Median	1 st quartile	3 th quartile
2017	8278	2.70	3.98	0.10	52.65	1.20	0.54	2.92
2018	6561	1.55	2.60	0.10	46.19	0.62	0.32	1.63
2019	7567	2.70	4.25	0.10	74.49	1.30	0.58	2.95
2020	1630	2.48	4.19	0.10	52.21	0.91	0.48	2.42
2021	6010	4.04	7.03	0.10	79.13	1.59	0.73	4.11
2022	8336	2.66	4.78	0.10	79.27	1.00	0.50	2.67

Toluene								
year	N	Mean	S.D.	Min.	Max.	Median	1 st quartile	3 th quartile
2017	8292	5.37	4.89	0.14	44.70	4.10	1.94	7.16
2018	6562	4.74	4.82	0.15	55.28	3.34	1.63	6.17
2019	7564	4.71	5.29	0.10	64.62	3.26	1.45	6.18
2020	1628	3.74	3.96	0.14	48.16	2.70	1.21	5.11
2021	6012	5.86	6.46	0.11	69.36	3.90	1.64	7.56
2022	7237	4.14	5.31	0.10	72.80	2.30	0.80	5.59

Paulínia (PL)

Benzene								
year	N	Mean	S.D.	Min.	Max.	Median	1 st quartile	3 th quartile
2017	7816	1.35	1.82	0.10	26.28	0.70	0.36	1.52
2018	7690	1.32	1.98	0.10	17.41	0.57	0.29	1.32
2019	6663	1.26	1.61	0.10	18.84	0.62	0.31	1.50
2020	46	0.86	0.51	0.14	2.27	0.75	0.45	1.18
2021	5869	0.96	1.78	0.10	22.24	0.37	0.20	0.80
2022	4975	1.29	2.19	0.10	29.66	0.40	0.20	1.20

Toluene								
year	N	Mean	S.D.	Min.	Max.	Median	1 st quartile	3 th quartile
2017	7829	3.01	3.89	0.10	48.65	1.68	0.78	3.75
2018	7727	3.30	5.14	0.10	78.62	1.64	0.69	3.72
2019	6851	3.53	4.44	0.10	84.50	2.16	0.88	4.68
2020	80	4.22	2.59	0.67	11.92	3.52	2.47	5.54
2021	6052	2.19	5.55	0.10	91.60	0.60	0.27	1.69
2022	4850	2.92	6.06	0.10	81.10	0.90	0.30	2.80

Pinheiros (PN)

Benzene								
year	N	Mean	S.D.	Min.	Max.	Median	1 st quartile	3 th quartile
2017	8289	1.08	0.92	0.10	8.30	0.79	0.45	1.43
2018	8611	1.90	1.70	0.10	9.93	1.40	0.75	2.39
2019	8039	0.87	0.96	0.10	22.45	0.54	0.28	1.14
2020	5400	0.86	1.03	0.10	12.17	0.49	0.26	0.94
2021	1330	1.17	0.96	0.10	14.52	0.90	0.54	1.53
2022						-		

Toluene								
year	N	Mean	S.D.	Min.	Max.	Median	1 st quartile	3 th quartile
2017	8299	5.02	5.03	0.13	49.60	3.58	1.99	6.20
2018	8615	6.86	7.58	0.23	95.70	4.43	2.46	8.00
2019	8248	4.88	6.61	0.10	98.50	2.70	1.24	5.70
2020	7640	5.02	6.65	0.10	85.12	2.88	1.36	6.10
2021	1586	4.22	3.47	0.16	47.43	3.37	1.84	5.50
2022						-		

São José dos Campos (SJC)

Benzene								
---------	--	--	--	--	--	--	--	--

year	N	Mean	S.D.	Min.	Max.	Median	1 st quartile	3 th quartile
2017	7618	0.56	0.62	0.10	18.34	0.38	0.21	0.70
2018	7311	0.62	1.19	0.10	18.15	0.35	0.18	0.66
2019	8525	0.45	0.38	0.10	4.90	0.35	0.17	0.60
2020	7624	0.45	0.40	0.10	14.22	0.40	0.17	0.60
2021	5925	0.78	0.73	0.10	5.54	0.56	0.30	0.90
2022	4837	0.64	0.69	0.10	6.93	0.40	0.20	0.80

Toluene

year	N	Mean	S.D.	Min.	Max.	Median	1 st quartile	3 th quartile
2017	7527	1.37	2.75	0.10	81.56	0.59	0.28	1.40
2018	7133	1.65	4.94	0.10	92.80	0.55	0.27	1.25
2019	8526	1.52	4.18	0.10	97.54	0.52	0.25	1.18
2020	7598	7.06	16.94	0.10	196.22	0.92	0.37	3.99
2021	7196	5.86	13.32	0.10	186.14	2.19	0.78	4.74
2022	6757	1.86	2.46	0.10	38.50	1.00	0.43	2.33

São José dos Campos - Vista Verde (SJC_VV)

Benzene

year	N	Mean	S.D.	Min.	Max.	Median	1 st quartile	3 th quartile
2017	7531	1.69	1.91	0.10	18.66	0.93	0.51	1.97
2018	8267	1.29	1.56	0.10	14.73	0.71	0.39	1.49
2019	8334	0.91	1.07	0.10	8.93	0.49	0.25	1.13
2020	6356	1.28	1.74	0.10	18.59	0.53	0.25	1.46
2021	8397	0.83	1.03	0.10	9.48	0.43	0.22	0.91
2022	8075	0.70	0.84	0.10	8.29	0.40	0.20	0.80

Toluene

year	N	Mean	S.D.	Min.	Max.	Median	1 st quartile	3 th quartile
2017	7538	4.15	5.43	0.10	66.86	2.20	0.95	5.13
2018	8299	3.58	4.22	0.10	56.64	2.00	0.94	4.46
2019	8350	3.93	5.57	0.10	85.23	2.16	0.86	4.95
2020	6286	5.35	7.53	0.10	79.18	2.35	0.89	6.55
2021	8454	3.19	4.57	0.10	86.42	1.79	0.77	3.95
2022	8130	2.50	3.02	0.10	42.31	1.41	0.70	3.13

It is possible to determine the variability of the data through the interquartile intervals between the first and third quartile. Thus, the highest variability and values of benzene and toluene happened with the highest amplitude, as well as the average concentrations (Figure 4.13).

Highest mean concentrations for benzene were observed in 2017 for Capuava: 2.7 $\mu\text{g m}^{-3}$, followed by Cubatão: 1.8 $\mu\text{g m}^{-3}$; 2018 – Cubatão: 2.4 $\mu\text{g m}^{-3}$ and Capuava: 1.5 $\mu\text{g m}^{-3}$; 2019 – Capuava: 2.7 $\mu\text{g m}^{-3}$ and Cubatão: 2.0 $\mu\text{g m}^{-3}$; 2020 – Capuava: 2.5

$\mu\text{g m}^{-3}$ and Cubatão: $1.3 \mu\text{g m}^{-3}$; 2021 – Capuava: $4.0 \mu\text{g m}^{-3}$ and Cubatão: $1.5 \mu\text{g m}^{-3}$; 2022 – Capuava: $2.7 \mu\text{g m}^{-3}$ and Cubatão: $2.0 \mu\text{g m}^{-3}$. For toluene highest mean concentrations were observed in 2017 for Capuava: $5.4 \mu\text{g m}^{-3}$, followed by Pinheiros: $5.0 \mu\text{g m}^{-3}$; 2018 – Pinheiros: $6.9 \mu\text{g m}^{-3}$ and Capuava: $4.7 \mu\text{g m}^{-3}$; 2019 – Pinheiros: $4.9 \mu\text{g m}^{-3}$ and Capuava: $4.7 \mu\text{g m}^{-3}$; 2020 – São José dos Campos: $7.1 \mu\text{g m}^{-3}$ and São José dos Campos – Vista Verde: 5.4 ; 2021 – Capuava and São José dos Campos with the same value: $5.9 \mu\text{g m}^{-3}$ and 2022 – Cubatão: $6.2 \mu\text{g m}^{-3}$ and Capuava: $4.1 \mu\text{g m}^{-3}$ (Figure 4.13).

In this context, we concluded that benzene presented higher annual mean concentrations at the sites located in industrialized areas, however, a less clear profile was observed for toluene values, since the highest concentrations were observed, mainly, for AQS that represents industrial and urban-traffic emissions, and for 2022, at industrial areas only.

It is important to highlight that these higher concentration for benzene and toluene at Capuava AQS reinforces the importance of exploring, in more detail, the emissions of local industries and their impacts on the environment and on the health of the population.

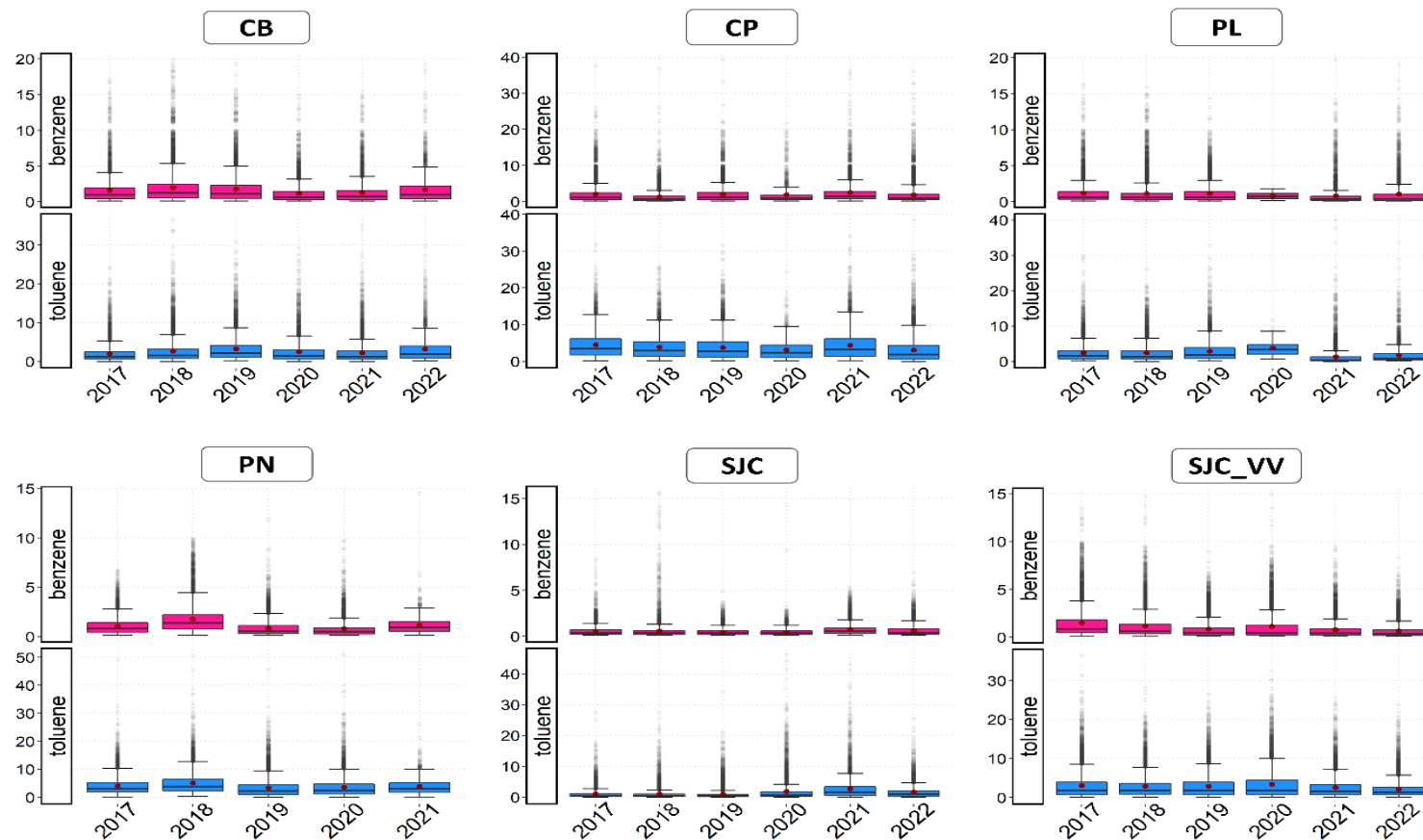


Figure 4.13. Annual boxplots of 1 h concentrations ($\mu\text{g m}^{-3}$) for benzene, and toluene at CETESB AQS, from 2017 to 2022, were CB: Cubatão, CP: Capuava, PL: Paulínia, PN: Pinheiros, SJC: São José dos Campos and SJC_VV: São José dos Campos – Vista Verde. Boxplot width and the lower and upper hinges correspond to the first and third quartiles (the 25th and 75th percentiles). Lower whisker: smallest observation greater than or equal to lower hinge - 1.5 * IQR (interquartile range), above 75th percentile. Upper whisker: largest observation less than or equal to upper hinge + 1.5 * IQR, below 25th percentile. The middle is the median (50% quantile), and the red point is the mean value. Points beyond the end of the whiskers are “outliers”, which correspond to values > 1.5 and < 3 times the standard deviation (sd). The data were presented on the Y axis with an appropriate scale for good visualization of the percentiles and the mean in relation to the median.

4.3.3. Seasonal and diurnal profiles

Figure 4.14 shows the seasonal variations for benzene and toluene at different AQS for each year (2017 to 2022). Monthly averages were similar in summer and spring (with maximum ranged from 5 to 10 $\mu\text{g m}^{-3}$) and in winter and autumn (with maximum ranged from 10 to 15 $\mu\text{g m}^{-3}$). These observations agree with previous studies in São Paulo (Dominutti et al., 2016; Nogueira et al., 2017; Coelho et al., 2021).

For toluene, highest values were observed at autumn and winter. But it is not possible to observe a clear trend for benzene, a possible explanation for that, is associated to the relatively constant emissions from the industries, like was observed in Korea (Kim et al., 2019; Coelho et al., 2023).

Previous studies evaluated VOCs in São Paulo, associated diurnal profiles of this compounds to traffic emissions, that presenting higher concentrations during rush hours rush hours maximum at 9:00 a.m. and after 6:00 p.m. (Martins; Andrade, 2008; Brito et al., 2015; Dominutti et al., 2016). Figure 4.15 shows the average profiles for benzene and toluene for all AQS, during 2017 to 2022. For traffic site (Pinheiros), the observed profiles agree with the common traffic emissions with an increase in concentrations from 6:00 to 9:00 a.m. and after 6:00 p.m. For urban site (São José dos Campos) it is possible to observe a decrease in concentration after 6:00 a.m. without any considerable variation of concentration along the day, and an increase after 6:00 p.m. Probably this peak was associated with meteorological conditions, like development of the nocturnal boundary layer or thermal inversion events. For industrial sites (Cubatão, Capuava, Paulínia and São José dos Campos – Vista Verde), benzene shows a profile with higher concentrations from 6 p.m. to 6 a.m. Toluene showed a divergent profile, showed an increase in concentrations after 2 p.m. Especially for Cubatão and Capuava, at this hour it is possible to observe the secondary maximum concentration of the day. This particularity of diurnal profiles at industrial areas of São Paulo was discussed for Capuava AQS region at previous studies (Coelho et al., 2021; Coelho et al., 2023).

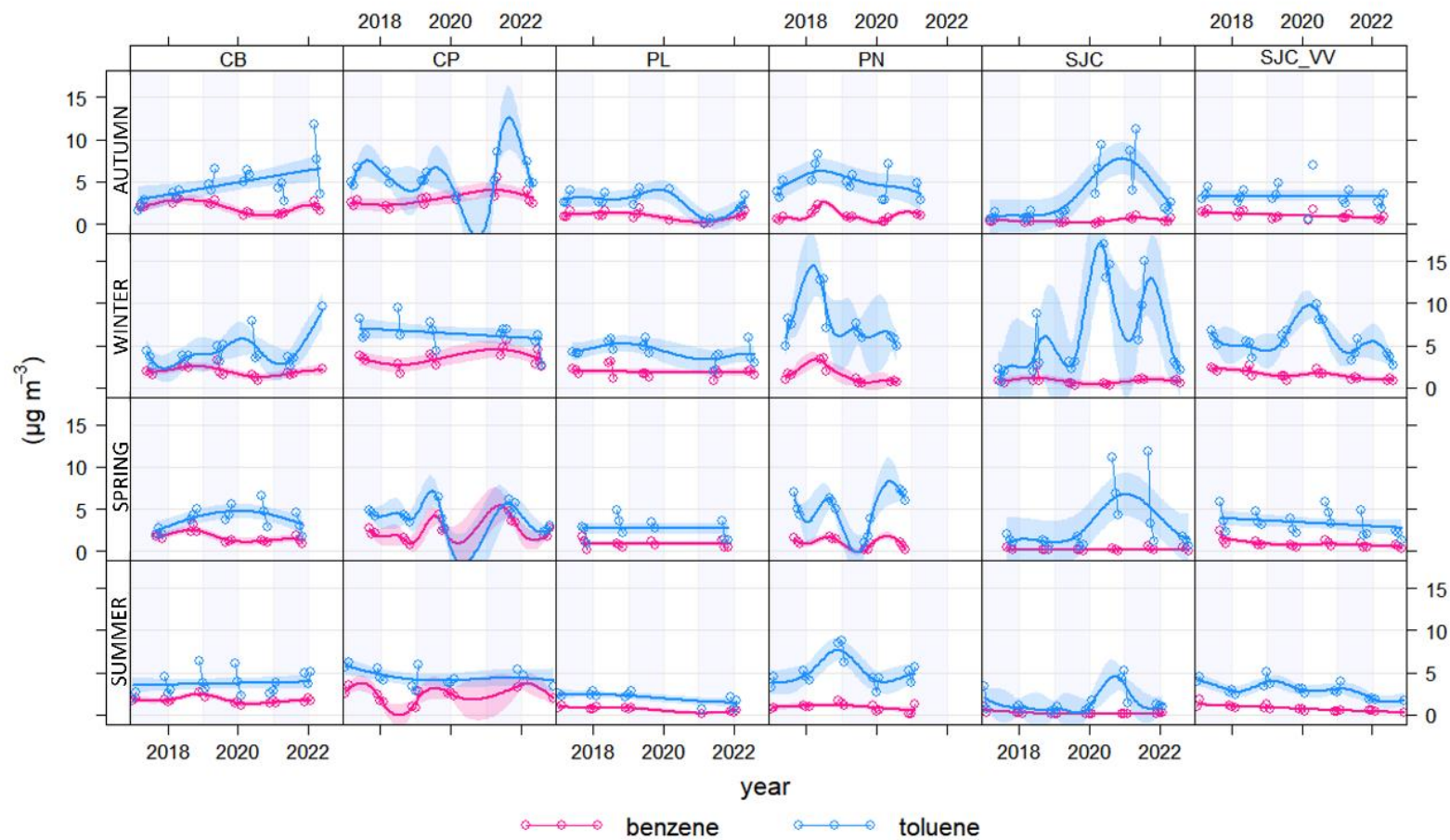


Figure 4.14. Seasonal trends for benzene and toluene at CETESB AQS, from 2017 to 2022, were CB: Cubatão, CP: Capuava, PL: Paulínia, PN: Pinheiros, SJC: São José dos Campos and SJC_VV: São José dos Campos – Vista Verde. Points corresponds to the monthly mean concentrations. Autumn: March, April and May; Winter: June, July and August; Spring: September, October and November; Summer: December, January and February.

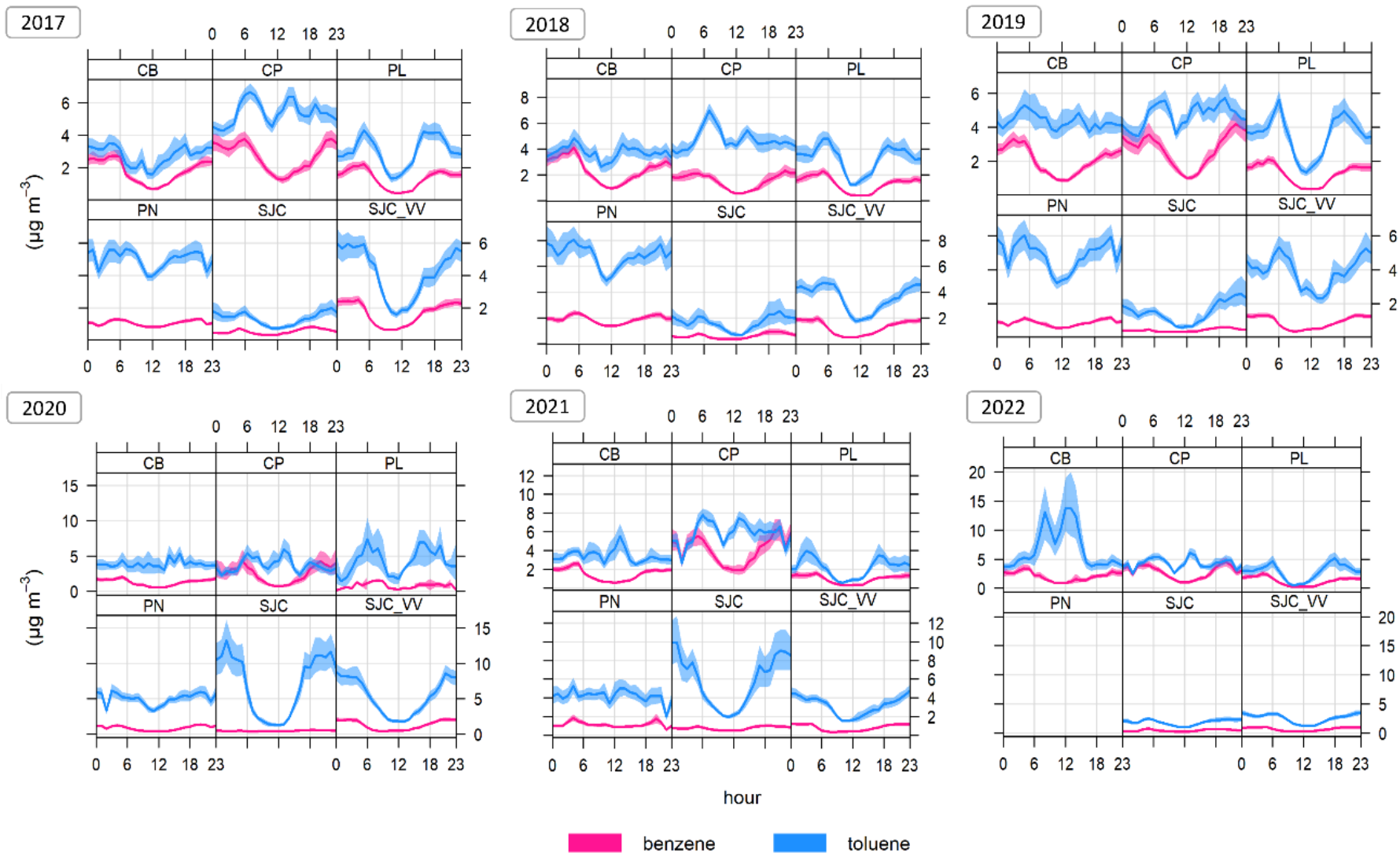


Figure 4.15. Hourly average profiles for benzene, and toluene at CETESB AQS, from 2017 to 2022, were CB: Cubatão, CP: Capuava, PL: Paulínia, PN: Pinheiros, SJC: São José dos Campos and SJC_VV: São José dos Campos – Vista Verde.

4.3.4. Ratios and correlation for benzene and toluene

Ratios of benzene/toluene (B/T) have been widely used to obtain preliminary information about sources (Tiwari et al. 2010; Kumar et al. 2018). Benzene and toluene are emitted from vehicle fuel combustion at an approximate ratio of 0.5 (Jiang et al. 2017); ratios above this value indicate other emission sources. Table 4.2 shows the comparison of ratio values among different AQS, for each year of monitoring.

The B/T ratios ranged from 0.06 to 0.69. Most of the ratios showed values ≤ 0.5 , which indicates that the main source of these compounds was fossil fuel burning from vehicles, despite the presence of industries in the region. However, it is important to highlight the Cubatão and Capuava stations, that present ratios above 0.5, were: Cubatão – 2017 and 2018: 0.65 and Capuava – 2019: 0.57; 2020: 0.66; 2021: 0.69; 2022: 0.64. In this case, these AQS are to be under the influence of other emission sources, like local industries.

Figure 4.16 presents the scatter plots and linear correlations. The linear correlation has been analyzed in order to evaluate the contribution from similar emission sources (Parrish et al., 1998; Ait-Helal et al., 2014).

Benzene and toluene concentrations could be directly influenced not only by emissions and atmospheric transport but also by chemical reactions due to the reactivity of these compounds (Coelho et al., 2021; Coelho et al., 2023). Positive correlation between benzene and toluene for 2017-2022 at Cubatão was ranged from 0.37 to 0.65; Capuava: 0.31 to 0.45; Paulínia: 0.38 to 0.49; Pinheiros: 0.56 to 0.85; São José dos Campos: 0.19 to 0.65 and São José dos Campos – Vista Verde: 0.45 to 0.83. In this way it is possible to consider that pollutants can be emitted by the same sources. Pinheiros AQS shows the strongest correlations for the period, indicating the higher influence of traffic emissions. But, as discussed in previous study, a possible explanation for low correlations between them, at other sites, is that the differences in the intensity and constancy of industrial emissions (Coelho et al., 2023).

Table 4.2. Comparison of B/T ratios observed in different AQS, for each year of monitoring (2017-2022). Ratios ≥ 0.5 are bolded.

Year of monitoring	Ratio (B/T)	Site
2017	0.65	CB
	0.50	CP
	0.45	PL
	0.22	PN
	0.41	SJC
	0.41	SJC-VV
2018	0.65	CB
	0.33	CP
	0.40	PL
	0.28	PN
	0.37	SJC
	0.36	SJC-VV
2019	0.48	CB
	0.57	CP
	0.36	PL
	0.18	PN
	0.29	SJC
	0.23	SJC-VV
2020	0.34	CB
	0.66	CP
	0.20	PL
	0.17	PN
	0.06	SJC
	0.24	SJC-VV
2021	0.44	CB
	0.69	CP
	0.44	PL
	0.28	PN
	0.13	SJC
	0.26	SJC-VV
2022	0.32	CB
	0.64	CP
	0.44	PL
	-	PN
	0.35	SJC
	0.28	SJC-VV

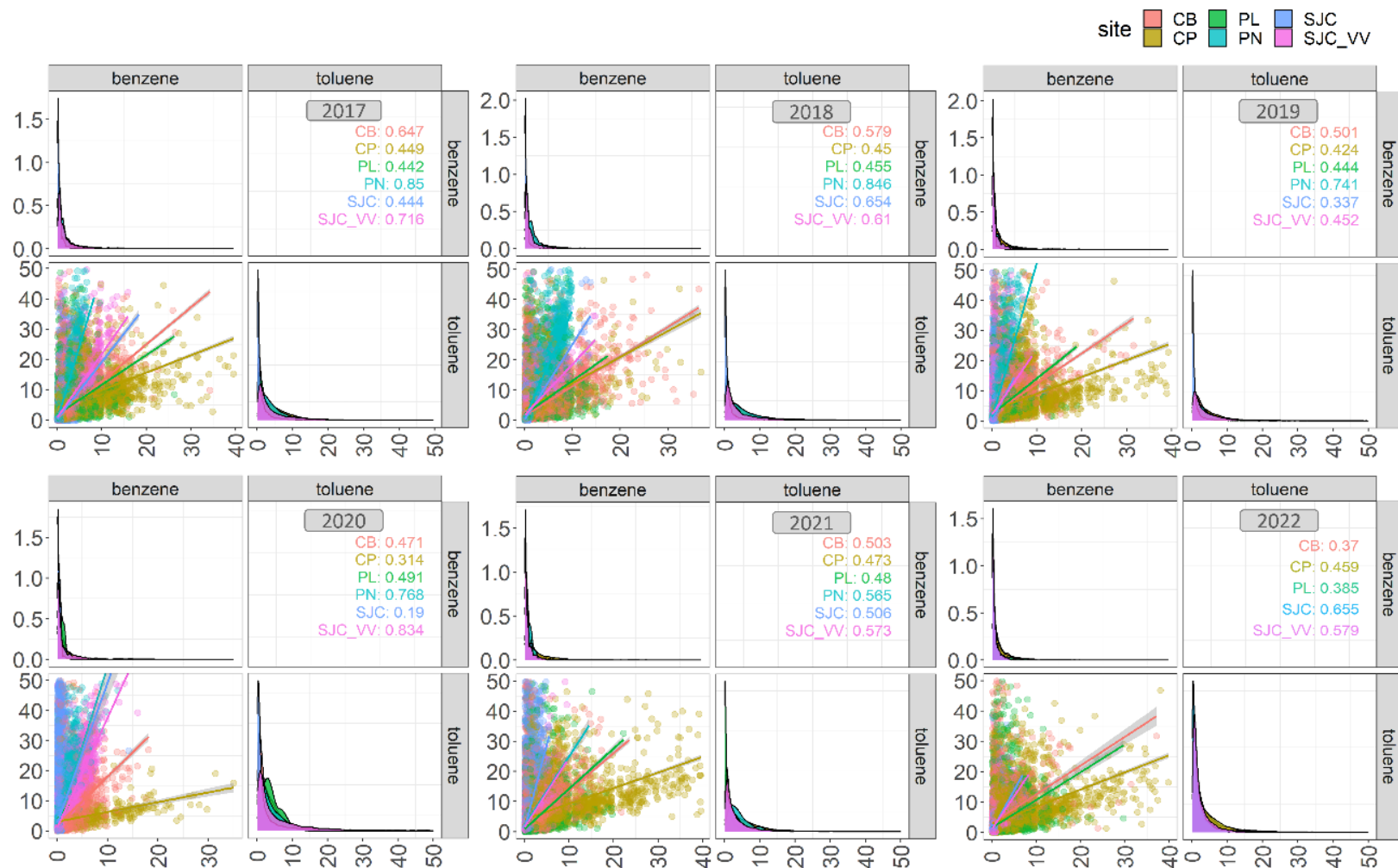


Figure 4.16. Scatter plots and respective linear regression for benzene and toluene at CETESB AQS, from 2017 to 2022, were CB: Cubatão, CP: Capuava, PL: Paulínia, PN: Pinheiros, SJC: São José dos Campos and SJC_VV: São José dos Campos – Vista Verde. The correlation coefficient (Pearson) is presented in different colors, that corresponds with each station, and the curves represent the concentration distribution at sites (in $\mu\text{g m}^{-3}$).

4.3.5. O₃ and SOA formation potentials

Secondary pollutant formation metrics were applied to evaluate the potential impacts that benzene and toluene concentrations in the area vicinity of AQS, that might imply on the local atmosphere. Figure 4.17 shows the results of the OFP and SOAFP in the period (2017-2022) for each site.

Benzene showed potentials ranged from 0.5 to 2.9 $\mu\text{g m}^{-3}$ (OFP) and 2.2 to 20.2 $\mu\text{g m}^{-3}$ (SOAFP) with highest values at Capuava, since the OFP is directly influenced by the concentrations, Capuava is the AQS that shows the highest benzene concentrations, as previous discussed here (Figure – indicar o boxplot). In general, toluene depicted higher potentials for OFP (ranged from 5.5 to 28.2 $\mu\text{g m}^{-3}$) and SOAFP (7.8 to 38.1 $\mu\text{g m}^{-3}$), at all AQS during the period. The ability to form SOA is also related to the one to form O₃ for toluene, which have previously been reported as compound that mostly contributed to both potentials (Wu et al. 2017; Coelho et al., 2021).

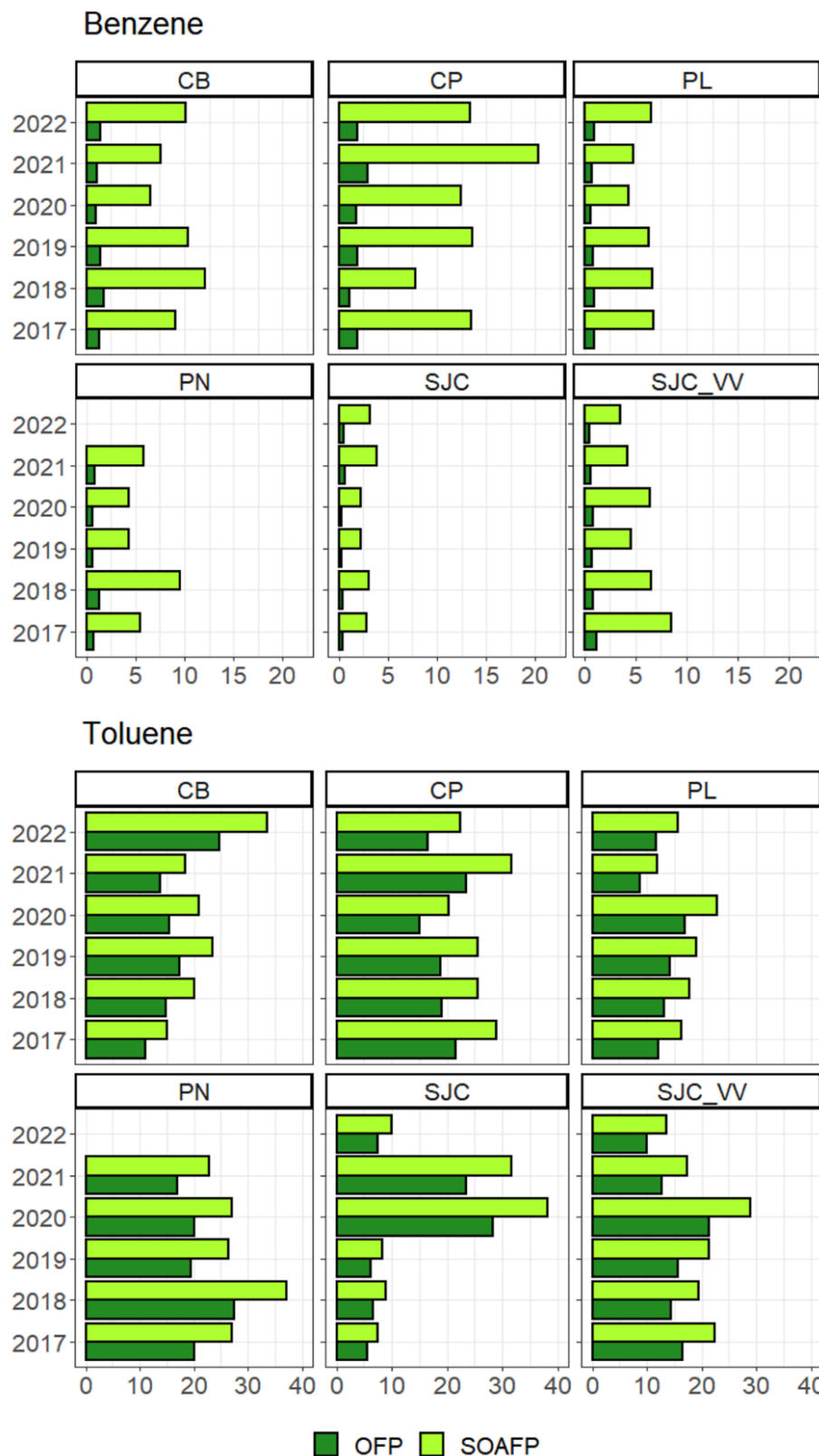


Figure 4.17. Ozone Formation Potential (OFP) and Secondary Organic Aerosol Formation Potential (SOAFP) estimation for benzene and toluene at CETESB AQS, from 2017 to 2022, were CB: Cubatão, CP: Capuava, PL: Paulínia, PN: Pinheiros, SJC: São José dos Campos and SJC_VV: São José dos Campos – Vista Verde.

4.3.6. Exposure risk

We provide an estimation of non-cancer and cancer risk to analyze the hazard of benzene and toluene inhalation for people who live, work, or circulate daily on the areas that AQS are inserted. Table 4.3 shows the estimated factors for each site and year of monitoring.

EC ranges from 0.15 to 2.35 $\mu\text{g m}^{-3}$ with higher values for toluene. HQ values less than 1 imply that there are not health effects expected, because the exposure is below the reference limit (Miri et al., 2016; Tohid et al., 2019; Ly et al., 2020). The values obtained during our study ranged from 0.0001 to 0.045 and do not exceed the U.S. EPA recommendation (< 1), and the cumulative non-cancer hazard index (HI) was in average 0.09, suggesting that HQ was negligible (Table 4.3). Our results agree with previous study at an industrial area, where HQ values ranged from 0.001 to 0.11 (Tohid et al., 2019; Coelho et al., 2021). US EPA recommended values for LCR less than 1×10^{-6} . In the present study the LCR for benzene ranges for 1.0×10^{-6} to 1.0×10^{-5} . Averaged LCR for each site indicating a probable cancer risk, followed by Capuava: 6.9×10^{-6} (seven times higher than the US EPA recommended); Cubatão: 4.8×10^{-6} (four times higher); Paulínia: 3.0×10^{-6} and Pinheiros: 3.0×10^{-6} (three times higher); São José dos Campos – Vista Verde: 2.9×10^{-6} (~three times higher) and São José dos Campos: 1.5×10^{-6} (~ two times higher) (Table 4.3). Our results are in agreement with previous study at urban and industrial areas (Tsai et al., 2019; Tohid et al., 2019; Bretón et al., 2020; Ly et al., 2020; Coelho et al., 2021).

Table 4.3. Calculated values of exposure concentration (EC), lifetime cancer risk (LCR), hazard quotient (HQ) and hazard index (HI) for CETESB AQS, from 2017 to 2022, were CB: Cubatão, CP: Capuava, PL: Paulínia, PN: Pinheiros, SJC: São José dos Campos and SJC_VV: São José dos Campos – Vista Verde. Inhalation exposure reference (RFC) and inhalation risk (IR) were obtained from U.S. EPA (IRIS) for each compound.

Site	Year		EC	LCR EPA recommendation <1 x 10 ⁻⁶	HQ <1	HI \sum^{HQ}
CB	2017	Benzene	0.60	4.68 x 10 ⁻⁶	0.0200	0.13
		Toluene	0.92		0.0002	
	2018	Benzene	0.81	6.29 x 10 ⁻⁶	0.0269	0.0002
		Toluene	1.24		0.0002	
	2019	Benzene	0.69	5.38 x 10 ⁻⁶	0.0230	0.0003
		Toluene	1.45		0.0003	
	2020	Benzene	0.44	3.41 x 10 ⁻⁶	0.0146	0.0003
		Toluene	1.29		0.0003	
	2021	Benzene	0.50	3.91 x 10 ⁻⁶	0.0167	0.0002
		Toluene	1.14		0.0002	
	2022	Benzene	0.67	5.23 x 10 ⁻⁶	0.0224	0.0004
		Toluene	2.07		0.0004	
CP	2017	Benzene	0.90	7.01 x 10 ⁻⁶	0.0300	0.18
		Toluene	1.79		0.0004	
	2018	Benzene	0.52	4.03 x 10 ⁻⁶	0.0172	0.0003
		Toluene	1.58		0.0003	
	2019	Benzene	0.90	7.02 x 10 ⁻⁶	0.0300	0.0003
		Toluene	1.57		0.0003	
	2020	Benzene	0.83	6.45 x 10 ⁻⁶	0.0275	0.0002
		Toluene	1.25		0.0002	
	2021	Benzene	1.35	<u>1.05 x 10⁻⁵</u>	0.0449	0.0004
		Toluene	1.95		0.0004	
	2022	Benzene	0.89	6.91 x 10 ⁻⁶	0.0295	0.0003
		Toluene	1.38		0.0003	
PL	2017	Benzene	0.45	3.52 x 10 ⁻⁶	0.0151	0.08
		Toluene	1.00		0.0002	
	2018	Benzene	0.44	3.42 x 10 ⁻⁶	0.0146	0.0002
		Toluene	1.10		0.0002	
	2019	Benzene	0.42	3.28 x 10 ⁻⁶	0.0140	0.0002
		Toluene	1.18		0.0002	
	2020	Benzene	0.29	2.23 x 10 ⁻⁶	0.0095	0.0003
		Toluene	1.41		0.0003	
	2021	Benzene	0.32	2.50 x 10 ⁻⁶	0.0107	0.0001
		Toluene	0.73		0.0001	
	2022	Benzene	0.43	3.36 x 10 ⁻⁶	0.0144	0.0002
		Toluene	0.97		0.0002	
PN	2017	Benzene	0.36	2.82 x 10 ⁻⁶	0.0120	0.07
		Toluene	1.67		0.0003	

	2018	Benzene	0.63	4.94×10^{-6}	0.0211	
		Toluene	2.29		0.0005	
	2019	Benzene	0.29	2.27×10^{-6}	0.0097	
		Toluene	1.63		0.0003	
	2020	Benzene	0.29	2.23×10^{-6}	0.0095	
		Toluene	1.67		0.0003	
	2021	Benzene	0.39	3.04×10^{-6}	0.0130	
		Toluene	1.41		0.0003	
	2022	Benzene	-	-	-	
		Toluene	-	-	-	
SJC	2017	Benzene	0.19	1.47×10^{-6}	0.0063	0.04
		Toluene	0.46		0.0001	
	2018	Benzene	0.21	1.61×10^{-6}	0.0069	
		Toluene	0.55		0.0001	
	2019	Benzene	0.15	1.16×10^{-6}	0.0050	
		Toluene	0.15		0.0050	
	2020	Benzene	0.15	1.18×10^{-6}	0.0051	
		Toluene	2.35		0.0005	
	2021	Benzene	0.26	2.02×10^{-6}	0.0086	
		Toluene	1.95		0.0004	
	2022	Benzene	0.21	1.67×10^{-6}	0.0072	
		Toluene	0.62		0.0001	
SJC_VV	2017	Benzene	0.56	4.38×10^{-6}	0.0187	0.08
		Toluene	1.38		0.0003	
	2018	Benzene	0.43	3.36×10^{-6}	0.0143	
		Toluene	1.19		0.0002	
	2019	Benzene	0.30	2.38×10^{-6}	0.0102	
		Toluene	1.31		0.0003	
	2020	Benzene	0.43	3.32×10^{-6}	0.0142	
		Toluene	1.78		0.0004	
	2021	Benzene	0.28	2.15×10^{-6}	0.0092	
		Toluene	1.06		0.0002	
	2022	Benzene	0.23	1.83×10^{-6}	0.0078	
		Toluene	0.83		0.0002	

4.5. Conclusions

Six years of data from different official AQS data was analyzed in order to provide an overview of the status of industrial emissions in São Paulo state.

Spatial observations about localization for AQS in relation to industrial sources distance and polar plots of concentrations influenced by the wind directions for

pollutant concentration variations during the day, showed that the each AQS as well-positioned for these pollutants' measurements.

Benzene presented higher annual mean concentrations at the sites located in industrialized areas, however, a less clear profile was observed for toluene, since the higher concentrations were observed for industrial or urban-traffic areas. Additionally diurnal profiles of toluene at industrial areas do not corresponds to typical traffic emissions.

Despite the contribution of industrial emission, B/T ratios indicated that the main sources of these pollutants were related to traffic emissions. Positive correlations were observed between them for all AQS, but poorer correlations at industrial sites probably is related to the differences in the intensity and constancy of local industrial emissions.

About secondary pollutants formation, benzene presented higher potential do form O₃ at Capuava AQS, toluene showed high contributions for O₃ and SOA potential formation at all sites.

The evaluation of potential health impacts and cancer risk demonstrates the non-cancer hazard for toluene was negligible, but the lifetime cancer risk calculated for benzene to each site in the period (2017-2022) showed one highest value, in comparison with other AQS evaluated here, to Capuava in 2021, the cancer risk is ten times higher than the US EPA recommendation.

Chapter 5. Conclusions

In order to understanding the role of HCs from industrial emissions, some observations are appointed, such as, at air samples data we highlighted the higher concentrations at industrial site in comparison with the traffic site. Among them, the most abundant HCs were aromatics, with higher contributions of toluene, benzene, xylenes, and cumene. When we analyze the AQS monitoring data, we observed that benzene presented higher annual mean concentrations at the sites located in industrialized areas. In this case, we concluded that industrial emissions are an additional source of HCs for an impacted by traffic emissions area like MASP.

The evaluations of ratios and correlations of BTEX, showed that despite vehicular emissions were the main sources of these compounds around Capuava complex, there is the influence from industrial sources among others. For AQS monitoring, positive correlations were observed between then for all AQS at each year, but poorer correlations at industrial sites probably is related to the differences in the intensity and constancy of local industrial emissions. Furthermore, near-field simulations evaluated the dispersion of pollutants of industrial origin, estimated concentrations of VOC, depicted a linear correlation indicated that Capuava complex could be responsible for more than 60% of benzene concentrations in the Capuava AQS. However, little is known about the emissions inventory or VOC speciation for industrial emissions.

Concentration variations for different seasons was examined. At winter and autumn are similar for air samples and AQS data. Especially for benzene we do not observe a clear pattern, a possible explanation for that, is associated to the relatively constant emissions from the industries.

For both air sampling and AQS monitoring data, sites related urban-traffic emissions, the diurnal profiles presented maximum values compatible to rush hour (vehicle circulation). For industrial sites, different HCs species do not show a

significant variation, especially for toluene, we identified an uncommon pattern, with increase in concentrations (maximum values, in some cases) in the afternoon (~2 p.m.).

Multiyear trends are analyzed on basis of AQS monitoring (for being the only part of the dataset with data for different years), during the six years of observations, it is not possible to determine one trend of increasing or decreasing of concentrations for benzene and toluene.

O₃ formation potential is directly influenced by the concentration of each compound, even if on the MIR scale, its value is comparatively not the most reactive. The ability to form SOA is also related to the one to form O₃, this pattern is observed for toluene and m,p-xylene at the present work. Our air samples with HCs (C₆-C₁₁), showed aromatics compounds represented ~98% and ~68% of the total SOA and O₃ formation estimations, respectively. In general, the site closely to the petrochemical complex depicted higher potentials.

In comparison with the CETESB stations evaluated here, benzene presented higher potential do form O₃ at Capuava AQS (0.5 to 2.9 µg m⁻³) and toluene showed high contributions for O₃ and SOA potential formation at all sites, ranged from 5.5 to 28.2 µg m⁻³ (O₃ potential) and 7.8 to 38.1 µg m⁻³ (SOA potential).

Our measurements at two sites in Capuava region showed the lifetime cancer risk for benzene was six times higher than the EPA recommendations. Our overview of six years of official monitoring data shows the lifetime cancer risk on average, for each station was three times higher than the recommendations, but it is needed to highlight that the Cubatão and Capuava stations was five and seven times higher, respectively. Additionally, the highest value found in this work is for Capuava in 2021 (Lifetime cancer risk: 1.0×10^{-5}), it was ten times higher than the EPA recommendation (1.0×10^{-6}). Additionally, when we analyzed the episode of uncontrolled emissions at Capuava, AERMOD simulations showed that the VOC plume had the potential to

reach a large part of Mauá and Santo André municipalities and the neighborhoods of east side of MASP, with the potential to affect the health of more than 1 million inhabitants, these observations evidenced the need to improve more details and strategies of industrial emissions controls, especially for areas like Capuava, that have residents less than 0.5 km away the complex.

Even though the governmental local inventories consider the emissions from industrial activities, a lack of industrial profile and activities is observed. Therefore, more details about speciation profiles are needed to improve the representation of industrial emissions in inventories and to better estimate their effects on the atmosphere.

Chapter 6. Future perspectives

Based on the conclusions presented in this thesis, some points are suggested for future works:

- Continue with air samples in different places (industrial areas without MASP).
- Simultaneous air samplings in industrialized areas and in any area that represented an urban background.
- Collect data of emissions inventories for other industries by environmental impact assessments (EIAs), in order to provide a dispersion study for each petrochemical complex in São Paulo state.
- Considering the great contribution in the formation of secondary pollutants, elucidate the chemical composition of SOA, for these industrialized areas.
- Use the dataset from this work to elucidate the source apportionment of HCs by Positive Matrix Factorization (PMF), for example.

APPENDIX I: Publications and presentations at scientific meetings

- Coelho, M.S.**, Corrêa, T., Fornaro, A. Breakthrough Volume for hydrocarbons (C₆ -C₁₁) sampling by Tenax-TA cartridges in urban atmosphere. In: Simpósio Latino-Americano de Química Analítica Ambiental, XIV, 2019, Bento Gonçalves. Anais.
- Corrêa, T., **Coelho, M.S.**, Fornaro, Study of atmospheric NMHC concentrations in urban green areas with different source profiles. In: Simpósio Latino-Americano de Química Analítica Ambiental, XIV, 2019, Bento Gonçalves. Anais.
- Coelho, M.S.**; Dominutti, P.A.; Boian, C.; dos Santos, T.C.; Nogueira, T.; Oliveira, C.A.V.B.d.S.; Fornaro, A., 2021. Non-methane hydrocarbons in the vicinity of a petrochemical complex in the Metropolitan Area of São Paulo, Brazil. *Air Qual. Atmos. Health*, 14, 967–984. <https://doi.org/10.1007/s11869-021-00992-1>.
- Coelho, M.S.**; Dominutti, P.A. Industrial emissions are an additional source of hydrocarbons in the megacity of São Paulo. Latin America Early Career Earth System Scientist Network. Online. 2021. <https://laearlycareer.wixsite.com/latinamericaeaccess/single-post/industrial-emissions-are-an-additional-source-of-hydrocarbons-in-the-megacity-of-s%C3%A3o-paulo>
- Coelho, M.S.** Qualidade do ar na Região Metropolitana de São Paulo: Uma discussão sobre a química atmosférica e a contribuição das emissões industriais de hidrocarbonetos menos o metano. In: Encontro de Pós-Graduação – Universidade de São Paulo, II, 2021, São Paulo. E-Pôster. <https://youtu.be/1JR7stfOk2I>
- dos Santos, T.C., Dominutti, P., Pedrosa, G.S., **Coelho, M.S.**, Nogueira, T., Borbon, A., Souza, S.R., Fornaro, A., 2022. Isoprene in urban Atlantic forests: Variability, origin, and implications on the air quality of a subtropical megacity. *Sci. Total Environ.* 824. <https://doi.org/10.1016/j.scitotenv.2022.153728>.
- Coelho, M.S.** “Estimativa do impacto na qualidade do ar resultante das emissões não-controladas do polo petroquímico de Capuava na região do grande ABC”. Online. 02.18.2022. <https://www.youtube.com/live/ZVuuXyoYYRQ?feature=share>
- Coelho, M.S.**; Zacharias, D.C.; de Paulo, T.S.; Ynoue, R.Y.; Fornaro, A., 2023. Air Quality Impact Estimation Due to Uncontrolled Emissions from Capuava Petrochemical Complex in the Metropolitan Area of São Paulo (MASP), Brazil. *Atmosphere*, 14, 577. <https://doi.org/10.3390/atmos14030577>.
- Fornaro, A.; **Coelho, M.S.**; Zacharias, D.C.; de Paulo, T.S.; Ynoue, R.Y. 2023. Air Quality Impact Estimation from Capuava Petrochemical Complex in the Metropolitan Area of São Paulo, Brazil. In: 46^a Reunião Anual da Sociedade Brasileira de Química, 2023, Água de Lindóia, Anais.

APPENDIX II: Publishing rights - license details

A) License of use

This Agreement between Monique Silva Coelho ("You") and Springer Nature ("Springer Nature") consists of your license details and the terms and conditions provided by Springer Nature and Copyright Clearance Center.

License Number 5401990073281

License date Oct 04, 2022

Licensed Content Publisher Springer Nature

Licensed Content Publication Air Quality, Atmosphere & Health

Licensed Content Title Non-methane hydrocarbons in the vicinity of a petrochemical complex in the Metropolitan Area of São Paulo, Brazil

Licensed Content Author Monique Silva Coelho et al

Licensed Content Date Feb 24, 2021

Type of Use Thesis/Dissertation

B) Open Access Journal - For articles published under an open access Creative Common (CC BY) license, any part of the article may be reused without permission provided.



atmosphere

an Open Access Journal by MDPI



Air Quality Impact Estimation Due to Uncontrolled Emissions from Capuava Petrochemical Complex in the Metropolitan Area of São Paulo (MASP), Brazil

Monique Silva Coelho; Daniel Constantino Zacharias; Tayná Silva de Paulo; Rita Yuri Ynoue; Adalgiza Fornaro

Atmosphere 2023, Volume 14, Issue 3, 577

References

- ABC, 2017. ABC DO ABC Available online: Atuação da Brasken no Polo Petroquímico do Grande ABC. URL <https://www.abcdabc.com.br/abc/noticia/atuacao-braskem-polo-petroquimico-grande-abc-50400> (accessed 8.14.20).
- ABC DO ABC. Available online: <https://www.abcdabc.com.br/abc/noticia/atuacao-braskem-polo-petroquimico-grande-abc-50400> (accessed on 14 August 2020).
- ABC, D.d.G. Forte Cheiro de Queimado Preocupa Moradores Da Região Available online: <https://www.dgabc.com.br/Noticia/3705274/forte-cheiro-de-queimado-preocupa-moradores-da-regiao> (accessed on 9 April 2021).
- ABC, D.d.G. Moradores Vizinhos Relatam Aumento Da Poluição Do Ar Available online: <https://www.dgabc.com.br/Noticia/3679176/moradores-vizinhos-relatam-aumento-da-poluicao-do-ar> (accessed on 16 February 2021).
- Ait-Helal, W., Borbon, A., Sauvage, S., De Gouw, J.A., Colomb, A., Gros, V., Freutel, F., Crippa, M., Afif, C., Baltensperger, U., Beekmann, M., Doussin, J.F., Durand-Jolibois, R., Fronval, I., Grand, N., Leonardis, T., Lopez, M., Michoud, V., Miet, K., Perrier, S., Prévôt, A.S.H., Schneider, J., Siour, G., Zapf, P., Locoge, N., 2014. Volatile and intermediate volatility organic compounds in suburban Paris: Variability, origin and importance for SOA formation. *Atmos. Chem. Phys.* 14, 10439–10464. <https://doi.org/10.5194/acp-14-10439-2014>
- Alvim, D.S., Gatti, L.V., Corrêa, S.M., Chiquetto, J.B., de Souza Rossatti, C., Pretto, A., Santos, M.H., Yamazaki, A., Orlando, J.P., Santos, G.M., 2017. Main ozone-forming VOCs in the city of Sao Paulo: observations, modelling and impacts. *Air Qual. Atmos. Heal.* 10, 421–435. <https://doi.org/10.1007/s11869-016-0429-9>
- Alvim, D.S., Gatti, L.V., Corrêa, S.M., Chiquetto, J.B., Santos, G.M., Rossatti, C. de S., Pretto, A., Rozante, J.R., Figueroa, S.N., Pendharkar, J., Nobre, P., 2018. Determining VOCs reactivity for ozone forming potential in the megacity of São Paulo. *Aerosol Air Qual. Res.* 18, 2460–2474. <https://doi.org/10.4209/aaqr.2017.10.0361>
- Alvim, D.S., Gatti, L.V., Santos, M.H. dos, Yamazaki, A., 2011. Estudos dos compostos orgânicos voláteis precursores de ozônio na cidade de São Paulo. *Eng. Sanit. e Ambient.* 16, 189–196. <https://doi.org/10.1590/S1413-41522011000200013>
- An, J., Zhu, B., Wang, H., Li, Y., Lin, X., Yang, H., 2014. Characteristics and source apportionment of VOCs measured in an industrial area of Nanjing, Yangtze River Delta, China. *Atmos. Environ.* 97, 206–214. <https://doi.org/10.1016/j.atmosenv.2014.08.021>
- Andrade, M. de F., Kumar, P., de Freitas, E.D., Ynoue, R.Y., Martins, J., Martins, L.D., Nogueira, T., Perez-Martinez, P., de Miranda, R.M., Albuquerque, T., Gonçalves, F.L.T., Oyama, B., Zhang, Y., 2017. Air quality in the megacity of São Paulo: Evolution over the last 30 years and future perspectives. *Atmos. Environ.* 159, 66–82. <https://doi.org/10.1016/j.atmosenv.2017.03.051>
- Atkinson, R., 2000. Atmospheric chemistry of VOCs and NO. *Atmos. Environ.* 34, 2063–2101. [https://doi.org/https://doi.org/10.1016/S1352-2310\(99\)00460-4](https://doi.org/https://doi.org/10.1016/S1352-2310(99)00460-4)
- Atkinson, R.; Arey, J. Atmospheric degradation of volatile organic compounds atmospheric degradation of volatile organic compounds. *Chem. Rev.* 2003, 103, 4605–4638. <https://doi.org/10.1021/cr0206420>.
- Arulprakasajothi, M.; Chandrasekhar, U.; Yuvarajan, D.; Teja, M.B. An analysis of the implications of air pollutants in Chennai. *Int. J. Ambient. Energy* 2020, 41, 209–213. <https://doi.org/10.1080/01430750.2018.1443504>.
- Bali, K.; Kumar, A.; Chourasiya, S. Emission estimates of trace gases (VOCs and NO_x) and their reactivity during biomass burning period (2003–2017) over Northeast India. *J. Atmospheric Chem.* 2021, 78, 17–34. <https://doi.org/10.1007/s10874-020-09413-6>.
- Bergstra, A.D.; Brunekreef, B.; Burdorf, A. The Influence of Industry-Related Air Pollution on Birth Outcomes in an Industri-alized Area. *Environ. Pollut.* 2021, 269, 115741. <https://doi.org/10.1016/j.envpol.2020.115741>.

- Białowicz, J.S.; Rogula-Kozłowska, W.; Krasuski, A. Contribution of landfill fires to air pollution—An assessment methodology. *Waste Manag.* 2021, 125, 182–191. <https://doi.org/10.1016/j.wasman.2021.02.046>.
- Braskem, 2017. Busca de produtos Available online: URL <http://www.braskem.com/busca-de-produtos> (accessed 8.13.20).
- Bretón, J.G.C., Bretón, R.M.C., Morales, S.M., Kahl, J.D.W., Guarnaccia, C., del Carmen Lara Severino, R., Marrón, M.R., Lara, E.R., de la Luz Espinosa Fuentes, M., Chi, M.P.U., Sánchez, G.L., 2020. Health risk assessment of the levels of BTEX in ambient air of one urban site located in Leon, Guanajuato, Mexico during two climatic seasons. *Atmosphere (Basel)*. 11. <https://doi.org/10.3390/atmos11020165>
- Brito, J., Wurm, F., Yáñez-Serrano, A.M., De Assunção, J.V., Godoy, J.M., Artaxo, P., 2015. Vehicular Emission Ratios of VOCs in a Megacity Impacted by Extensive Ethanol Use: Results of Ambient Measurements in São Paulo, Brazil. *Environ. Sci. Technol.* 49, 11381–11387. <https://doi.org/10.1021/acs.est.5b03281>
- Baltrenas, P., Baltrenaite, E., Sereviciene, V., Pereira, P., 2011. Atmospheric BTEX concentrations in the vicinity of the crude oil refinery of the Baltic region. *Environ. Monit. Assess.* 182, 115–127. <https://doi.org/10.1007/s10661-010-1862-0>
- Bloss, C., Wagner, V., Jenkin, M.E., Volkamer, R., Bloss, W.J., Lee, J.D., Heard, D.E., Wirtz, K., Martin-Reviejo, M., Rea, G., Wengwe, J.C., Pilling, M.J., 2005. Development of a detailed chemical mechanism (MCMv3.1) for the atmospheric oxidation of aromatic hydrocarbons. *Atmos. Chem. Phys.* 5, 541–664. <https://doi.org/https://doi.org/10.5194/acp-5-641-2005>
- Boian, C., Brumatti, M.M., Fornaro, A., 2015. Avaliação preliminar das concentrações de COV no entorno do Polo Petroquímico de Capuava, Mauá-SP. *Rev. Hipótese* 1, 15–28.
- Borrás, E., Tortajada-Genaro, L.A., 2011. Determination of oxygenated compounds in secondary organic aerosol from isoprene and toluene smog chamber experiments. *Int. J. Environ. Anal. Chem.* 92, 110–124. <https://doi.org/https://doi.org/10.1080/03067319.2011.572164>
- Carter, W.P.L., 2013. SAPRC Atmospheric Chemical Mechanisms and VOC Reactivity Scales Available online: URL <https://intra.engr.ucr.edu/~carter/SAPRC/> (accessed 11.30.19).
- Carter, W.P.L., 2010. Development of the SAPRC-07 chemical mechanism. *Atmos. Environ.* 44, 5324–5335. <https://doi.org/10.1016/j.atmosenv.2010.01.026>
- Carter, W.P.L., 1994. Development of Ozone Reactivity Scales for Volatile Organic Compounds. *Air Waste* 44, 881–899. <https://doi.org/10.1080/1073161X.1994.10467290>
- Carlsaw, D.C.; Ropkins, K. Openair—An R package for air quality data analysis. *Environ. Model. Softw.* 2012, 27–28, 52–61. <https://doi.org/10.1016/j.envsoft.2011.09.008>.
- Carvalho, V.S.B., Freitas, E.D., Martins, L.D., Martins, J.A., Mazzoli, C.R., Andrade, M. de F., 2015. Air quality status and trends over the Metropolitan Area of São Paulo, Brazil as a result of emission control policies. *Environ. Sci. Policy* 47, 68–79. <https://doi.org/10.1016/j.envsci.2014.11.001>
- Caumo, S., Vicente, A., Custódio, D., Alves, C., Vasconcelos, P., 2018. Organic compounds in particulate and gaseous phase collected in the neighbourhood of an industrial complex in São Paulo (Brazil). *Air Qual. Atmos. Heal.* 11, 271–283. <https://doi.org/10.1007/s11869-017-0531-7>
- Cerqueira, J.S.; de Albuquerque, H.N.; Sousa, F..A.S.. Atmospheric pollutants: Modeling with AERMOD software. *Air Qual. Atmosphere Health* 2018, 12, 21–32. <https://doi.org/10.1007/s11869-018-0626-9>.
- Cimorelli, A.J.; Perry, S.G.; Venkatram, A.; Weil, J.C.; Paine, R.B.; Wilson, R.B.; Russell, R.L.; Peters, W.D., Brode, R.W. AERMOD: A dispersion model for industrial source applications. part I: General model formulation and boundary layer characterization. *J. Appl. Meteorol. Climatol.* 2005, 44.
- CET - Companhia de Engenharia de Tráfego. Mobilidade no Sistema Viário Principal Volumes 2018. Outubro/2019. URL <http://www.cetsp.com.br/media/969813/relatorio-msvp-2018.pdf> (accessed 3.20.23).

- CETESB, 2022. Qualidade Do Ar No Estado de São Paulo. 2022, 228. Available online: <http://cetesb.sp.gov.br/ar/publicacoes-relatorios/> (accessed on 30 February 2022).
- CETESB, 2020. Companhia Ambiental do Estado de São Paulo. Available online: Qualidade do Ar. URL <https://cetesb.sp.gov.br/ar/qualar/> (accessed 2.16.20).
- CETESB, 2019. Qualidade do Ar no Estado de São Paulo 2018 210. Série Relatórios/ CETESB, ISSN 0103-4103
- CETESB, 2018. Qualidade do Ar no Estado de São Paulo 2017 198. Série Relatórios/ CETESB, ISSN 0103-4103
- CETESB Multa Empresas Do Polo Petroquímico Capuava. Available online: <https://cetesb.sp.gov.br/blog/2021/04/14/cetesb-multa-empresas-do-polo-petroquimico-capuava/>(accessed on 10 June 2021).
- CETESB. Poluição Do Ar: Gerenciamento e Controle de Fontes. Conform. Ambient. Com Requisitos Técnicos E Legais 2017, 2, 254.
- Cetin, E., Odabasi, M., Seyfioglu, R., 2003. Ambient volatile organic compound (VOC) concentrations around a petrochemical complex and a petroleum refinery. *Sci. Total Environ.* 312, 103–112. [https://doi.org/10.1016/S0048-9697\(03\)00197-9](https://doi.org/10.1016/S0048-9697(03)00197-9)
- Chang, J.C.; Hanna, S.R. Air quality model performance evaluation. *Meteorol. Atmos. Phys.* 2004, 87, 167–196. <https://doi.org/10.1007/s00703-003-0070-7>.
- Cheng, H.R., Guo, H., Saunders, S.M., Lam, S.H.M., Jiang, F., Wang, X.M., Simpson, I.J., Blake, D.R., Louie, P.K.K., Wang, T.J., 2010. Assessing photochemical ozone formation in the Pearl River Delta with a photochemical trajectory model. *Atmos. Environ.* 44, 4199–4208. <https://doi.org/10.1016/j.atmosenv.2010.07.019>
- Chiarelli, S. P.; Amador Pereira, L.A.; Nascimento Saldiva, P.H.d.; Ferreira Filho, C.; Bueno Garcia, M.L.; Ferreira Braga, A.L.; Conceição Martins, L. The association between air pollution and blood pressure in traffic controllers in Santo Andre, São Paulo, Brazil. *Environ. Res.* 2011, 111, 650–655. <https://doi.org/10.1016/j.envres.2011.04.007>.
- Chiquetto, J.B., 2008. Padrões atmosféricos associados a concentrações de ozônio troposférico na Região Metropolitana de São Paulo. Universidade de São Paulo.
- Coelho, M.S.; Dominutti, P.A.; Boian, C.; dos Santos, T.C.; Nogueira, T.; Oliveira, C.A.V.B.d.S.; Fornaro, A. Non-methane hydrocarbons in the vicinity of a petrochemical complex in the Metropolitan Area of São Paulo, Brazil. *Air Qual. Atmos. Health* 2021, 14, 967–984. <https://doi.org/10.1007/s11869-021-00992-1>.
- Coelho, M.S., Corrêa, T., Fornaro, A., 2019. Breakthrough Volume for hydrocarbons (C₆-C₁₁) sampling by Tenax-TA cartridges in urban atmosphere. In: Simpósio Latino-Americano de Química Analítica Ambiental, XIV, 2019, Bento Gonçalves. Anais.
- COFIP ABC, 2019. COMITÊ DE FOMENTO INDUSTRIA DO POLO DO GRANDE ABC. Available online: Histórico e perfil econômico. URL <http://www.cofipabc.com.br/index.asp?ID=16> (accessed 8.14.20).
- Cui, Y.; Ji, D.; He, J.; Kong, S.; Wang, Y. In situ continuous observation of hourly elements in PM_{2.5} in urban Beijing, China: Occurrence levels, temporal variation, potential source regions and health risks. *Atmos. Environ.* 2020, 222, 117164. <https://doi.org/10.1016/j.atmosenv.2019.117164>.
- Debevec, C., Sauvage, S., Gros, V., Sciare, J., Pikridas, M., Stavroulas, I., Salameh, T., Leonardis, T., Gaudion, V., Depelchin, L., Fronval, I., Sarda-Esteve, R., Baisnée, D., Bonsang, B., Savvides, C., Vrekoussis, M., Locoge, N., 2017. Origin and variability in volatile organic compounds observed at an Eastern Mediterranean background site (Cyprus). *Atmos. Chem. Phys.* 17, 11355–11388. <https://doi.org/10.5194/acp-17-11355-2017>
- Derwent, R.G., Jenkin, M.E., Utembe, S.R., Shallcross, D.E., Murrells, T.P., Passant, N.R., 2010. Secondary organic aerosol formation from a large number of reactive man-made organic compounds. *Sci. Total Environ.* 408, 3374–3381. <https://doi.org/10.1016/j.scitotenv.2010.04.013>
- Dominutti, P.A., Nogueira, T., Borbon, A., Andrade, M. de F., Fornaro, A., 2016. One-year of NMHCs

- hourly observations in São Paulo megacity: meteorological and traffic emissions effects in a large ethanol burning context. *Atmos. Environ.* 142, 371–382.
<https://doi.org/10.1016/j.atmosenv.2016.08.008>
- Dominutti, P.; Nogueira, T.; Fornaro, A.; Borbon, A. One Decade of VOCs Measurements in São Paulo megacity: composition, variability, and emission evaluation in a biofuel usage context. *Sci. Total Environ.* 2020, 738, 139790. <https://doi.org/10.1016/j.scitotenv.2020.139790>.
- Damuchali, A.M.; Guo, H. Developing an odour emission factor for an oil refinery plant using reverse dispersion modeling. *Atmos. Environ.* 2020, 222, 117167.
<https://doi.org/10.1016/j.atmosenv.2019.117167>.
- Dumanoglu, Y., Kara, M., Altiok, H., Odabasi, M., Elbir, T., Bayram, A., 2014. Spatial and seasonal variation and source apportionment of volatile organic compounds (VOCs) in a heavily industrialized region. *Atmos. Environ.* 98, 168–178.
<https://doi.org/https://doi.org/10.1016/j.atmosenv.2014.08.048>
- Evo, C.P.R., Ulrych, B.K., Takegawa, B., Soares, G., Nogueira, G., Oliveira, L.O. de, Golfetti, M., Milazzotto, P.H., Martins, L.C., 2011. Poluição do ar e internação por insuficiência cardíaca congestiva em idosos no município de Santo André. *Arq. Bras. Ciências da Saúde* 36, 6–9.
<https://doi.org/10.7322/abcs.v36i1.68>
- Friedrich, R., Obermeier, A., 1999. Anthropogenic Emissions of Volatile Organic Compounds, in: Hewitt, C. (Ed.), *Reactive Hydrocarbons in the Atmosphere*. Academic Press, pp. 1–39.
- Gao, Y.; Li, M.; Wan, X.; Zhao, X.; Wu, Y.; Liu, X.; Li, X. Important contributions of alkenes and aromatics to VOCs emissions, chemistry and secondary pollutants formation at an industrial site of central Eastern China. *Atmos. Environ.* 2021, 244, 117927.
<https://doi.org/10.1016/j.atmosenv.2020.117927>.
- Gentner, D.R., Isaacman, G., Worton, D.R., Chan, A.W.H., Dallmann, T.R., Davis, L., Liu, S., Day, D.A., Russell, L.M., Wilson, K.R., Weber, R., Guha, A., Harley, R.A., 2012. Elucidating secondary organic aerosol from diesel and gasoline vehicles through detailed characterization of organic carbon emissions. *Natl. Acad. Sci. United States Am.*
<https://doi.org/www.pnas.org/cgi/doi/10.1073/pnas.1212272109>
- Gutiérrez, M.C.; Hernández-Ceballos, M.A.; Márquez, P.; Chica, A.F.; Martín, M.A. Identification and simulation of atmospheric dispersion patterns of odour and VOCs generated by a waste treatment plant. *Atmos. Pollut. Res.* 2023, 14, 101636. <https://doi.org/10.1016/j.apr.2022.101636>.
- GREC, 2020. Climate Study Group (GREC/ USP). Available online: Relatórios Mensais. URL http://www.grec.iag.usp.br/data/monitoramentoclimatico_BRA.php (accessed 11.24.20).
- Grosjean, D., Seinfeld, J.H., 1989. Parameterization of the Formation of Secondary Organic Aerosols. *Atmos. Environ.* 23, 1733–1747. [https://doi.org/https://doi.org/10.1016/0004-6981\(89\)90058-9](https://doi.org/https://doi.org/10.1016/0004-6981(89)90058-9)
- Harrison, R.M.; Allan, J.; Carruthers, D.; Heal, M.R.; Lewis, A.C.; Marnier, B.; Murrells, T.; Williams, A. Non-exhaust vehicle emissions of particulate matter and voc from road traffic: A review. *Atmos. Environ.* 2021, 262, 118592. <https://doi.org/10.1016/j.atmosenv.2021.118592>.
- Hadei, M., Hopke, P.K., Shahsavani, A., Moradi, M., Yarahmadi, M., Emam, B., Rastkari, N., 2018. Indoor concentrations of VOCs in beauty salons; association with cosmetic practices and health risk assessment. *J. Occup. Med. Toxicol.* 13, 1–9. <https://doi.org/10.1186/s12995-018-0213-x>
- Hennig, T.A.; Kretsch, J.L.; Pessagno, C.J.; Salamonowicz, P.H.; Stein, W.L. The shuttle radar topography mission. In: Westort, C.Y. (eds) *Digital Earth Moving*. Lecture Notes in Computer Science, vol 2181. Springer, Berlin, Heidelberg. 2001, 2181, 65–77. https://doi.org/10.1007/3-540-44818-7_11.
- IAG/ USP, 2020. Meteorological Station. Available online: Solicitação de dados. URL http://www.estacao.iag.usp.br/sol_dados.php (accessed 11.24.20).
- IBGE, 2017. Instituto Brasileiro de Geografia Estatística. Available online: Estimativa da População. URL <https://www.ibge.gov.br/> (accessed 5.16.19).
- Jacobson, M.Z., 2002. Basics and History of Discovery of Atmospheric Chemicals, in: *Atmospheric*

- Pollution History, Science and Regulation. Cambridge University Press, New York, p. 412.
- Jenkin, M.E., Derwent, R.G., Wallington, T.J., 2017. Photochemical ozone creation potentials for volatile organic compounds: Rationalization and estimation. *Atmos. Environ.* 163, 128–137. <https://doi.org/10.1016/j.atmosenv.2017.05.024>
- Jia, C., Mao, X., Huang, T., Liang, X., Wang, Y., Shen, Y., Jiang, W., Wang, H., Bai, Z., Ma, M., Yu, Z., Ma, J., Gao, H., 2016. Non-methane hydrocarbons (NMHCs) and their contribution to ozone formation potential in a petrochemical industrialized city, Northwest China. *Atmos. Res.* 169, 225–236. <https://doi.org/10.1016/j.atmosres.2015.10.006>
- Jiang, Z., Grosselin, B., Daële, V., Mellouki, A., Mu, Y., 2017. Seasonal and diurnal variations of BTEX compounds in the semi-urban environment of Orleans, France. *Sci. Total Environ.* 574, 1659–1664. <https://doi.org/10.1016/j.scitotenv.2016.08.214>
- Johnson, M.R.; Devillers, R.W.; Thomson, K.A. Quantitative field measurement of soot emission from a large gas flare using sky-LOSA. *Environ. Sci. Technol.* 2011, 45, 345–350.
- Kim, S., Kwon, H., Lee, M., Seo, Y., Choi, S., 2019. Spatial and temporal variations of volatile organic compounds using passive air samplers in the multi-industrial city of Ulsan, Korea. *Environ. Sci. Pollut. Res.* <https://doi.org/https://doi.org/10.1007/s11356-018-4032->
- Kamara, A.A.; Harrison, R.M. Analysis of the air pollution climate of a central urban roadside supersite: London, Marylebone road. *Atmos. Environ.* 2021, 258, 118479. <https://doi.org/10.1016/j.atmosenv.2021.118479>.
- Kansal, A., 2009. Sources and reactivity of NMHCs and VOCs in the atmosphere: A review. *J. Hazard. Mater.* 166, 17–26. <https://doi.org/10.1016/j.jhazmat.2008.11.048>
- Kawashima, A.B.; Martins, L.D.; Rafee, S.A.A.; Rudke, A.P.; de Moraes, M.V.; Martins, J.A. Development of a spatialized atmospheric emission inventory for the main industrial sources in Brazil. *Environ. Sci. Pollut. Res.* 2020, 27, 35941–35951. <https://doi.org/10.1007/s11356-020-08281-7>.
- Kelleghan, D.B.; Hayes, E.T.; Everard, M.; Curran, T.P. Predicting atmospheric ammonia dispersion and potential ecological effects using monitored emission rates from an intensive laying hen facility in Ireland. *Atmos. Environ.* 2021, 247, 118214. <https://doi.org/10.1016/j.atmosenv.2021.118214>.
- Kroll, J.H., Seinfeld, J.H., 2008. Chemistry of secondary organic aerosol: Formation and evolution of low-volatility organics in the atmosphere 42, 3593–3624. <https://doi.org/10.1016/j.atmosenv.2008.01.003>
- Kumar, A., Singh, D., Kumar, K., Singh, B.B., Jain, V.K., 2018. Distribution of VOCs in urban and rural atmospheres of subtropical India: temporal variation, source attribution, ratios, OFP and risk assessment. *Sci. Total Environ.* 613, 492–501. <https://doi.org/http://dx.doi.org/10.1016/j.scitotenv.2017.09.096>
- Lee, S.C., Chiu, M.Y., Ho, K.F., Zou, S.C., Wang, X., 2002. Volatile organic compounds (VOCs) in urban atmosphere of Hong Kong. *Chemosphere* 48, 375–382. [https://doi.org/10.1016/S0045-6535\(02\)00040-1](https://doi.org/10.1016/S0045-6535(02)00040-1)
- Leuchner, M., Rappenglück, B., 2010. VOC source-receptor relationships in Houston during TexAQS-II. *Atmos. Environ.* 44, 4056–4067. <https://doi.org/10.1016/j.atmosenv.2009.02.029>
- Lin, Y.C.; Lai, C.Y.; Chu, C.P. Air Pollution diffusion simulation and seasonal spatial risk analysis for industrial areas. *Environ. Res.* 2021, 194, 110693. <https://doi.org/10.1016/j.envres.2020.110693>.
- Liu, Y.; Wang, H.; Jing, S.; Peng, Y.; Gao, Y.; Yan, R.; Wang, Q.; Lou, S.; Cheng, T.; Huang, C. Strong regional transport of volatile organic compounds (VOCs) during wintertime in Shanghai megacity of China. *Atmos. Environ.* 2021, 244, 117940. <https://doi.org/10.1016/j.atmosenv.2020.117940>.
- Ly, B.T., Kajii, Y., Nguyen, T.Y.L., Shoji, K., Van, D.A., Do, T.N.N., Nghiem, T.D., Sakamoto, Y., 2020. Characteristics of roadside volatile organic compounds in an urban area dominated by gasoline vehicles, a case study in Hanoi. *Chemosphere* 254, 126749. <https://doi.org/10.1016/j.chemosphere.2020.126749>

- Macêdo, M.F.M.; Ramos, A.L.D. Vehicle atmospheric pollution evaluation using AERMOD. Model at avenue in a Brazilian capital city. *Air Qual. Atmos. Health* 2020, 13, 309–320. <https://doi.org/10.1007/s11869-020-00792-z>.
- Mao, W.; Wang, W.; Jiao, L.; Zhao, S.; Liu, A. Modeling air quality prediction using a deep learning approach: Method optimization and evaluation. *Sustain. Cities Soc.* 2021, 65, 102567. <https://doi.org/10.1016/j.scs.2020.102567>.
- Martins, L.D., 2006. Sensibilidade da formação do ozônio troposférico às emissões veiculares na Região Metropolitana de São Paulo. Universidade de São Paulo, Instituto de Astronomia, Geofísica e Ciências Atmosféricas.
- Martins, L.D., Andrade, M.F., 2008. Ozone formation potentials of volatile organic compounds and ozone sensitivity to their emission in the megacity of São Paulo, Brazil. *Water. Air. Soil Pollut.* 195, 201–213. <https://doi.org/10.1007/s11270-008-9740-x>
- McEwen, J.D.N.; Johnson, M.R. Black carbon particulate matter emission factors for buoyancy-driven associated gas flares. *J. Air Waste Manag. Assoc.* 2012, 62, 307–321. <https://doi.org/10.1080/10473289.2011.650040>.
- Michalik, J.; Machaczka, O.; Jirik, V.; Heryan, T.; Janout, V. Air pollutants over industrial and non-industrial areas: Historical concentration estimates. *Atmosphere* 2022, 13, 1–15. <https://doi.org/10.3390/atmos13030455>.
- Miller, L., Xu, X., Wheeler, A., Atari, D.O., Grgicak-mannion, A., Luginaah, I., 2011. Spatial Variability and Application of Ratios between BTEX in Two Canadian Cities. *Sci. World J.* 11, 2536–2549. <https://doi.org/10.1100/2011/167973>
- Miri, M., Rostami, M., Shendi, A., Reza, H., Ebrahimi, H., Ahmadi, E., Taban, E., Gholizadeh, A., Yazdani, M., Mohammadi, A., Azari, A., 2016. Chemosphere Investigation of outdoor BTEX: Concentration, variations, sources, spatial distribution, and risk assessment. *Chemosphere* 163, 601–609. <https://doi.org/10.1016/j.chemosphere.2016.07.088>
- Monks, P.S., Granier, C., Fuzzi, S., Stohl, A., Williams, M.L., Akimoto, H., Amann, M., Baklanov, A., Baltensperger, U., Bey, I., Blake, N., Blake, R.S., Carslaw, K., Cooper, O.R., Dentener, F., Fowler, D., Fragkou, E., Frost, G.J., Generoso, S., Ginoux, P., Grewe, V., Guenther, A., Hansson, H.C., Henne, S., Hjorth, J., Hofzumahaus, A., Huntrieser, H., Isaksen, I.S.A., Jenkin, M.E., Kaiser, J., Kanakidou, M., Klimont, Z., Kulmala, M., Laj, P., Lawrence, M.G., Lee, J.D., Liousse, C., Maione, M., McFiggans, G., Metzger, A., Mieville, A., Moussiopoulos, N., Orlando, J.J., O'Dowd, C.D., Palmer, P.I., Parrish, D.D., Petzold, A., Platt, U., Pöschl, U., Prévôt, A.S.H., Reeves, C.E., Reimann, S., Rudich, Y., Sellegri, K., Steinbrecher, R., Simpson, D., ten Brink, H., Theloke, J., van der Werf, G.R., Vautard, R., Vestreng, V., Vlachokostas, C., von Glasow, R., 2009. Atmospheric composition change - global and regional air quality. *Atmos. Environ.* 43, 5268–5350. <https://doi.org/10.1016/j.atmosenv.2009.08.021>
- Na, K., Song, C., Cocker, D.R., 2006. Formation of secondary organic aerosol from the reaction of styrene with ozone in the presence and absence of ammonia and water. *Atmos. Environ.* 40, 1889–1900. <https://doi.org/10.1016/j.atmosenv.2005.10.063>
- Nogueira, T., Dominutti, P.A., Fornaro, A., Andrade, M.d.F., 2017. Seasonal trends of formaldehyde and acetaldehyde in the megacity of São Paulo. *Atmosphere*. <https://doi.org/10.3390/atmos8080144>
- NTP, 2016. National Toxicology Program. Available online: Report on Carcinogens. URL <https://ntp.niehs.nih.gov/ntp/roc/content/profiles/benzene.pdf> (accessed 8.14.20).
- Orlando, J.P., Alvim, D.S., Yamazaki, A., Corrêa, S.M., Gatti, L.V., 2010. Ozone precursors for the São Paulo Metropolitan Area. *Sci. Total Environ.* 408, 1612–1620. <https://doi.org/10.1016/j.scitotenv.2009.11.060>
- Otto, D.; Molhave, L.; Rose, G.; Hudnell, H.K.; House, D. Neurobehavioral and sensory irritant effects of controlled exposure to a complex mixture of volatile organic compounds. *Neurotoxicol. Teratol.* 1990, 12, 649–652. [https://doi.org/10.1016/0892-0362\(90\)90079-R](https://doi.org/10.1016/0892-0362(90)90079-R).
- Parrish, D.D., Trainer, M., Young, V., Goldan, P.D., Kuster, W.C., Jobson, B.T., Fehsenfeld, F.C.,

- Lonneman, W.A., Zika, R.D., Farmer, C.T., Riemer, D.D., Rodgers, M.O., 1998. Internal consistency tests for evaluation of measurements of anthropogenic hydrocarbons in the troposphere. *J. Geophys. Res.* 103, 339–359. <https://doi.org/https://doi.org/10.1029/98JD01364>
- Parveen, N.; Siddiqui, L.; Sarif, N.; Islam, S.; Khanam, N.; Mohibul, S. Industries in Delhi: Air pollution versus respiratory morbidities. *Process. Saf. Environ. Prot.* 2021, 152, 495–512. <https://doi.org/10.1016/j.psep.2021.06.027>.
- Pecha, P.; Tichý, O.; Pechová, E. Determination of radiological background fields designated for inverse modelling during atypical low wind speed meteorological episode. *Atmos. Environ.* 2021, 246. <https://doi.org/10.1016/j.atmosenv.2020.118105>.
- Pereira, G.M., Ellen da Silva Caumo, S., Mota do Nascimento, E.Q., Parra, Y.J., de Castro Vasconcellos, P., 2019. Polycyclic aromatic hydrocarbons in tree barks, gaseous and particulate phase samples collected near an industrial complex in São Paulo (Brazil). *Chemosphere* 237. <https://doi.org/10.1016/j.chemosphere.2019.124499>
- PerkinElmer, 2020. Tenax TA. Available online: URL <https://www.perkinelmer.com/> (accessed 8.12.20).
- Petrobras, 2020. Refinaria Capuava Available online: Informações gerais. URL <https://petrobras.com.br/pt/nossas-atividades/principais-operacoes/refinarias/refinaria-capuava-recap.htm> (accessed 3.10.20).
- Pisso, I.; Sollum, E.; Grythe, H.; Kristiansen, N.I.; Cassiani, M.; Eckhardt, S.; Arnold, D.; Morton, D.; Thompson, R.L.; Groot Zwaaftink, C.D.; et al. The lagrangian particle dispersion model FLEXPART version 10.4. *Geosci. Model Dev.* 2019, 12, 4955–4997. <https://doi.org/10.5194/gmd-12-4955-2019>.
- Pirhalla, M.; Heist, D.; Perry, S.; Tang, W.; Brouwer, L. Simulations of dispersion through an irregular urban building array. *Atmos. Environ.* 2021, 258, 118500. <https://doi.org/10.1016/j.atmosenv.2021.118500>.
- Rajabi, H., Hadi Mosleh, M., Mandal, P., Lea-Langton, A., Sedighi, M., 2020. Emissions of volatile organic compounds from crude oil processing - Global emission inventory and environmental release. *Sci. Total Environ.* 727, 138654. <https://doi.org/10.1016/j.scitotenv.2020.138654>
- Ras, M.R., Borrull, F., Marcé, R.M., 2009. Sampling and preconcentration techniques for determination of volatile organic compounds in air samples. *Trends Anal. Chem.* 28, 347–361. <https://doi.org/10.1016/j.trac.2008.10.009>
- Ragothaman, A.; Anderson, W.A. Air quality impacts of petroleum refining and petrochemical industries. *Environment* 2017, 4, 1–16. <https://doi.org/10.3390/environments4030066>.
- Roukos, J., Riffault, V., Locoge, N., Plaisance, H., 2009. VOC in an urban and industrial harbor on the French North Sea coast during two contrasted meteorological situations. *Environ. Pollut.* 157, 3001–3009. <https://doi.org/10.1016/j.envpol.2009.05.059>
- Saiki, M., Alves, E.R., Marcelli, M.P., 2007. Analysis of lichen species for atmospheric pollution biomonitoring in the Santo André municipality, São Paulo, Brazil. *J. Radioanal. Nucl. Chem.* 273, 543–547. <https://doi.org/10.1007/s10967-007-0906-6>
- Salameh, T., Borbon, A., Afif, C., Sauvage, S., Leonardis, T., Gaimoz, C., Locoge, N., 2016. Composition of gaseous organic carbon during ECOCEM in Beirut, Lebanon: new observational constraints for VOC anthropogenic emission evaluation in the Middle East. *Atmos. Chem. Phys. Discuss.* 1–32. <https://doi.org/10.5194/acp-2016-543>
- Salameh, T., Sauvage, S., Afif, C., Borbon, A., Locoge, N., 2015. Source apportionment vs. emission inventories of non-methane hydrocarbons (NMHC) in an urban area of the Middle East: local and global perspectives in the Middle East. *Atmos. Chem. Phys.* 15, 26795–26837. <https://doi.org/10.5194/acpd-15-26795-2015>
- Sekar, A.; Varghese, G.K.; Ravi Varma, M.K. Analysis of benzene air quality standards, monitoring methods and concentrations in indoor and outdoor environment. *Heliyon* 2019, 5, e02918. <https://doi.org/10.1016/j.heliyon.2019.e02918>.
- Shao, P., An, J., Xin, J., Wu, F., Wang, J., Ji, D., Wang, Y., 2016. Source apportionment of VOCs and the

- contribution to photochemical ozone formation during summer in the typical industrial area in the Yangtze River Delta, China. *Atmos. Res.* 176–177, 64–74.
<https://doi.org/10.1016/j.atmosres.2016.02.015>
- Sharma, S., Giri, B., Patel, K.S., 2016. Ambient volatile organic compounds in the atmosphere of industrial central India. *J. Atmos. Chem.* 73, 381–395. <https://doi.org/10.1007/s10874-016-9329-5>
- Silva, C.M. Da, Silva, L.L. Da, Corrêa, S.M., Arbilla, G., 2017. Speciation analysis of ozone precursor volatile organic compounds in the air basins of the Rio de Janeiro metropolitan area. *Rev. Virtual Quim.* 9, 1887–1909. <https://doi.org/10.21577/1984-6835.20170111>
- Simpson, I.J., Blake, N.J., Barletta, B., Diskin, G.S., Fuelberg, H.E., Gorham, K., Huey, L.G., Meinardi, S., Rowland, F.S., Vay, S.A., Weinheimer, A.J., Yang, M., Blake, D.R., 2010. Characterization of trace gases measured over alberta oil sands mining operations: 76 speciated C2–C10 volatile organic compounds (VOCs), CO₂, CH₄, CO, NO, NO₂, NO_y, O₃ and SO₂. *Atmos. Chem. Phys.* 10, 11931–11954. <https://doi.org/10.5194/acp-10-11931-2010>
- Song, S., Shon, Z., Kang, Y., Kim, K., Han, S., Kang, M., Bang, J., Oh, I., 2019. Source apportionment of VOCs and their impact on air quality and health in the megacity of Seoul. *Environ. Pollut.* 247, 763–774. <https://doi.org/10.1016/j.envpol.2019.01.102>
- Squizzato, R.; Nogueira, T.; Martins, L.D.; Martins, J.A.; Astolfo, R.; Machado, C.B.; Andrade, M.d.F.; Freitas, E.D.d. Beyond megacities: Tracking air pollution from urban areas and biomass burning in Brazil. *Clim. Atmos. Sci.* 2021, 4, s41612–s021.
- Tadano, Y.S.; Mazza, R.A.; Tomaz, E. Modelagem Da Dispersão De Poluentes Atmosféricos No Município De Paulínia (Brasil) Empregando O Iscst3. *Mecânica Comput.* 2010, XXIX, 15–18.
- Thera, B.T.P., Dominutti, P., Öztürk, F., Salameh, T., Sauvage, S., Afif, C., Çetin, B., Gaimoz, C., Keleş, M., Evan, S., Borbon, A., 2019. Composition and variability of gaseous organic pollution in the port megacity of Istanbul: Source attribution, emission ratios, and inventory evaluation. *Atmos. Chem. Phys.* 19, 15131–15156. <https://doi.org/10.5194/acp-19-15131-2019>
- Tiwari, V., Hanai, Y., Masunaga, S., 2010. Ambient levels of volatile organic compounds in the vicinity of petrochemical industrial area of Yokohama, Japan. *Air Qual. Atmos. Heal.* 3, 65–75.
<https://doi.org/10.1007/s11869-009-0052-0>
- Tohid, L., Sabeti, Z., Sarbakhsh, P., Zoroufchi, K., Shakerkhatibi, M., Rasoulzadeh, Y., Rahimian, R., Darvishali, S., 2019. Spatiotemporal variation, ozone formation potential and health risk assessment of ambient air VOCs in an industrialized city in Iran. *Atmos. Pollut. Res.* 10, 556–563. <https://doi.org/10.1016/j.apr.2018.10.007>
- Tsai, J.H., Gu, W.T., Chung, I.I., Chiang, H.L., 2019. Airborne air toxics characteristics and inhalation health risk assessment of a metropolitan industrial complex. *Aerosol Air Qual. Res.* 19, 2477–2489. <https://doi.org/10.4209/aaqr.2019.08.0422>
- Tyovenda, A.A.; Ayua, T.J.; Sombo, T. Modeling of gaseous pollutants (CO and NO₂) emission from an industrial stack in Kano City, Northwestern Nigeria. *Atmos. Environ.* 2021, 253, 118356.
<https://doi.org/10.1016/j.atmosenv.2021.118356>.
- Ueda, A.C., 2010. Estudo de Compostos Orgânicos Voláteis na Atmosfera da Região Metropolitana de Campinas. Universidade Estadual de Campinas.
- Ueda, A.C., Tomaz, E., 2011. BTEX concentrations in the atmosphere of the metropolitan area of Campinas (São Paulo, Brazil). *Trans. Ecol. Environ.* 147, 211–217.
<https://doi.org/10.2495/AIR110191>
- United States Environmental Protection Agency, 2016. Integrated Risk Information System (IRIS) Available online: <http://www.epa.gov> (accessed 6.30.20).
- United States Environmental Protection Agency, 1999. Determination of Volatile Organic Compounds in Ambient Air Using Active Sampling on to Sorbent Tubes, 2nd ed, 17-24.
- United States Environmental Protection Agency. CMAQ: Community Multiscale Air Quality Modeling System. Available online: <https://www.epa.gov/cmaq/frequent-cmaq-questions> (accessed on 25 October 2022).

- United States Environmental Protection Agency Air Quality Dispersion Modeling – Preferred and Recommended Models. Available online: <https://www.epa.gov/scram/air-quality-dispersion-modeling-preferred-and-recommended-models#aermod> (accessed on 9 August 2022).
- United States Environmental Protection Agency Air Quality Dispersion Modeling – Alternative Models. Available online: <https://www.epa.gov/scram/air-quality-dispersion-modeling-alternative-models#calpuff> (accessed on 28 September 2022).
- Valverde, M.C.; Coelho, L.H.; de Oliveira Cardoso, A.; Paiva Junior, H.; Brambila, R.; Boian, C.; Martinelli, P.C.; Valdam-brini, N.M. Urban climate assessment in the ABC Paulista Region of São Paulo, Brazil. *Sci. Total Environ.* 2020, 735, 139303. <https://doi.org/10.1016/j.scitotenv.2020.139303>.
- Venkatram, A.; Brode, R.; Cimorelli, A.; Lee, R.; Paine, R.; Perry, S.; Peters, W.; Weil, J.; Wilson, R. A complex terrain dispersion model for regulatory applications. *Atmos. Environ.* 2001, 35, 4211–4221. [https://doi.org/10.1016/S1352-2310\(01\)00186-8](https://doi.org/10.1016/S1352-2310(01)00186-8).
- Vemado, F., Pereira Filho, A.J., 2016. Severe weather caused by heat island and sea breeze effects in the metropolitan area of são paulo, Brazil. *Adv. Meteorol.* 2016. <https://doi.org/10.1155/2016/8364134>
- Vestenius, M.; Hopke, P.K.; Lehtipalo, K.; Petäjä, T.; Hakola, H.; Hellén, H. Assessing volatile organic compound sources in a boreal forest using positive matrix factorization (PMF). *Atmos. Environ.* 2021, 259. <https://doi.org/10.1016/j.atmosenv.2021.118503>.
- Waked, A., Sauvage, S., Borbon, A., Gauduin, J., Pallares, C., Vagnot, M.P., Léonardis, T., Locoge, N., 2016. Multi-year levels and trends of non-methane hydrocarbon concentrations observed in ambient air in France. *Atmos. Environ.* 141, 263–275. <https://doi.org/10.1016/j.atmosenv.2016.06.059>
- Wang, J.L., Chew, C., Chang, C.Y., Liao, W.C., Lung, S.C.C., Chen, W.N., Lee, P.J., Lin, P.H., Chang, C.C., 2013. Biogenic isoprene in subtropical urban settings and implications for air quality. *Atmos. Environ.* 79, 369–379. <https://doi.org/10.1016/j.atmosenv.2013.06.055>
- Warneke, C., Gouw, J.A. de, Holloway, J.S., Peischl, J., Ryerson, T.B., Atlas, E., Blake, D., Trainer, M., Parrish, D.D., 2012. Multiyear trends in volatile organic compounds in Los Angeles, California: Five decades of decreasing emissions. *J. Geophys. Res. Atmos.* 117. <https://doi.org/https://doi.org/10.1029/2012JD017899>
- Weber, S., Uzu, G., Calas, A., Chevrier, F., Besombes, J.L., Charron, A., Salameh, D., Ježek, I., Močnik, G., Jaffrezo, J.L., 2018. An apportionment method for the oxidative potential of atmospheric particulate matter sources: Application to a one-year study in Chamonix, France. *Atmos. Chem. Phys.* 18, 9617–9629. <https://doi.org/10.5194/acp-18-9617-2018>
- Wei, W., Cheng, S., Li, G., Wang, G., Wang, H., 2014. Characteristics of ozone and ozone precursors (VOCs and NO_x) around a petroleum refinery in Beijing, China. *J. Environ. Sci. (China)* 26, 332–342. [https://doi.org/10.1016/S1001-0742\(13\)60412-X](https://doi.org/10.1016/S1001-0742(13)60412-X)
- WHO, 2018. World Health Organization. Available online: Ambient outdoor air Pollution. URL [https://www.who.int/en/news-room/fact-sheets/detail/ambient-\(outdoor\)-air-quality-and-health](https://www.who.int/en/news-room/fact-sheets/detail/ambient-(outdoor)-air-quality-and-health) (accessed 8.14.20).
- WHO, 2021. World Health Organization. Air Quality Guidelines: particulate matter (PM_{2.5} and PM₁₀), ozone, nitrogen dioxide, sulfur dioxide and carbon monoxide. 2021. <https://apps.who.int/iris/handle/10665/345329>. (Accessed on 20 November 2022).
- Wu, W., Zhao, B., Wang, S., Hao, J., 2017. Ozone and secondary organic aerosol formation potential from anthropogenic volatile organic compounds emissions in China. *J. Environ. Sci. (China)* 53, 224–237. <https://doi.org/10.1016/j.jes.2016.03.025>
- Wu, X., Huang, W., Zhang, Y., Zheng, C., Jiang, X., Gao, X., Cen, K., 2015. Characteristics and uncertainty of industrial VOCs emissions in China. *Aerosol Air Qual. Res.* 15, 1045–1058. <https://doi.org/10.4209/aaqr.2014.10.0236>
- Xu, H.; Li, Y.; Feng, R.; He, K.; Ho, S.S.H.; Wang, Z.; Ho, K.F.; Sun, J.; Chen, J.; Wang, Y.; et al. Comprehensive characterization and health assessment of occupational exposures to volatile

- organic compounds (VOCs) in Xi'an, a major city of Northwestern China. *Atmos. Environ.* 2021, 246, 118085. <https://doi.org/10.1016/j.atmosenv.2020.118085>.
- Yuan, B., Shao, M., Lu, S., Wang, B., 2010. Source profiles of volatile organic compounds associated with solvent use in Beijing, China. *Atmos. Environ.* 44, 1919–1926. <https://doi.org/10.1016/j.atmosenv.2010.02.014>
- Yuan, Z., Zhong, L., Kai, A., Lau, H., Zhen, J., Louie, P.K.K., 2013. Volatile organic compounds in the Pearl River Delta: Identification of source regions and recommendations for emission-oriented monitoring strategies. *Atmos. Environ.* 76, 162–172. <https://doi.org/10.1016/j.atmosenv.2012.11.034>
- Zaccarelli-Marino, M.A., 2012. Chronic autoimmune thyroiditis in industrial areas in Brazil: A 15-year survey. *J. Clin. Immunol.* 32, 1012–1018. <https://doi.org/10.1007/s10875-012-9703-2>
- Zaccarelli-Marino, M.A., André, C.D.S., Singer, J.M., 2016. Overt Primary Hypothyroidism in an Industrial Area in São Paulo, Brazil: The Impact of Public Disclosure. *Int. J. Environ. Res. Public Heal.* 13, 1161. <https://doi.org/10.3390/ijerph13111161>
- Zhang, Y., Mu, Y., Liu, J., Mellouki, A., 2012. Levels, sources and health risks of carbonyls and BTEX in the ambient air of Beijing, China. *J. Environ. Sci.* 24, 124–130. [https://doi.org/10.1016/S1001-0742\(11\)60735-3](https://doi.org/10.1016/S1001-0742(11)60735-3)
- Zaccarelli-Marino, M.A.; Alessi, R.; Balderi, T.Z.; Martins, M.A.G. Association between the occurrence of primary hypothyroidism and the exposure of the population near to industrial pollutants in São Paulo State, Brazil. *Int. J. Environ. Res. Public Health* 2019, 16, 1–11. <https://doi.org/10.3390/ijerph16183464>.
- Zhang, Z., Wang, H., Chen, D., Li, Q., Thai, P., Gong, D., Li, Y., Zhang, C., Gu, Y., Zhou, L., Morawska, L., Wang, B., 2017. Emission characteristics of volatile organic compounds and their secondary organic aerosol formation potentials from a petroleum refinery in Pearl River Delta, China. *Sci. Total Environ.* 584–585, 1162–1174. <https://doi.org/10.1016/j.scitotenv.2017.01.179>
- Zheng, J., Shao, M., Che, W., Zhang, L., Zhong, L., Zhang, Y., Streets, D., 2009. Speciated VOC Emission Inventory and Spatial Patterns of Ozone Formation Potential in the Pearl River Delta, China. *Environ. Sci. Technol.* 43, 8580–8586. <https://doi.org/https://doi.org/10.1021/es901688e>
- Zhang, Q.; Sun, L.; Wei, N.; Wu, L.; Mao, H. The characteristics and source analysis of VOCS emissions at roadside: Assess the impact of ethanol-gasoline implementation. *Atmos. Environ.* 2021, 263, 118670. <https://doi.org/10.1016/j.atmosenv.2021.118670>.